



RESEARCH & DEVELOPMENT

**Institute for Transportation Research & Education,
North Carolina State University**

Traffic Analysis Tools: Assessment, Comparison and Validation Study

FINAL REPORT

NCDOT Project 2020-30

FHWA/NC/2020-30

MAY 2022

TECHNICAL REPORT DOCUMENTATION PAGE

1. Report No. FHWA/NC/2020-30	2. Government Accession No.	3. Recipient's Catalog No.	
4. Title and Subtitle: Traffic Analysis Tools: Assessment, Comparison and Validation Study		5. Report Date: February 21, 2022	
		6. Performing Organization Code	
7. Author(s) Nagui M. Roupail, Shoaib Samandar, Richard Chase, Guangchuan Yang, George List and Gyoungsoon Chun		8. Performing Organization Report No. ITRE/ NC State University	
9. Performing Organization Name and Address Institute for Transportation Research and Education North Carolina State University Centennial Campus Box 8601, Raleigh, NC		10. Work Unit No.	
		11. Contract or Grant No. NCDOT Project 2020-30	
12. Sponsoring Agency Name and Address North Carolina Department of Transportation Research and Analysis Group, 104 Fayetteville Street Raleigh, North Carolina 27601		13. Type of Report and Period Covered Draft Final Report, August 2019- January 2022	
		14. Sponsoring Agency Code NCDOT/NC/2020-30	
15. Supplementary Notes: In cooperation with the U.S. DOT and Federal Highway Administration.			
16. Abstract: This report summarizes the findings of a research project aimed at assessing the accuracy of both analytical and microsimulation tools in describing the operational performance of a variety of intersection and interchange types under North Carolina conditions. The three tools evaluated in this study were SYNCHRO10, SIDRA9 and Trans Modeler5. In addition, some basic comparisons with the FHWA CAP-X sketch planning tool was carried out for some sites. The original, Pre-Covid scope of work was to cover ten congested interrupted flow facilities in the field. The revised scope reduced the field effort to six sites, including an isolated and coordinated signalized intersection; a single lane roundabout; a traditional diamond interchange; an offset intersection and a continuous flow intersection with an additional two alternative intersection (AI) sites (Diverging Diamond Interchange and a Reduced Conflict Intersection) processed via a sensitivity analysis to variations in demand volumes, capacity and control conditions. The team carried out all fieldwork using high-resolution videos taken from one or two drones at a height of 300-400 ft., supplemented with ground based cameras and Blue Tooth units as needed. All video data were then post-processed via a third party vendor, Data From Sky (DFS). The processed videos enabled the team to generate individual vehicle ID's and their position, in the field of view. Subsequently the field data produced multiple performance measures at the point, segment and facility levels. Five of the field sites, located in five different NC counties, involved signalized intersections. Measurements of saturation flow rates at those sites produced values that were below expectations, in the range of 1,520-1,770 pc/hr./lane. This is likely to be generating lower movement capacities than are currently being assumed in NC modeling studies. These rates were needed for model calibration in this study for both Synchro and SIDRA. In the case of Trans Modeler microsimulation, saturation flow rates are entered using a headway buffer parameter. The research has developed a graphical plot relating the buffer value and saturation flow rate, which can be used to calibrate the input for a specific saturation flow rate value. In general, when field conditions were operating in the LOS range A-C, all three models generated performance measures (PMs) that were close to each other and to the field value. However, under congested conditions, the analytical models tended to overestimate the field PMs, while the microsimulation model tended to slightly underestimate them. Part of the problem is related to the presence of initial and final queues in estimating the true traffic demand volumes (as opposed to the discharge flow rate in traditional traffic counts). The team recommends the use of a microsimulation model in those cases, with due attention to including the initial queue effects on delays. Another limitation discovered in both SIDRA and SYNCHRO (and HCM6) was their inability to generate correct Origin Destination based LOS measures in the field at both the CFI and offset intersections. The team was able to generate an alternative analytical approach that was validated at both those sites. Finally, the team also developed a new methodology for the field estimation of the critical headway value for roundabouts in Trans Modeler, which is explained in detail in Chapter 4 of this report. Additional work is needed to further develop the analytical approach for application to all alternative intersection cases.			
17. Key Words SYNCHRO, Trans Modeler, SIDRA, Calibration, Validation		18. Distribution Statement: Unlimited	
19. Security Classification (this report): Unclassified	20. Security Classification Unclassified	21. No. Pages: 122	22. Price
Form DOT F 1700.7 (8-72)		Reproduction of completed page authorized	

DISCLAIMER

The contents of this report reflect the views of the author(s) and not necessarily the views of the University. The author(s) are responsible for the facts and the accuracy of the data presented herein. The contents do not necessarily reflect the official views or policies of either the North Carolina Department of Transportation or the Federal Highway Administration at the time of publication. This report does not constitute a standard, specification, or regulation.

ACKNOWLEDGEMENTS

The research team acknowledges the North Carolina Department of Transportation for supporting and funding this project. We extend our thanks to the project Steering and Implementation Committee: Mike Reese, Jim Dunlop, David Olsen, Joseph Hummer, and Matthew Carlisle. Many thanks also to our R&A project coordinator Dr. Stephanie Bolyard.

EXECUTIVE SUMMARY

The state of North Carolina continues to experience significant growth both in terms of its population and levels of economic growth. The transportation infrastructure must be able to accommodate both mobility needs, especially in the highway sector where travel demands continues to outpace all other modes. Decisions on what type of highway improvements are necessary and cost effective will often rely on traffic models to estimate the benefits and costs of such improvements. Thus, testing the ability of these models to reflect real-world field observations is an important task that NCDOT has recognized and initiated. This research represents one important step in that direction.

The scope of this research focused on two analytical traffic models and a microsimulation model that are currently used for congestion management purposes at NCDOT. These include Synchro (Version 10), SIDRA (version 9) and Trans Modeler (Version 5) respectively. The original scope of work at the outset was to collect field data at 10 sites. Due Covid-19 travel and traffic impacts, the team was forced to reduce that number to 6 sites, along with two additional sites where only model sensitivities were tested. Sites included two signalized intersections, an offset intersection, a roundabout, a traditional diamond interchange, a continuous flow intersection, a diverging diamond interchange and a reduced conflict intersection. In addition, some limited comparisons with the FHWA CAP-X sketch planning approach were also carried out.

In general, the field observations indicated that both analytical and microsimulation models yielded very similar results (within one LOS range) to each other and to the field data, when the facility was operating at acceptable levels of service, say A to C. Under congested conditions, however, the analytical models tended to overestimate delays and travel times, while the simulation model slightly under-predicted the same. One issue with all three models tested is whether they could correctly account for the effect of initial and final queues during the congested periods. This research has proposed a method to account for those effects. Another possible contributing factor to congestion is the general finding regarding measured saturation flow rates, which in this study ranged from 1550-1800, with only one observation across all sites yielding a value above 1,800 pc/hr./lane. This is despite the fact that data were collected in five different NC counties, and with presumably differing population factors.

Two additional key contributions from this research include: (a) a method to field calibrate the critical headway in Trans Modeler to estimate roundabout capacity, and (b) an alternative analytical approach to estimating delays at facilities with multiple intersections (RCI, CFI, Offset, MUT, etc.). The proposed analytical approach addresses a key deficiency in both Sidra and Synchro which tended to overestimate delays by a significant margin at both the offset and CFI sites in the field. The research also generated a simple graphical plot relating the “headway buffer” in Trans Modeler to the resulting saturation flow rate. This will enable modeler to pick the correct buffer value associated with their preferred saturation flow rate input.

Table of Contents

1	Chapter 1: Introduction.....	11
1.1	Project Objectives	11
1.2	Project Scope.....	12
1.3	Scope Reduction due to COVID-19.....	12
1.4	Project Tasks	13
1.5	Report Organization	13
2	Chapter 2: Literature Review	15
2.1	Existing Selection Methods.....	16
2.2	Performance Measure Comparison	17
2.3	Simulation Verification, Validation, and Calibration	18
2.4	Details about Specific Tools	20
2.5	Conclusion.....	21
3	Chapter 3: Isolated Signalized Intersection	22
3.1	Site Description	22
3.2	Data Collection and Extraction Method.....	22
3.2.1	Data Collection	22
3.2.2	Demand Volume Extraction	24
3.2.3	Signal Timing Extraction.....	24
3.3	Field Performance Measures	25
3.4	Models' Testing and Calibration.....	26
3.5	Model Validation.....	28
3.6	Summary and Discussion.....	29
4	Chapter 4: Single Lane Roundabout.....	31
4.1	Site Description	31
4.2	Data Collection and Extraction Method.....	32
4.3	Field Performance Measures	33
4.4	Models' Testing and Calibration.....	34
4.5	Models' Validation.....	37
4.6	Summary and Discussion.....	38
5	Chapter 5: Coordinated Signalized Intersection	40
5.1	Site Description	40

5.2	Data Collection and Extraction Method.....	41
5.2.1	Data Collection	41
5.2.2	Demand Volume Extraction	43
5.2.3	Signal Timing Extraction.....	44
5.2.4	Field Performance Measures.....	44
5.3	Model Testing and Calibration.....	46
5.4	Model Validation.....	47
5.5	Summary and Discussion.....	49
6	Chapter 6: Offset Intersection.....	51
6.1	Site Description	51
6.2	Data Collection and Extraction	52
6.2.1	Data Collection	52
6.2.2	Demand Volume Extraction	53
6.2.3	Signal Data Extraction	53
6.2.4	Field Performance Measures.....	54
6.3	Models' Testing and Calibration.....	55
6.4	Model Validation.....	56
6.5	Summary and Discussion.....	57
7	Chapter 7: Continuous Flow Intersection.....	59
7.1	Site Description	59
7.2	Data Collection and Extraction	60
7.2.1	Data Collection	60
7.2.2	Demand Volume Extraction	61
7.2.3	Signal Data Extraction	62
7.2.4	Field Performance Measures.....	62
7.3	Models' Testing and Calibration.....	63
7.4	Model Validation.....	64
7.5	Addressing the Limitations of Analytical Models at CFI's	64
7.6	Summary and Discussion.....	67
8	Chapter 8: Traditional Diamond Interchange.....	69
8.1	Site Description	69
8.2	Data Collection and Extraction	70
8.2.1	Data Collection	70

8.2.2	Demand Volume Extraction	71
8.2.3	Signal Data Extraction	72
8.2.4	Field Performance Measures.....	73
8.3	Models' Testing and Calibration.....	74
8.4	Model Validation.....	74
8.5	Summary and Discussion.....	76
9	Chapter 9: Critical Movement Analysis and CAP-X	78
9.1	Isolated Signalized Intersection in Chapter 3.....	78
9.2	Single Lane Roundabout in Chapter 4	81
9.3	Coordinated Signalized Intersection in Chapter 5.....	85
9.4	Offset Intersection in Chapter 6	88
9.5	Continuous Flow Intersection in Chapter 7.....	92
9.6	Traditional Diamond Interchange in Chapter 8.....	94
9.7	Summary of Results	96
10	Chapter 10: Sensitivity Analysis.....	98
10.1	RCI Analysis	99
10.2	Findings.....	100
10.3	DDI Analysis.....	106
10.4	Findings.....	107
10.5	Summary and Conclusions.....	111
11	Chapter 11 Summary, Conclusions and Guidance	113
11.1	Summary and Conclusions.....	113
11.2	General Guidance.....	117
11.3	Model Use Guidance.....	118

List of Figures

Figure 2-1: Verification, Validation and Calibration Method Source: Park (15).....	20
Figure 3-1: Location of Isolated Intersection at NC50 and NC-42	22
Figure 3-2: Geometric Layout of NC-50 and NC-42.....	23
Figure 3-3: Processed Drone Video Showing Vehicle ID's and Sensor Locations.....	23
Figure 3-4: Travel Time for SB-TH Vehicles by Arrival Time at Upstream Sensor	26
Figure 3-5: Sample Headway Buffer vs. Saturation Flow Rate.....	27
Figure 3-6: Time in System Comparisons for Video 2.....	29
Figure 3-7: Control Delay Components: SYNCHRO vs. SIDRA	29
Figure 4-1: Location of the single lane roundabout site	31
Figure 4-2: Roundabout Geometric Layout.....	31
Figure 4-3: Screenshot of drone video at the roundabout.....	32
Figure 4-4: Critical headway definition using the conflict zone concept	35
Figure 4-5: SIDRA9 vs Field Average Travel Speeds for (a) SB and (b) EB Approaches	37
Figure 4-6: TransModeler vs Field Average Travel Speeds for (a) SB and (b) EB Approaches .	38
Figure 5-1: Aerial View of Oleander Dr. and S. College Rd. Intersection.....	40
Figure 5-2: Geometric Layout of Oleander Dr. and S. College Rd.	41
Figure 5-3: Drone's Flight Sequence	42
Figure 5-4: Processed Drone Video for Oleander Dr. and S. College Rd Showing Vehicle ID's and Entry and Exit Sensor Locations for EB-TH and EB-L Movements.....	43
Figure 5-5: Travel Time for EB-TH and EB-LT Vehicles by Arrival Time at Upstream Sensor	46
Figure 5-6: Time in System for EB Through at Oleander Dr. and S. College Rd. Intersection...	48
Figure 5-7: Components of time-in-system for EB approach at Oleander Dr. and S. College Rd. intersection.....	49
Figure 6-1: Plan View of Offset Intersection at Capital, Highwoods and Westinghouse Blvd....	51
Figure 6-2: Geometric Layout of the Offset Intersection	52
Figure 6-3: DFS Processed Screenshot of Offset Intersection with Vehicle Trajectory IDs, OD Labels and Location of Virtual Sensors.....	52
Figure 6-4: Signal Phasing Plan at the Offset Intersection	54
Figure 6-5: Travel Time Profiles for (a) EB-TH and (b) SB-L Movements at Offset Intersection	55
Figure 6-6: Initial Model Validation Results at the Offset Intersection	56
Figure 6-7: Validation Results Post Recalibration of SIDRA Model.....	57
Figure 7-1: Plan view of Continuous Flow Intersection NC 16 and Mt Holly-Huntersville Rd..	59
Figure 7-2: Geometric Layout of the CFI at NC 16 and Mt Holly-Huntersville Rd	60
Figure 7-3: DFS Processed Screenshot of a) Main Intersection and b) North Westbound Intersection at NC 16 and Mt Holly-Huntersville Rd along with trajectory IDs and Location of Travel Time Sensors	61
Figure 7-4: Signal Phasing Plan for Main and North Westbound Intersections of CFI	62
Figure 7-5: Travel Time Profiles for (a) WB TH and (b) WB LT Movements in Upstream Section and for (c) WB TH and (d) WB LT Movements in Downstream Section.....	63
Figure 7-6: Model Validation Results for the two movements on the Westbound Approach.....	64

Figure 7-7: Arrival and Departure Flows for the WB-LT Movement Intersection of Brookshire and Mount Holly CFI..... 66

Figure 8-1: Plan View of Traditional Diamond Interchange at I-85 and NC 86 with Indicated Origin and Destination Labels 69

Figure 8-2: Geometric Layout of the I-85 and NC 86 Interchange 70

Figure 8-3: DFS Processed Screenshot of the North Intersection on NC86 and I-85 along With Trajectory IDs and Location of Travel Time Sensors 71

Figure 8-4: Signal Phasing Plan at the Offset Intersection 72

Figure 8-5:: Travel Time Profiles for (a) SB-TH, (b) SB-R and (c) WB-L Movements at the North Intersection 73

Figure 8-6: Model Validation Results at North Intersection by Turning Movement 75

Figure 8-7: Model Validation Results Based on NB and SB Route Travel Time 76

Figure 9-1: Isolated Signalized Intersection CAP-X Outputs..... 79

Figure 9-2: Isolated Signalized Intersection CAP-X Inputs 80

Figure 9-3: Single Lane Roundabout CAP-X Results 82

Figure 9-4: Single Lane Roundabout CAP-X Inputs 83

Figure 9-5: 1x2 Roundabout CAP-X Results 84

Figure 9-6: 1x2 Roundabout CAP-X Inputs 85

Figure 9-7: Coordinated Signalized Intersection CAP-X Results 86

Figure 9-8: Coordinated Signalized Intersection CAP-X Inputs 87

Figure 9-9: Offset Intersection First Zone CAP-X Results 89

Figure 9-10: Offset Intersection First Zone CAP-X Inputs 90

Figure 9-11: Offset Intersection Second Zone CAP-X Results 91

Figure 9-12: Offset Intersection Second Zone CAP-X Inputs..... 92

Figure 9-13: Continuous Flow Intersection CAP-X Results 93

Figure 9-14: Continuous Flow Intersection CAP-X Inputs 94

Figure 9-15: Traditional Diamond Interchange CAP-X Inputs and Results..... 95

Figure 10-1: Reduced Conflict Intersection / NC-55 & Holly Springs Road / New Hill Road / 35°39'27.86"N / 78°50'54.99"W 99

Figure 10-2: Aerial View of the Diverging Diamond Interchange on US-17 (and US-74 and US-76) at Village Road / River Road in Leland, NC 107

List of Tables

Table 1-1 Intersection and Interchange and Tools Considered at Project Inception	12
Table 2-1 Summary Table of Each Simulation Tool Type.....	16
Table 2-2 Interpretations of Measures of Effectiveness for Micro- and Macroscopic Models	18
Table 3-1: Demand Volume Estimation at NC-50 and NC-42.....	24
Table 3-2: Average Phase Duration during Data Collection	25
Table 3-3: Field Measurements of Key Movement Performance Measures	25
Table 3-4: Field Observations of Saturation Flow Rate	27
Table 3-5: Time in System Comparisons: Field vs. Models for NC50 SB Movements.....	28
Table 4-1: Estimated Demand Volumes by Turning Movement at the Roundabout	33
Table 4-2: Movement-based field observations.....	34
Table 4-3: Estimates of Gap Acceptance Parameters by Model and Calibration Method *	36
Table 5-1: Demand Volume Estimation at Oleander Dr. and S. College Rd.	44
Table 5-2: Average Phase Duration during Data Collection	44
Table 5-3: Field Measurements of Key Movement Performance Measures	45
Table 5-4: Field Observations of Saturation Flow Rate	46
Table 5-5: Time in System Comparisons: Field vs. Models for Oleander Dr. EB Movements ...	48
Table 6-1: Estimated Demand Flow Rates at the Two Offset Intersections.....	53
Table 6-2: Origin Destination Hourly Demands at Offset Intersection.....	53
Table 6-3: Field Saturation Flow Rates by Movement.....	56
Table 7-1: Estimated Demand Flow Rate at the Intersection	62
Table 7-2: Proposed Travel Time Estimation Method for WB-L Traffic at Main Intersection ...	66
Table 8-1: Estimated Demand Flow Rates at the Two Intersections.....	71
Table 8-2: Origin Destination Hourly Demands at Interchange.....	72
Table 8-3: Calibrated Entry, Negotiating and Exit Speeds for Key Movements.....	74
Table 9-1: CAPX vs. Models Comparison Table- Intersection Level Performance	97
Table 10-1: Saturation Flow Rates Per Lane / NC-55 & Holly Springs Road / New Hill Road	100
Table 10-2: Differences in the Saturation Flow Rates / TransModeler versus Synchro / NC-55 & Holly Springs Road / New Hill Road	101
Table 10-3: Displayed Greens by Scenario / NC-55 & Holly Springs Road / New Hill Road ..	102
Table 10-4: Differences in Displayed Greens / TransModeler versus Synchro / NC-55 & Holly Springs Road / New Hill Road.....	102
Table 10-5: V/C Ratios by Scenario / NC-55 & Holly Springs Road / New Hill Road.....	103
Table 10-6: Differences in V/C Ratios / TransModeler versus Synchro / NC-55 & Holly Springs Road / New Hill Road.....	103
Table 10-7: “Maximum” Queue Length / NC-55 & Holly Springs Road / New Hill Road.....	104
Table 10-8: Differences in “Maximum” Queue Length / NC-55 & Holly Springs Road / New Hill Road.....	104
Table 10-9: Queue Capacity Utilization / NC-55 & Holly Springs Road / New Hill Road.....	105
Table 10-10: Differences in Queue Capacity Utilization / NC-55 & Holly Springs Rd / New Hill Rd.....	105
Table 10-11: Average Delay Sensitivities / NC-55 & Holly Springs Road / New Hill Road	106

Table 10-12: Differences in Average Delays / NC-55 & Holly Springs Road / New Hill Road	106
Table 10-13: Displayed Greens by Scenario / US-17 at Village Road / River Road	108
Table 10-14: V/C Ratios by Scenario / US-17 at Village Road / River Road	109
Table 10-15: Queue Length Sensitivities / US-17 at Village Road / River Road.....	109
Table 10-16: Queue Capacity Utilization / US-17 at Village Road / River Road	110
Table 10-17: Average Delay Sensitivities / US-17 at Village Road / River Road	111
Table 11-1: Summary of Model Assessment Results	116

1 Chapter 1: Introduction

The past couple of decades have seen an increasing amount of diversity in intersection and interchange designs, exemplified by the proliferation of roundabouts and “alternative intersections” (such as the Reduced Conflict Intersection (RCI), Diverging Diamond Interchange (DDI) and Continuous Flow Intersection (CFI))at both the state and national levels. Specifically, the North Carolina Department of Transportation has been a leader in implementing several innovative intersection solutions to handle the ever increasing demand in many of the state urban and suburban centers.

Thus the need for reliable traffic analysis tools to assess current intersection operations, and to predict future performance cannot be overstated. For example, transportation and traffic models are currently being used in the state project prioritization process. In addition, many states that already have or plan to develop an ICE (Intersection Control Evaluation) process must rely on some type of analytical or simulation tool to determine the most optimal type of control across multiple alternatives. Generally speaking, users have access to three classes of modeling approaches. These include sketch planning approaches (e.g. CAPX, VJUST, and HCM Planning and Preliminary Engineering Method), analytical models (e.g. HCM6, SIDRA and SYNCHRO) and microsimulation models (e.g. SIMTRAFFIC, VISSIM and TransModeler).

The selected modeling approach must have the appropriate sensitivities to issues and options of concern to the analyst. For example, micro simulation may be the best (or the only) choice when the complexity of the interactions within the system exceeds the ability of available analytic approaches to obtain a solution. The main theme is that the analyst should use simulation whenever it improves the accuracy of the predicted performance. Often, this is because the interactions between system parts are too complex to study analytically; or the cascading effects of varying demand across time cannot be addressed analytically. The reverse comment pertains to analytical approaches: there is no need for simulation if the system parts are operating independently and/or the phenomena are not complex. Data availability is also essential. The inputs must be available to make the simulation-based analysis possible. Additionally, each modeling approach may be utilized at different stages of the planning and design lifecycle of a project. At the end, however, the overarching question remains: to what extent are the various modeling approaches accurate, when compared to field observations, and under which classes of intersection designs and traffic loadings? That is the core need for the research that this report aspires to answer.

1.1 Project Objectives

The objectives of this study can be summarized as follows:

- 1) Document differences between traffic analysis tools as it relates to each phase of a project’s lifecycle, including conditions such as location (urban vs. rural), under vs. oversaturated traffic state and duration of the analysis period
- 2) Test a subset of tools utilizing previous NCDOT Congestion Management Projects, and
- 3) Develop recommendations for incorporation of the findings of the tool testing.

A note regarding model validation and performance measures: in this report, travel time or time in the system was used as the performance measure. This was done to avoid the issue of having to assume an approach and exit speeds that were equivalent to the speed limit, since in most cases that assumption was not borne by the field data. In addition, the team refrained from using statistical tests to compare the model performance measures against field data. This was primarily to overcome the issues of large sample size that tend to produce outcomes of significance, even when the practical differences between field and model predictions are small. Secondly, as level of service (LOS) uses ranges of performance metrics (for example control delay at signals), it made sense to assess the differences from a practical standpoint, for example at the same or within one LOS range.

1.2 Project Scope

The scope of this research is limited both in terms of the variety of intersection designs and controls, as well as the diversity in the analysis tools being considered. Our initial approach, subsequent to the recommendations from the project StIC committee at the project kickoff meeting, was to focus on tools that are routinely used by the NCDOT Congestion Management Unit, as well as on a variety of designs both traditional and alternative. The tools tested in this project were CAPX, SYNCHRO 10, SIDRA9 and TransModeler 5. Not all the tools were tested on all intersections. Table 1-1 shows the scope of analyses that were agreed upon at the start of the project in August 2019.

Table 1-1 Intersection and Interchange and Tools Considered at Project Inception

Intersection / Interchange Type	CAP-X	SYNCHRO 10	SIDRA9	TransModeler 5
Isolated Signal				
Coordinated Signal				
Signalized Arterial				
Single Lane Roundabout				
Multilane Roundabout				
Reduced Conflict Intersection				
Offset Intersection				
Traditional Diamond Interchange				
Continuous Flow Intersection				
Diverging Diamond Interchange				

■ Field data collected ■ Model Sensitivity analysis

1.3 Scope Reduction due to COVID-19

The original project schedule called for Task 4 on “*Field and Project Data Collection*” to take place in the period from April through October 2020. This timeline coincided with the worse period of the COVID-19 pandemic, paralyzing both our data collection capabilities, and also impacting the normal traffic demand due to the various lockdown experienced during the core pandemic period. As a result, the team presented to the StIC several options ranging from full field data collection, to a hybrid data collection including limited site data

collection, and sensitivity analysis for others, to no field data collection and reliance on model sensitivity analysis.

Fortunately, after considerable delays, the research team was able to collect field data at six of the sites depicted in Table 1-1. Those are highlighted in the darker color. We were also able to conduct sensitivity analysis for two sites namely an RCI and a DDI and have included an assessment of the SIDRA model in most of the sites where we had field data. All in all, the team believes that sufficient field data has been collected, extracted and analyzed across models to enable us to meet the original project objectives.

1.4 Project Tasks

For the purpose of documentation, the original proposal listed 8 project tasks as follows:

Task 1: Kickoff Meeting

Task 2: Literature Review

Task 3: Develop Analysis Framework & Data Collection Plan

Task 4: Field and Project Data Collection

Task 5: Perform Analyses on the Tools

Task 6: Conduct Assessment, Comparison and Validation across the Tools

Task 7: Develop Recommendations for the Optimal Use of the Tools

Task 8: Develop Final Report

1.5 Report Organization

This research report is organized in a manner very similar to the layout in Table 1-1. Since the objective is to be able to compare across models and design types, we have dedicated a separate chapter for each intersection or interchange type, in order to ascertain which (if any) modeling approach best fits the observed field performance and under what conditions. This format allows for direct comparison of model performance for a given geometry and traffic condition rather than grouping all results of a model type separately. In order to ensure a fair comparison across models, the research team ensures that all models were properly calibrated prior to comparing performance. This will become evident to the reader of the intersection chapters. Below are the report chapters following this Chapter 1, Introduction.

Chapter 2 presents the **literature review** focused models, their calibration and validation.

Chapter 3 describes the site, data, models and findings for the **Isolated Signalized Intersection** at NC50 and NC42 in Johnston County.

Chapter 4 describes the site, data, models and findings for the **Single Lane Roundabout** at Pullen and Stinson in Wake County

Chapter 5 describes the site, data, models and findings for the **Coordinated Signalized Intersection** at College and Oleander Rd in New Hanover County.

Chapter 6 describes the site, data, models and findings for **the Offset Intersection** at Capital Blvd. and Highwood and Westinghouse in Wake County

Chapter 7 describes the site, data, models and findings for the **Continuous Flow Intersection** at Brookshire and Mount Holly/ Huntersville Rd in Mecklenburg County

Chapter 8 describes the site, data, models and findings for the **Traditional Diamond Interchange** at I-85 and NC-86 in Orange County

Chapter 9 provides an overall intersection or network comparison across models using the **CAP-X tool**

Chapter 10 summarizes the **SYNCRHO and TransModeler** Sensitivities for the **Reduced Conflict Intersection (RCI) and the Diverging Diamond Interchange (DDI)**.

Chapter 11 concludes the report and provide guidance for the optimal use of the tools considered in this research

2 Chapter 2: Literature Review

Given the focus of the project, this literature review focuses on tools that are used when examining intersections for geometric enhancements or operational changes. It also compares the “advantages” of using simulation with the “expedience” of using analytical methods. From NCDOT’s perspective, TransModeler is the simulation model of choice; so, it is contrasted with three analytical options: Cap-X, Synchro, and Sidra. The literature review also focuses on prior studies where the intent was to provide guidance about tool selection. Supportive, but of secondary importance, is an examination of the differences that exist between simulation- and analytically based approaches for such assessments.

In general, the tools available for analyzing “intersection performance” fall into one of the following categories, as described by the Traffic Analysis Toolbox Volume I: Traffic Analysis Tools Primer (1):

- 1) Sketch-planning tools
- 2) Travel demand models
- 3) Analytical/deterministic tools (HCM-based)
- 4) Traffic signal optimization tools
- 5) Microscopic simulation models
- 6) Mesoscopic simulation models
- 7) Macroscopic simulation models

The three that are most often used for traffic operational assessment are options 3, 5, and 7. The analytical/deterministic tools use equations and/or logic to derive performance results from specified inputs. The inputs are typically movement-specific demand volumes, geometric configurations of the approaches, and average values for signal cycle lengths and splits. The outputs are v/c (volume-to-capacity) ratios, delays, and queue lengths. In contrast, micro- and macroscopic simulation tools emulate the movement of vehicles in time and space, through a network, to develop an assessment of the system’s performance. They both use inputs about the system geometry, the temporal and spatial varying demands, and the signal control to specify the configuration of the systems, the inputs to which it is subjected, and how its operation is controlled. The difference lies in the level of detail provided. It is more detailed for microscopic models and less detailed for macroscopic ones.

For example, microscopic models use path specific, time varying average headways (input as flow rates) and headway distribution functions to generate vehicle arrival sequences. Macroscopic models use path specific, time varying flow rates and speed-volume-density relationships by segment to predict how those flow rates will cascade through the network. In both cases the models perform time- and/or event-based simulations of the movement of the vehicles through the system to create time- and location-based assessments of system performance. Generally, macroscopic models generate these outputs in a “broad brush” manner, focusing on flow rates, speeds, and densities, among adjacent system segments; while

microscopic models predict the trajectories of individual vehicles, in space and time, including, importantly, their interactions. Table 2-1 shows the differences between the macroscopic and microscopic options and lists several “software” examples of each (1). As can be seen, while macroscopic models use aggregated data, the microscopic models need more detailed information such as individual vehicle reaction times, car-following model parameters, and so on. Thus, microsimulation models are more time-consuming to employ. (2) However, they can provide more accurate results. Hence, this issue of selecting a tool to use is very important.

Table 2-1 Summary Table of Each Simulation Tool Type

Type	Macroscopic	Microscopic
Description	Based on the deterministic relationships of flow, speed, and density of the traffic stream.	Based on car-following and lane-change theory, individual vehicles are stochastically simulated.
Data Requirements	Relatively low	High
Time and Cost Effort	Relatively low	High
Level of Analysis	Planning, Preliminary Engineering, Design, Operation	Preliminary Engineering, Design, Operation
Examples	HCS, SIDRA, Synchro, VISTRO, Cap-X	Trans Modeler, VISSIM, CORSIM, Simtraffic

2.1 Existing Selection Methods

Selection methods in the existing literature (3, 4, 5, 6) appear aimed at having the analyst consider analytical tools first, followed by simulation (of either type). Also, between the two simulation options, a macroscopic model should be considered before using a microscopic one. This logic for this guidance is predicated on the increasing levels of data required, cost-intensity, and time-intensity. Two factors are often mentioned that encourage the analyst to do the selection in the opposite direction (micro-> macro -> analytical): 1) the existence of rapidly changing conditions (during the timeframe of interest, as in significant variations in the demands) and 2) the presence of “system effects” where the operation of one facility (intersection) has impacts on the operation of other facilities (e.g., closely spaced intersections where queues can spill back). Caltrans’ guidelines (3) list the following situations where microsimulation is seen to be the more appropriate tool to employ:

- Conditions that violate one or more basic assumptions of independence required by the analytical methods.
- The presence of physical conditions that are not covered well by the analytical method.
- Congestion that already exists at the beginning of the analysis period.
- Options are to be tested that involve changes in vehicle characteristics and/or driver behavior.

USDOT (4) has a spreadsheet-based method to select the appropriate type of tool. It involves several steps and uses scores for various criteria. Each criterion relates to the level of analysis scope, the facility type, the travel modes involved, the purpose of the analysis, and the performance measures of interest.

Several states have similar selection processes. For example, PennDOT [Pennsylvania] (7) uses the USDOT spreadsheet. It advises that, with the suggested tool type, a specific tool package should then be selected from those “authorized for use” by the state. ODOT [Oregon] (8) also uses the USDOT tool selection spreadsheet. However, it uses some additional questions to determine whether microsimulation is more appropriate or not. FDOT (5) has a simulation selection guideline that bases the choice on the facility, level of analysis, project need, and performance MOE based on their specific available simulation tool. This guidance suggests a specific tool based on tool characteristics and model outputs. VDOT (6) has created similar guidance. VDOT again focuses on tool selection driven by the purpose of the analysis. This also includes a description of each available simulation, calibration method, and traffic operations analysis tool selection matrix for specific analysis tool selection by type of facilities and traffic condition. Steven and Roupail (9) have provided NCDOT with guidance on appropriate tool selection for specific types of analyses. They evaluate various macroscopic simulation tool packages for signalized intersection analysis. Consequently, they develop recommendations for given traffic and geometric condition for NCDOT.

In the more general published literature, Fang and Elefteriadou (10) present guidelines for selecting a microsimulation tool depending on the characteristics of the interchange being studied (not necessarily intersections). They review AIMSUN, CORSIM, and VISSIM and identify each simulation program’s characteristics and limitations when traditional diamond interchange and single point interchange are to be assessed. Through delay comparisons of simulator outputs and field measurements, they conclude that the capability of simulating a given signal operation and MOE definitions provided in a simulator are critical considerations for selecting a simulation package for an interchange assessment.

Inherently, these selection guidelines are dependent upon and limited by the types of analysis tools available. They also make strong assumptions about the capabilities of the various tools. For example, the USDOT worksheet assumes every simulation model provides similar accuracy; and that the user (model chooser) has familiarity with and fluency in all the tools. This can lead to inappropriate tool selection. More generally, the selection guidelines do not consider whether the tool (model) can provide a sense of whether there are “errors” in the analysis caused by the limitations of the tool.

2.2 Performance Measure Comparison

The target MOEs which comprehensively represent traffic conditions should be considered carefully. Commonly used MOEs are described in the Traffic Analysis Toolbox, Volume VI: Definition, Interpretation, and Calculation of Traffic Analysis Tools Measures of Effectiveness. (11) The metrics mentioned are travel time, speed, delay, queues, stops, density, and travel-time variance. These MOEs are commonly recommended for tool evaluation because they are not only currently most used by public agencies to monitor the traffic performance but also can be used to derive other performance measures.

Another MOE that is often used is efficiency. Brilon (12) suggests “efficiency” as a performance measure. He optimizes this efficiency for interrupted and uninterrupted flow facilities to minimize economic loss. He defines the point that maximizes the economic benefit as being the appropriate threshold for differentiating between LOS D and E. In addition, he suggests expanding the assessment to a yearly basis to improve the defensibility of the results compared with the current hourly-based evaluation.

One challenge that is difficult to “overcome” is that the tools derive their performance metrics through very different methods. For example, they can all estimate “delay”, but how that is done differs among the methods, and even among “packages” that use the same method. A comparison of outputs from simulation tools should be cautious since some definitions of performance measure and output forms are different. (These comments are setting aside the issue about how the performance measurement definitions are different from field measurements. Users should review the user guide for the software employed before doing direct comparisons.) The Traffic Analysis Toolbox Volume III: Guidelines for Applying Traffic Microsimulation Modeling Software (13) briefly explains how the definitions are different between types of simulation when some performance measures are compared. Therefore, outputs from simulations should be adjusted to field measurement definitions.

Even if the comparison is between macroscopic simulations, adjustments can be required because each simulation can provide a different output format. Table 2-2 provides interpretations of three measures of effectiveness for macro- and microscopic models.

Table 2-2 Interpretations of Measures of Effectiveness for Micro- and Macroscopic Models

Type	Macroscopic	Microscopic
Delay/ LOS	<ul style="list-style-type: none"> • Calculates mean control delay for 15-min period within the hour. • Based on the signal approach. 	<ul style="list-style-type: none"> • Computes a control delay different for each run. • Based on the segment.
Density	<ul style="list-style-type: none"> • The unit of density is passenger car per mile. 	<ul style="list-style-type: none"> • The unit is vehicle per mile.
Queue	<ul style="list-style-type: none"> • Slow moving vehicles joining the rear of the queue are considered part of the queue 	<ul style="list-style-type: none"> • Slow moving vehicles and vehicles waiting to be served are not distinguished.

For example, SIDRA provides lane-by-lane outputs; but Synchro (and other, similar HCM-based procedures) provides outputs by lane group. This generates a need to post-process the results to ensure “eggs versus eggs” comparisons. In addition, some specific MOEs should be derived by available outputs for comparison because each simulation produces different outputs.

2.3 Simulation Verification, Validation, and Calibration

Since the analytical models are “top-down” and “equation-based”, their “verification” relates whether the equations being used by the model capture the cause-effect relationships extant in the situation(s) being examined. In the case of the HCM-based procedures, the model has been “calibrated” based on empirical data, and it has been validated through field studies. The

“calibration” issues relate to parameter values such as saturation flow rates, lost start-up time, “sneakers”, impacts of actuated control, and percent traffic arrivals on green.

Simulation-based models are more complicated. They are “bottom-up” assessment tools and derive their outputs based on “simulating” the way in which the system “behaves”. Verification, validation, and calibration are all important. The three steps are critical for modeler users regardless of the type of simulation tools used. Rakha, et al. (14) provide definitions of these ideas that are particularly useful:

- *Verification*: can the simulation program produce the desired output and it is correctly coded in the simulation program?
- *Calibration*: can the model “correctly” predict observed traffic conditions based on the parameter values that have been specified?
- *Validation*: can the model generally produce defensible results for a variety of situations?

Although Rakha, et al. (14) define verification and validation as being the responsibility of the model developer, simulation users must address these issues as well. Users must verify that their chosen simulation model can provide the desired output, and they must check that it is coded correctly. Park (15) defines this as testing the validity of the calibrated parameters with a dataset that is not used for calibration. Validation means checking the calibrated parameters. Most user manuals indicate how their model is to be verified and validated. In addition, these documents also provide definitions of the parameters employed and default values.

In practice, users of traffic analysis tools often encounter difficulty in collecting data for the model parameters. Particularly, data observation is harder when they elect to use microscopic simulation. This often leads to extensive use of default values without checking. However, it can be hard to reflect real local conditions because the defaults are based on countrywide observations. Thus, calibration and validation should be carried out for a reliable and credible result. Park (15) suggests the flow chart shown in Figure 2-1 for the calibration and validation process in the case of a microscopic simulation model.

Calibration is the process in which the best set of key parameters are found that allow the model to match a set of field measurements such as traffic volume, travel times, average speeds, and average delays. For example, if average travel time is the performance measure, lane-change distances, waiting times before diffusion, minimum headway, and so on could be key parameters and the estimated performance measure from a set of these parameters are compared to field measurement for validation until finding the best set of parameters. This iterative process helps ensure that credible outputs will be obtained

Calibration and validation techniques have been developed for specific models and facility types. For example, for roundabouts, Gagnon et al. (16) examine calibration options for popular macroscopic (SIDRA and RODEL) and microsimulation (PARAMICS, SimTraffic, and VISSIM) models. Li et al. (17) describe a VISSIM-specific roundabout calibration method. Chun et al. (18) indicate that definition of key parameters varies depending on the class of tools and describes appropriate way to estimate them.

Giuffrè et al. (19) present a calibration method for roundabout models using a genetic algorithm approach. For signalized intersections, Mathew and Radhakrishnan (20) describe how the static and dynamic characteristics of different vehicles should be considered in the calibration process. Bhattacharyya et al. (21) show how travel time distributions should be employed. Schroeder et al. (22) discuss the challenges of calibrating models of double-crossover diamond (DCD) interchanges. They observe that using queue length as a performance measure for model validation tends to be challenging, since there are definitional differences between simulated and field observed queues. Guo et al. (23) present a technique based on extreme value theory to calibrate models of signalized intersections in VISSIM.

2.4 Details about Specific Tools

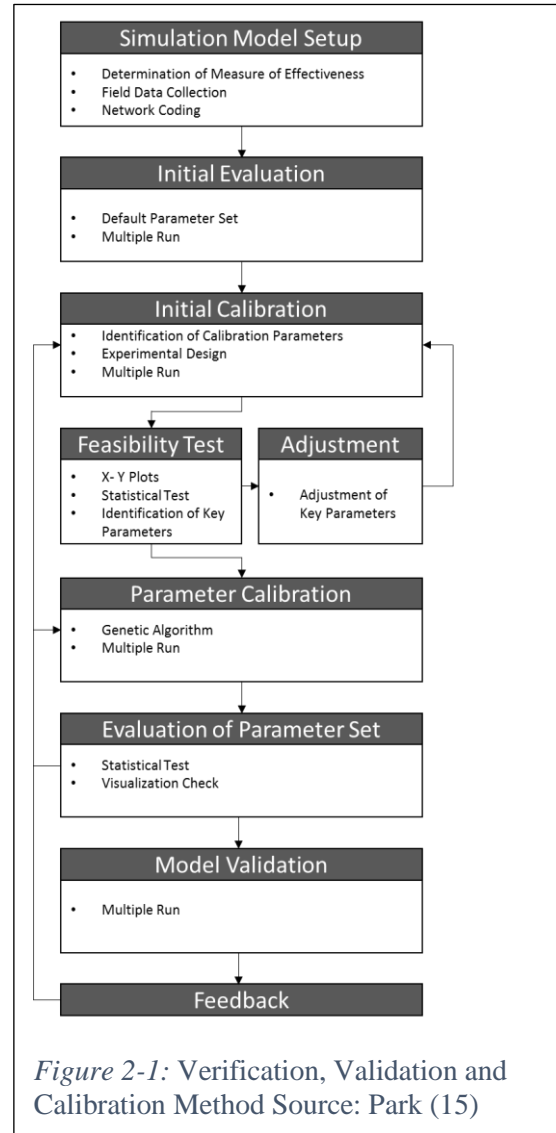
It is helpful to have detailed descriptions of specific tools. The ones that seem most pertinent here are:

HCM (Highway Capacity Manual)/ HCS (Highway Capacity Software) (24)

The HCM is the most popular document in the transportation field including various facilities evaluation methodology which has been developed during the past 60 years. The HCM provides a level of service (LOS) criteria for interrupted and uninterrupted facilities and the definition of various traffic performance measures. HCS is a computer program that facilitates the use of HCM methods. Although the tool is applicable to most facilities, it is not well equipped to develop signal timing plans or do signal timing optimization.

Cap-X (25)

Cap-X is a macroscopic simulation tool employed for assessing various intersection control types simultaneously. It is a very scope-limited tool that relies strictly on a critical lane analysis. As a result, it helps to identify the potential candidate control types which improve operational and safety performance. The tool consists of several input and output tabs. Key required inputs are the volume of each direction, simple geometric data of each alternative. Consequently, volume to capacity ratio for designed intersection is computed and shows ranks of each alternative based on the v/c ratio on the summary tab.



SIDRA (26)

SIDRA is a macroscopic analysis tool that can be used to assess the performance of a wide range of facility types and operating conditions. NCDOT uses it principally to evaluate the performance of roundabouts. Unlike the HCM methods, SIDRA does lane-by-lane analyses. It also can consider the impacts of geometric restrictions such as short lanes. It does provide an option for following the HCM methods.

Synchro (27)

Synchro is a macroscopic analysis model that is often used to design, model, and analyze signalized and unsignalized intersections. It is compatible with SimTraffic which is a microsimulation and can create animation. In addition, arterial segment modeling is also possible. This tool has been used to optimize traffic signal timings for an isolated intersection, an arterial or a network in several studies. (28), (29)

TransModeler (30)

Transmodeler is a microscopic simulation tool. It can be integrated with TransCAD which is a well-known travel demand tool. Like other microsimulation models, facilities and network analysis that is not available in macroscopic simulation can be carried out considering a variety of detail parameters.

2.5 Conclusion

Given the focus of the project, this literature review has focused on tools that are used when examining intersections for geometric enhancements or operational changes. It also compares the “advantages” of using simulation with the “expedience” of using analytical methods. In general, the tools available for analyzing “intersection performance” fall into one of the following categories, as described by the Traffic Analysis Toolbox Volume I: Traffic Analysis Tools Primer (1). The three that most directly pertain here are analytical/ deterministic tools (e.g., HCM-based), microscopic simulation models, and macroscopic simulation models. Consequently, this literature review has focused principally on two of these, analytical models and microscopic simulation models; and more specifically on the tools that NCDOT uses on a regular basis: TransModeler (microscopic simulation) and three analytical options: Cap-X, Synchro, and Sidra.

3 Chapter 3: Isolated Signalized Intersection

As identified in Chapter 1, a set of real-world case studies were used to assess the value of the tools commonly used by NCDOT to do performance assessment. Among the sites was a signalized intersection at NC-50 and NC-42 in Johnston County (35.59278, -78.5992) in September 2020. It is located approximately two miles west of the NC-42 interchange with I-40. The intersection operates under actuated control although during the data collection period, traffic volumes were quite heavy, essentially maxing out all phases and still causing queuing on several approaches. Speed limit on NC-42 is 45 mph, and 55 mph on NC-50. Figure 3-1 gives a general view of the intersection.

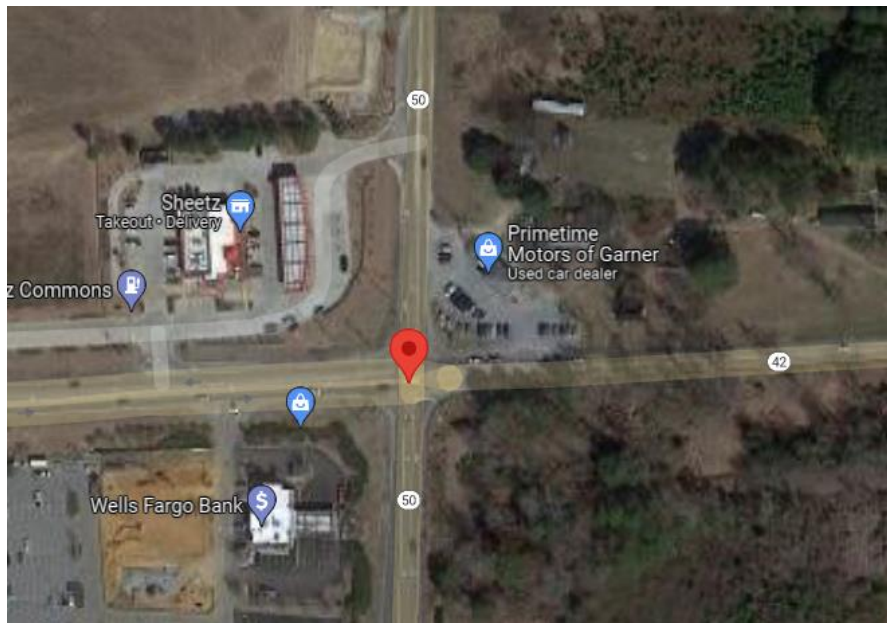


Figure 3-1: Location of Isolated Intersection at NC50 and NC-42

3.1 Site Description

The geometric layout for the site is shown in Figure 3-2. Basically, each entry approach has a through and right shared lane and an exclusive left turn pocket, with varying length on each approach. The approach of interest in this study was the SB through and right turn movement on NC50, as that approach was consistently congested and generated queues that spilled back beyond the data collection range at least through Pierce Rd to the north. This situation also represented a challenge to the modeling effort where a highly congested approach needed to be properly handled in both the analytical and simulation models.

3.2 Data Collection and Extraction Method

3.2.1 **Data Collection**

The primary data collection method was an ITRE drone that was flown above the site at an altitude of about 400 ft. Three drone videos were taken during the afternoon shoulder and peak periods. The video quality was quite high enabling us to measure vehicle discharging on all

approaches, and gather the saturation flow rate for the subject SB approach. A ground camera was also positioned on the SB approach to collect signal timing data during the data collection period. Drone videos were then dispatched to a third party vendor (Data from Sky of DFS) for generating vehicle trajectories in the field of view. Figure 3-3 gives a screenshot of the vehicle IDs which were tracked at the intersection. Note that SB vehicles could not be detected beyond a distance of about 1,000 ft. from the stop line. As a result, our modeling efforts focused on SB vehicle traveling between an upstream and downstream sensors (shown in yellow) in Figure 3-3.

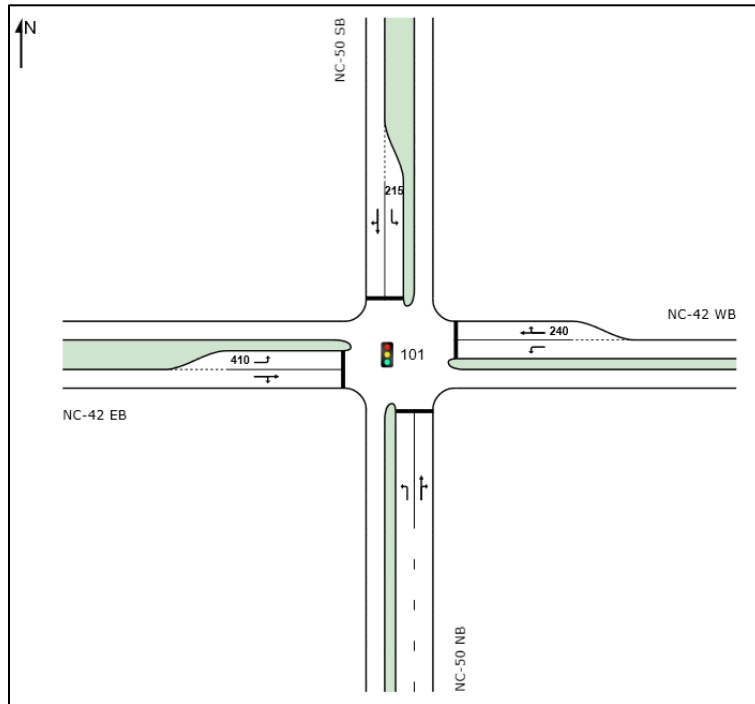


Figure 3-2: Geometric Layout of NC-50 and NC-42



Figure 3-3: Processed Drone Video Showing Vehicle ID's and Sensor Locations

The location of the upstream sensor was based on the system ability to detect 50% of the vehicles that eventually are fully detected at the stop line. The other 50% were undetected due to occlusion or small vehicle size. Thus, timestamp of undetected vehicles at upstream were supplemented manually, and all vehicles' travel time and delay were able to be measured.

Demand Volume Extraction

Demand volumes collected across the three video periods are given in Table 3-1. In all three periods, there were initial and final queues present at the start and the end of each period. Queue size varied from 15-25 vehicles. This added complexity to the problem as their effect on performance must be accounted for. For the models that are able to account for the presence of initial and ending queues in time duration (t), the demand flow rate was calculated as follows:

$$Demand\ Rate\ (T) = \frac{Discharged\ Veh\ in\ (T) + End\ Queue\ (T) - Initial\ Queue\ (T)}{T}$$

Table 3-1: Demand Volume Estimation at NC-50 and NC-42

Video 1	SB			NB			EB			WB			TOTAL
T = 469 sec	LT	TH	RT	LT	TH	RT	LT	TH	RT	LT	TH	RT	
Flow rate at Stopline (veh/h) *	61	391	38	107	207	100	84	522	84	169	506	8	2,279
Adj. flow rate (veh/h) **	35	220	22	107	207	100	84	522	84	169	506	8	2,065

Video 2	SB			NB			EB			WB			TOTAL
T = 489 sec	LT	TH	RT	LT	TH	RT	LT	TH	RT	LT	TH	RT	
Flow rate at Stopline (veh/h) *	44	375	37	132	213	37	103	515	140	125	441	37	2,199
Adj. flow rate (veh/h) **	33	277	27	132	213	37	103	515	140	125	441	37	2,080

Video 3	SB			NB			EB			WB			TOTAL
T = 613 sec	LT	TH	RT	LT	TH	RT	LT	TH	RT	LT	TH	RT	
Flow rate at Stopline (veh/h) *	6	399	29	123	211	65	82	411	65	141	493	23	2,050
Adj. flow rate (veh/h) **	5	335	25	123	211	65	82	411	65	141	493	23	1,980

* Less than one hour vehicle counts at the stop-line were converted to hourly flow rates

** The adjusted demand flow rates were calculated by taking account of the initial and final queue lengths per the equation above

3.2.2 Signal Timing Extraction

The signal timing data came from several sources: split monitor reports, signal plans from NCDOT and the ground camera installed on the SB approach. Average phase durations (used primarily for the analytical models) are shown in Table 3-2 for each video period. The microsimulation model utilized the actual controller settings for this intersection (not shown here). All four left turn movements operated in both protected and permissive phases. Interestingly, however, the SB left turn phase was rarely invoked, because of the queue spillback beyond the short pocket length. Thus it was very difficult in the field to estimate the true left turn demand and its travel time. As shown in the table, there was little variation in the displayed phase times, more likely due to most phases maxing out during the data collection period.

Table 3-2: Average Phase Duration during Data Collection

Movement in Phase	E/W-L	WB	E/W-TR	N/S-L	NB	N/S-TR	CYCLE
Avg.Phase Duration (sec)	Phase 1	Phase 2	Phase 3	Phase 4	Phase 5	Phase 6	LENGTH
Video 1	11	3	75	9	13	46	157
Video 2	11	3	81	9	13	46	163
Video 3	11	3	72	9	13	46	154

3.3 Field Performance Measures

For SB through and right vehicles the approach distance was about 860 ft and the exit distance beyond the stop line was 152 ft for through vehicles and 141 ft for right turning vehicles. Field observations for the SB through and right turn movements are shown in Table 3-3. Two key observations relate to the entry and average speed. Entry speed was observed to be much lower than the speed limit because the furthest upstream point for which we could detect vehicles was actually within the SB queue. This is important, since most analytical models (SIDRA and SYNCHRO) will assume that the field observations are taken at the back of the queue and therefore the entry speed is close to the speed limit. Secondly, the average travel speed is also very low, due to a significant number of cycle failures for the SB traffic, which receives on average only about 25% of the cycle green time per Table 3-2. Further confirmation can be gleaned from the observed individual through vehicles travel time shown in Figure 3-4. The seesaw pattern is explained by whether a vehicle is delayed by one or two cycles at the SB stop line. It relates the time spent in the system (between the two yellow virtual sensors) as a function of their arrival time at the upstream sensor. In the figure, the average travel time is shown by the dotted red line, and the free flow travel time by the dotted green line. Clearly this is a hyper congested approach by all performance indicators.

Table 3-3: Field Measurements of Key Movement Performance Measures

		Video 1	Video 2	Video 3
Travel Distance in System (ft.)	SB-TH	1,012	1,012	1,006
	SB-RT	1,001	1,001	1,001
Observed Average Entry and Negotiation Speed (mph)	SB-TH	18.9	16.5	21.6
	SB-RT	17.7	15.4	21.1
Observed Exit Speed (mph)	SB-TH	28.9	24.0	23.2
	SB-RT	28.2	28.3	28.7
Average time-in-system (sec)	SB-TH	146.8	163.1	159.7
	SB-RT	163.0	158.4	155.2
Average travel speed in system (mph)	SB-TH	4.70	4.23	4.30
	SB-RT	4.19	4.31	4.40

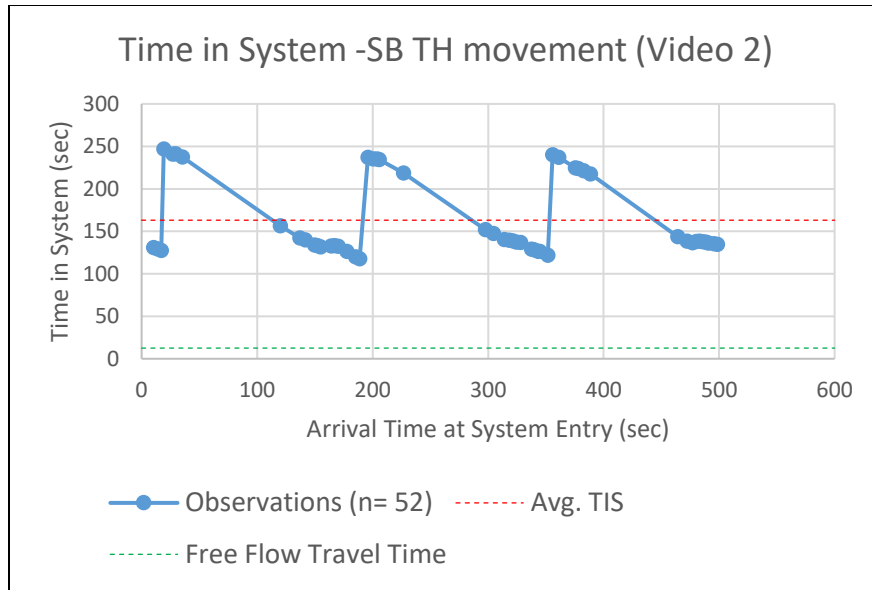


Figure 3-4: Travel Time for SB-TH Vehicles by Arrival Time at Upstream Sensor

3.4 Models' Testing and Calibration

The team's approach to model calibration was to deliver the most accurate input and calibration parameters in all models tested. This includes demand volume levels including any initial queues, signal timing parameters, actual entry speed and saturation flow rate.

Demand levels were reported earlier. The treatment of the initial queue, however, varied between models. SYNCHRO accepts as input a value for the initial queue similar to HCM6, while the current SIDRA model does not. In the latter model, the software developer recommended to the team that this queue be converted into an additional demand volume based on its magnitude and duration of observation. In TransModeler, the initial queue was generated as part of the model warm up period, after which statistics are collected. This queue was also limited to the position of the upstream sensor, which was about 25 vehicles. As mentioned earlier signal timing for SYNCHRO and SIDRA was recorded from the ground camera, while Trans-Modeler used the entire actuated control list of parameters to generate the timings.

Saturation flow headways were directly extracted from the DFS processed video by setting a virtual sensor at the stop line for the through and right shared lane, and tracking vehicle discharges. Table 3-4 below gives a summary of the observed saturation headways and resulting saturation flow rates from three video periods. The calibrated values appear to be much lower than the default ideal values cited in the Highway Capacity Manual (1,900 pc/h/pl) for signalized intersections. The base value used in SIDRA and SYNCHRO was the measured value of 1,700 veh /hr /lane, which was also adjusted for heavy vehicle and turning movements. In combination with the low g/C ratio available for the SB approach, those movements experience a high level of congestion.

Table 3-4: Field Observations of Saturation Flow Rate

Source	Number of Observations	Average Saturation headway	Saturation flow Rate (vphpl)
Video1	47	2.153	1672
Video 2	44	2.061	1747
Video 3	45	2.136	1685
Overall	136	2.118	1700

TransModeler uses a parameter name “Headway Buffer” as the means to calibrate a saturation flow rate. Generally speaking it reflects the required time buffer between a leading and following vehicle in car following mode. This necessitated that the team experiment with different values of headway buffer time to generate the appropriate saturation flow rate. A *sample* relationship between the two parameters is shown in Figure 3-5. For the particular SB movement tested in this study, an optimal headway buffer time in Trans Modeler of 0.65 seconds was selected. We should note that there is no facility in the model to vary the saturation flow rate between movements. Should that be needed, multiple runs will be required to account for the varying movement discharge rates.

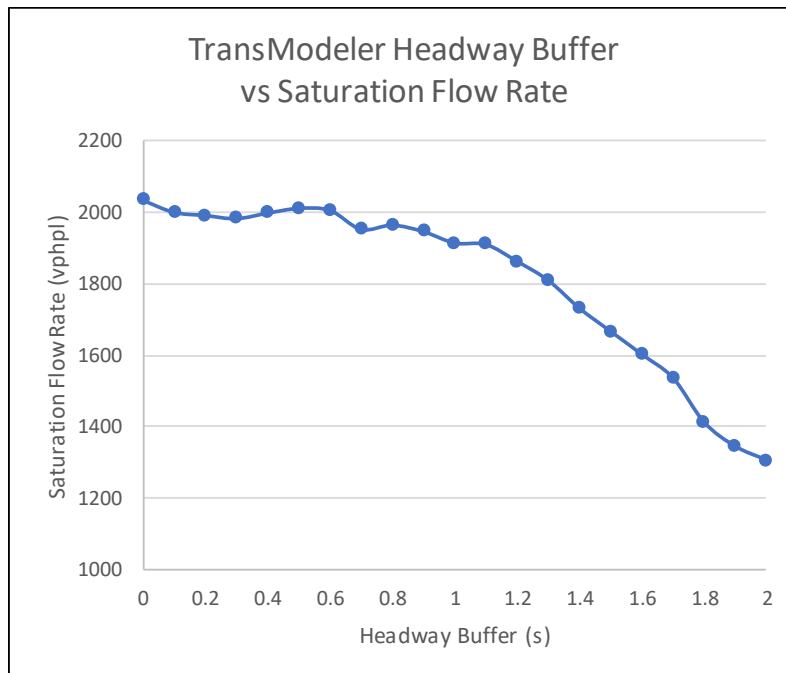


Figure 3-5: Sample Headway Buffer vs. Saturation Flow Rate

3.5 Model Validation

Before presenting the results, we provide a short note on how the different models can be used to estimate the travel time – or time in the system—between the upstream and downstream sensors for the through and right SB movements. By coding the approach and exit lengths to be equal to the setback of the upstream and downstream sensors shown in Figure 3-3, SIDRA will directly report the travel between them. SYNCHRO on the other hand does not report travel time, but strictly control delay at the signal. In this case, travel time is estimated as the control delay plus the free flow travel time (based on the field entry speed). TransModeler travel times are computed by setting virtual sensors in the simulation and tracking the vehicles’ time between the two sensors. Finally, in the case of SIDRA and SYNCHRO, we also present the estimated control delay components including the uniform delay (d_1 in HCM parlance), overflow (d_2), and initial queue (d_3) delays.

The travel time results for the three time periods are summarized in Table 3-5: Time in System Comparisons: Field vs. Models for NC50 SB Movements and a sample illustration of the Video 2 results are depicted in Figure 3-6 since all three periods show very similar trends in their estimation, regardless of which model is being evaluated. All models correctly estimate very high travel times, consistent with the field observations, and an LOS F. However, there were significant differences in the actual travel time values, especially for the analytical models. SIDRA overestimated delays by about 49% for both movements, but SYNCHRO estimation was more than double the field values. Trans Modeler on the other hand slightly underestimated the travel time for both movements but those were within 20 % of the field value in all three periods.

Further investigation of the high travel time overestimation of the SYNCHRO model results revealed the source. As mentioned earlier, SIDRA9 does not allow an initial queue, opting instead to convert it into additional demand, while SYNCHRO does allow it as input. This difference is evident when the various control delay components of both models are compared. Figure 3-7 delivers that comparison across the two models. It is evident that the primary reason for the overestimation of travel time in SYNCHRO is related to the estimation of the initial queue delay (or d_3 in Figure 3-7a). SIDRA on the other hand gives a higher value of overflow delay (or d_2 in Figure 3-7b) due to the increased demand or higher v/c ratio. Overall however, almost 65% of the SYNCHRO reported travel time can be traced back to the initial queue delay.

Table 3-5: Time in System Comparisons: Field vs. Models for NC50 SB Movements

		SB Movements					
		Video 1		Video 2		Video 3	
Average time in system (sec)		TH	RT	TH	RT	TH	RT
Field Measured Travel Time	Field	147	163	163	158	160	155
(Synchro) -Observed entry speed	Synchro 10	395	396	322	323	242	242
(SIDRA9) - Observed entry speed	SIDRA9	242	244	233	235	152	153
TransModeler	TransModeler 5	187	172	141	108	91	91

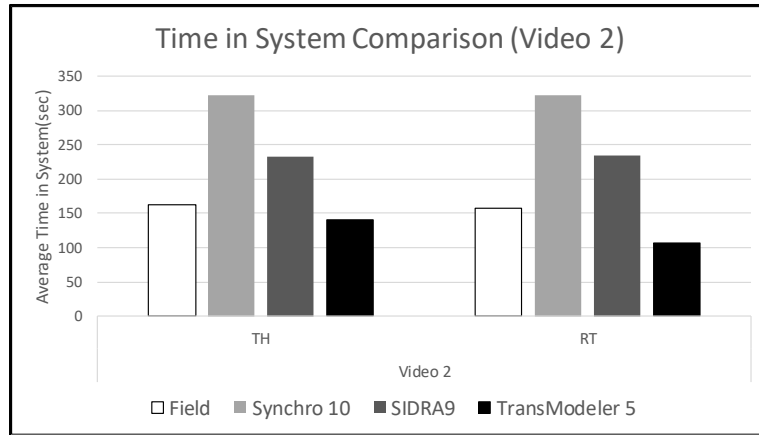


Figure 3-6: Time in System Comparisons for Video 2

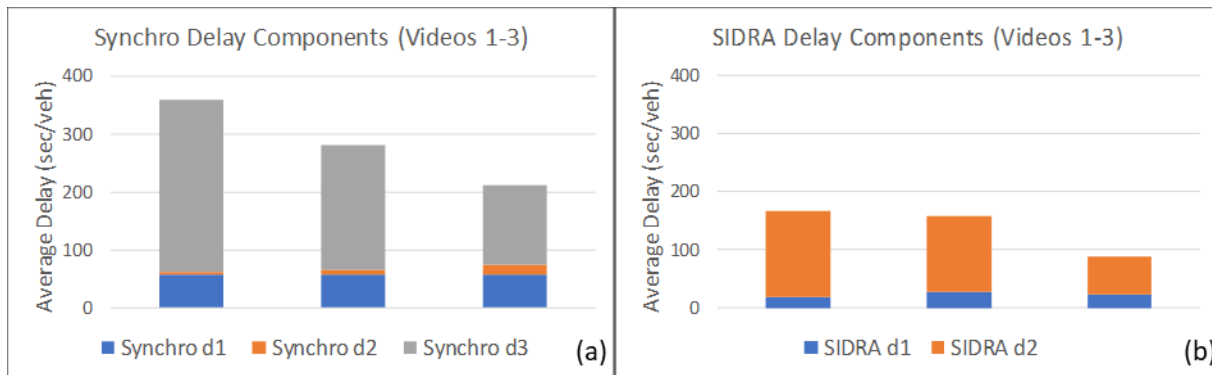


Figure 3-7: Control Delay Components: SYNCHRO vs. SIDRA

3.6 Summary and Discussion

This chapter summarizes the model assessment findings for the first data collection site included in this study. The site is an isolated intersection operating under fully actuated control. Data collection at that site used drone videos supplemented with ground cameras and extracted by a third party vendor, which enabled the team to produce vehicle trajectories within the field of view. The team selected the SB through and left movements for calibration and validation. Those movements generated extensive queuing that reached far beyond the field of view of the both the drone video and the imaging extraction program. Queues were caused by a combination of high demand and low capacity as those movements had low saturation flow rates (under 1,700) and low effective green to cycle ratio (about 26%). As a result, both model calibration and validation focused on a sub-section of the approach and exit links where vehicles could be detected and their trajectory confirmed. This also required the model inputs and outputs to be adapted to the limited sub-section that was investigated. Key related measures that were extracted from the field are the entry and exit speed in the sub-section, the maximum queues observed within the section, and the overall travel time, or time in system as the preferred validation performance measure. Key findings and lessons learned at this site include:

- 1) Counts taken at the stop line in the presence of an initial queue will tend to bias the estimation of demand volumes. A procedure for estimating demand within a time period must also account for the presence of initial and final queues.
- 2) Similarly, when queue lengths exceed the ability of the data collection equipment to measure them, consider limiting the data collection to within a smaller sub-section where most vehicles can be detected and their speed measured.
- 3) Based on 1 and 2, the team proposes that travel time (or time in system) to traverse the data collection sub-section be the selected performance measure for model validation. One advantage of this measure is that it makes no assumption regarding the free flow speed or travel time, which control delay does.
- 4) SIDRA9 cannot account for the presence of an initial queue, but can take its effect into account by adding a supplemental demand volume that is based on the initial queue size and the period duration.
- 5) SYNCHRO can accept an initial queue as input, but it appears that the initial queue delay effects it generates are much higher than those observed in the field.
- 6) Trans Modeler initial queue length coding requires an iterative process, where demand volumes are entered, and queue length measured at the end of the model warm up period. The process is repeated until the measured queue length closely match the initial queue in the field.
- 7) Signal timings were easily coded in SYNCHRO and SIDRA as the approach under study practically operated in a pre-timed control mode during data collection. Trans Modeler, however, required a substantial amount of effort to accurately code the signal controller settings
- 8) Saturation flow rate at that site was found to be quite low compared to the baseline value in the HCM (about 15% lower).
- 9) Base saturation flow rate in SYNCHRO and SIDRA is a direct input that can be varied by approach and is automatically adjusted for the presence of heavy and turning vehicles. In Trans Modeler, however, it is expressed as a “Headway Buffer”, a parameter related to saturation flow rate, but again requires an iterative approach to generate a match to the field saturation flow rate.
- 10) In general, Trans Modeler was best able to match the subsection travel time in the field, albeit with some underestimation. It was followed by SIDRA which overestimated the subsection travel time by a considerable margin. SYNCHRO had the largest difference with the field data. It appears that the main source of overestimation for that model is traced back to the initial queue delay—which is borrowed from the HCM6 signalized intersection chapter. That delay component by itself contributed to about 65% of the subsection travel time.

4 Chapter 4: Single Lane Roundabout

Upon recommendation from the project StIC, the Pullen Hillsborough single lane roundabout in Raleigh, NC (35.786111, -78.662417) was selected as a representative of moderately congested roundabouts in the state. The site is located near the NC State University campus and is abutted on both sides of Pullen Rd with two roundabouts at Stinson Drive on the south and Oberlin Rd on the north, as depicted in Figure 4-1 below. The speed limit on the intersecting roads is set at 35 mph.

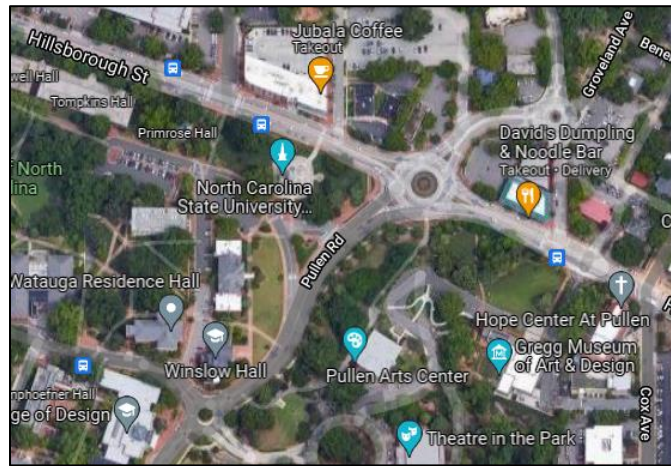


Figure 4-1: Location of the single lane roundabout site

4.1 Site Description

The geometric layout for the site is shown in Figure 4-2. Basically, each entry approach, except for the westbound traffic includes a slip right turn lane, along with a shared through and left lane. Traffic on the three slip lanes must yield to exiting traffic at the destination approach. The nearest traffic signal to the roundabout is on the west leg at Enterprise and Hillsboro. That signal sometimes results in traffic backing into the roundabout.

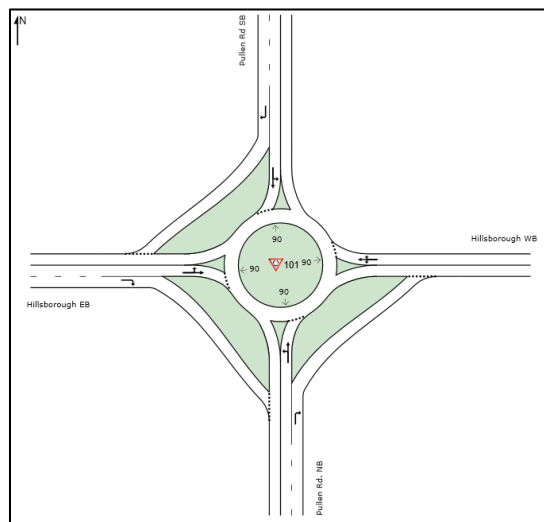


Figure 4-2: Roundabout Geometric Layout

4.2 Data Collection and Extraction Method

Data at this site focused on Origin-Destination demands from all four approaches, along with key calibration parameters and performance measures. For the purpose of this research, the team focused on the shared lanes on both the SB and EB approaches of the roundabout. Data were collected from a drone hovering at 300-400 ft. above the site, giving a bird-eye view of the entire roundabout. However, there were many instances where the queues on those approaches spilled back beyond the line of sight available from the drone video. This required the team to select performance measures than could be observed in the field. This is further explained in the next section. The raw video was processed through a third party vendor (Data from Sky or DFS) which generated full individual vehicle trajectories within the field of view of the drone. This high quality data enabled the team to generate all the required data both for model calibration and validation. Figure 4-3 shows a screenshot of a video depicting the observable view from the drone along with vehicle trajectories and their IDs. Yellow lines indicate positions of virtual sensors capturing selected OD travel times.

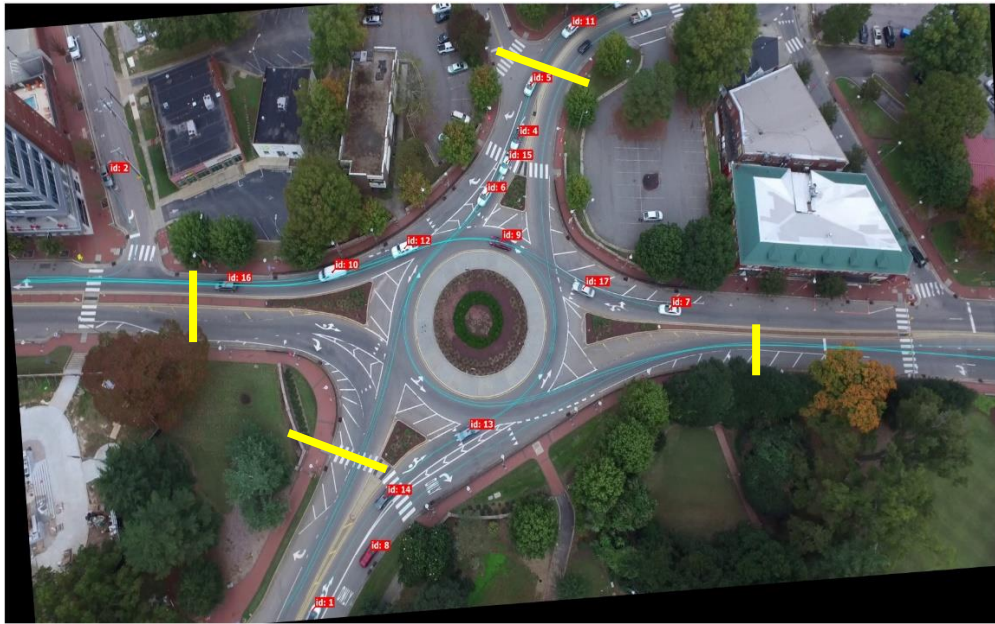


Figure 4-3: Screenshot of drone video at the roundabout

The OD demands were calculated on the basis of the observed trajectories discharging on each approach, while also accounting for the initial and final queues observed during data collection. As evidenced from the screenshot above, demand counts for the SB approach in particular as well as the EB approach could not be carried out upstream of the back of queue, even with the drone video because the back of queue often extended beyond the video frame. The team developed an approximate demand estimation method taking into account the size of both the initial and final queue. Because of the short battery life on the drone and the need to replace the battery multiple times during filming, four short videos were taken, and their data converted into hourly flow rates. The estimated OD demands by approach are shown in Table 4-1.

Table 4-1: Estimated Demand Volumes by Turning Movement at the Roundabout

Period	in VPH.	SB				NB				EB				WB			
		LT	TH	RT	UT	LT	TH	RT	UT	LT	TH	RT	UT	LT	TH	RT	UT
Video 1	Discharge	130	335	43	0	167	242	167	0	56	310	161	25	124	378	12	6
	Demand	130	335	43	0	167	242	167	0	58	320	167	26	121	369	12	6
Video 2	Discharge	88	284	44	0	202	296	170	0	69	258	145	25	57	309	13	6
	Demand	88	284	44	0	204	299	172	0	68	252	141	25	56	304	12	6
Video 3	Discharge	86	379	46	0	153	259	133	0	33	272	193	33	133	299	0	13
	Demand	78	344	42	0	155	262	134	0	32	262	185	32	131	294	0	13
Video 4	Discharge	118	421	81	0	185	288	155	7	52	370	192	30	126	310	15	7
	Demand	110	391	76	0	189	295	159	8	51	365	190	29	136	336	16	8
All	% Heavy Vehicles.	2	1	0	0	3	0	0	0	0	5	7	0	0	4	0	0

4.3 Field Performance Measures

To evaluate the overall validity of the models, performance measures such as stopped or control delay or back of queue have been widely used for model validation purposes. Control delay consists of the stopped delay at the yield line along with acceleration and deceleration delays to and from a cruise speed. In order to precisely measure control delay in the field, the actual vehicle travel time between the furthest upstream and downstream points at which vehicles travel at the cruise speed must be observable in the field. That travel time minus the free flow travel time over that same distance constitutes the control delay for that vehicle. Such a distance was not viewable within the video frame at the study site. As was evident from Figure 4-3, the back of queue often exceeded the range of the video frame. To avoid the constraints on measuring control delay or back of queue, the study opted for the use of the *time-in-system* measure for validation purposes. That measure is simply the travel time for a vehicle within the observable field of view. It varies by turning movement origin and destination and was selected as the most feasible measure for model validation under sight restricted conditions. A corollary measure to time in system is the average travel speed in the (observable) system which divides the movement travel distance by the time in system. Those two measures are obtained by recording the vehicles' timestamps at two observable upstream and downstream sensors and subtracting time at the upstream sensor from the downstream one. Figure 4-3 shows the locations of sensors (yellow lines) associated with SB an EB through and left movements.

In addition, because queues will extend beyond the sensor positions, the speed measured at the upstream sensors are likely to be lower than the default cruise speed in most cases. Thus, the corresponding entry and exit speeds at those sensors were also used as inputs on the subject approaches. Table 4-2 gives the field observed travel distance, average entry speed, negotiating speed (in the circle region) and exit speed. This enables the computation of average time-in-system, and average travel speed for the selected movements. Methods for extracting the performance measures counterparts in both analytical and microsimulation models are discussed later in the model validation section.

Table 4-2: Movement-based field observations

		Video 1		Video 2		Video 3		Video 4	
		SB	EB	SB	EB	SB	EB	SB	EB
Travel Distance in System (ft)	TH	397	646	397	646	397	646	367*	599*
	LT	638	612	638	612	638	612	638*	565*
Observed Entry Speed (mph)	TH	12.47	9.99	13.65	18.45	14.44	19.35	12.06	14.15
	LT	12.47	9.99	13.65	18.45	14.44	19.35	12.06	14.15
Observed Negotiation Speed (mph)	TH	15.64	16.03	15.64	16.03	16.16	15.57	15.33	15.06
	LT	14.33	15.44	14.75	14.89	14.10	14.82	13.81	14.00
Observed Exit Speed (mph)	TH	23.60	23.95	24.15	26.55	23.86	23.04	22.44	20.48
	LT	25.49	18.17	29.42	18.32	26.63	17.74	25.01	18.94
Average time-in-system (sec)	TH	31.26	45.73	33.25	25.00	27.06	29.17	30.81	41.03
	LT	39.70	51.89	36.10	27.20	36.48	33.38	34.67	42.97
Average travel speed in system (mph)	TH	8.66	9.63	8.14	17.61	10.00	15.10	8.12	9.95
	LT	10.96	8.04	12.05	15.34	11.92	12.50	12.55	8.97

* Because of slight change in the drone positioning in video 4, the sensor locations are modified.

4.4 Models' Testing and Calibration

This roundabout was used as the testbed for SIDRA9 (HCM defaults) and TransModeler. In order to match the inputs from the field into the model, link lengths in the case of the analytical models, and sensor locations in the case of the micro simulator were coded into the model. In addition to those inputs the key calibration parameters for a roundabout include the critical headway and follow on headway. For the analytical models, the team applied three different approaches using the Raff (32), Maximum Likelihood (30) and Siegloch (31) methods, the latter being the one used in the latest HCM release 6. All these modeling approaches require the estimation of accepted gaps, and – with the exception of Siegloch--also use rejected gaps in the circulating stream, as well as the number of approach vehicles entering in each accepted gap.

In the case of TransModeler, which is similar to VISSIM's gap acceptance process, the critical headway is estimated using a conflict zone between a circulating vehicle and an entry vehicle. The concept is illustrated in Figure 4-4 and is explained next. The critical headway and follow up headway are defined as t_c and t_f , respectively, and the conflict zone is marked with the checkered pattern. The start and end points of the conflict zone are labeled as C and A, respectively. The yield line is labeled B. In the case shown in the figure, the conflict zone has already cleared. Assume the distance between the front bumper of the circulating vehicle (in green) and point A is d_A' and the distance to C is d_C' . The distance between B and A is defined as d_A . If the speed of the circulating vehicle is s' and that of the entering vehicle is s , the conditions for gap acceptance are mathematically described next to the diagram in Figure 4-4.

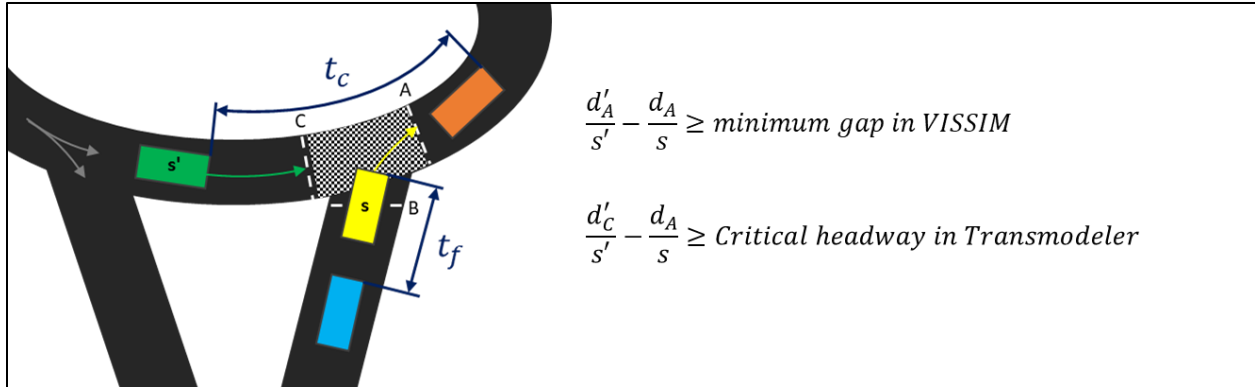


Figure 4-4: Critical headway definition using the conflict zone concept

Based on the above definitions, an accepted headway in TransModeler can simply be calculated by differentiating the measured timestamps when an entering vehicles in Figure 4-4 crosses sensor A and when the immediately following circulating vehicle s' passes sensor C. This method enables the analyst to measure all accepted headways according to the definition in TransModeler, and can thus generate the entire distribution of accepted headways. However, some accepted headways could be very large due to lack of demand on the circulating lane.

In order to estimate the rejected headways, one requires that a rejected lag be always associated with a stopped vehicle at or near sensor B. The timestamp when the entering vehicle is stopped is applicable here. The rejected headway process is modeled from the perspective of an approaching driver. A driver on the entering lane would first monitor the area between sensors C and A to verify if a circulating vehicle is about to cross that zone. If there are no vehicles between them when vehicle (s) then the lead vehicle space is clear. If not, the critical headway is not evaluated until the leading vehicle downstream of sensor B vehicle crosses sensor A. Next, the entry driver estimates when the lagging circulating vehicle (s') is expected to reach sensor C, at the instant vehicle (s) will (in theory) cross sensor A. If the lag is deemed acceptable, vehicle (i) will enter the roundabout, otherwise the driver will wait for the next opportunity and repeat the process as many times as needed until an acceptable headway is presented. Interestingly, some of the rejected headways could be negative – meaning that vehicle s' will cross sensor C before vehicle s is estimated to cross sensor A. (or $d'_C/s' < d_A/s$). Because the critical headway in TransModeler is founded on a very different definition than that used in all the analytical models, its calibrated value is likely to be quite different.

In all models, the value of the follow on headway is based on observations when multiple minor road vehicles accept a gap in the circulating lane. In the Siegloch approach, however, the follow on headway is simultaneously estimated with the critical headway.

Table 4-3 gives a summary of the calibration results by model. Note that in this case, data from the multiple videos were used to generate the results

Table 4-3: Estimates of Gap Acceptance Parameters by Model and Calibration Method *

Key Parameters	Model Platform	SB Approach	EB Approach
Critical headway- Raff’s method	SIDRA9	4.15	4.85
	TransModeler	0.98	1.46
Critical headway - MLE method	SIDRA9	4.41 (0.820)**	4.61 (1.152)**
	TransModeler	1.11 (0.799)*	1.55 (0.740)*
Critical headway – Siegloch method	SIDRA9	4.17	4.23
	TransModeler	Not applicable	Not applicable
Critical headway -default mean values	SIDRA9 / HCM	4.8	4.8
	TransModeler	1.05****	1.05****
Follow up headway field mean values (used directly in Raff’s and MLE)	SIDRA9	2.9	2.9
	TransModeler***	1.35****	1.35****
Follow-up headway – Siegloch method	SIDRA9	2.97	
	TransModeler	Not applicable	Not applicable
Follow up headway default mean values	SIDRA9 / HCM	2.5	2.5
	TransModeler***	0.3****	0.3****

* The critical headway definitions are different. Because of this the numerical values for the parameters cited in the table cannot be compared to assess whether they are the same or different for the same parameter.

** Standard deviation assuming critical headways follow a lognormal distribution

*** Buffer times in TransModeler adjusted for matching follow up headway in the field or default

**** The default values in TransModeler 5.0 are in percentage distributions; the numbers presented here are average values

It is clear from the above Table that most analytical model calibration approaches yielded similar ranges of critical and follow-on headways. Critical headways varied from 4.15-4.41 and the follow on headway using Siegloch was 2.97. Default HCM values for both were 4.8 and 2.5 respectively. It appears that the roundabout critical gap has dropped at that site, indicating an increase in capacity above the current defaults. On the other hand, the TransModeler calibration yielded values from 0.98-1.11, which contains the current default value of 1.06 seconds. The follow on headway observed in the field using Tans Modeler calibration method was 1.35 se compared to the default value of 0.30. It is important to note that in SIDRA (as well as SYNCHRO) the user is able to calibrate the critical headway *by approach*. In TransModeler, however, only one set of buffer times associated with the critical headways (akin to saturation flow rate) can be calibrated for the entire roundabout. This required us to make two separate runs for the SB and EB approach in order to code the different critical headways.

4.5 Models' Validation

To evaluate the validity and quantify the utility of the calibrated models, un-calibrated models were generated for comparison purposes. The un-calibrated scenarios assumed the following: (a) demand is measured at the yield-line, (b) approach cruise speed is equivalent to the posted speed limit (35 mph), link length is taken as 1,600 ft. (SIDRA9 default) and default gap acceptance parameters in HCM 6th for single lane roundabouts are entered. In SIDRA9, the actual travel time is reported as the equivalent of time-in-system observed in the field. However, the premise of the comparison is based on the same travel distance between field and model (16). In this research, average travel speed in the system is compared. Figure 4-5 (a) and (b) shows average travel speed results in SIDRA calibrated and un-calibrated models against the field for the SB and EB approaches, respectively. Also shown are the 95th percentile confidence intervals of the field mean, based on ± 2 standard errors from the mean, approximately.

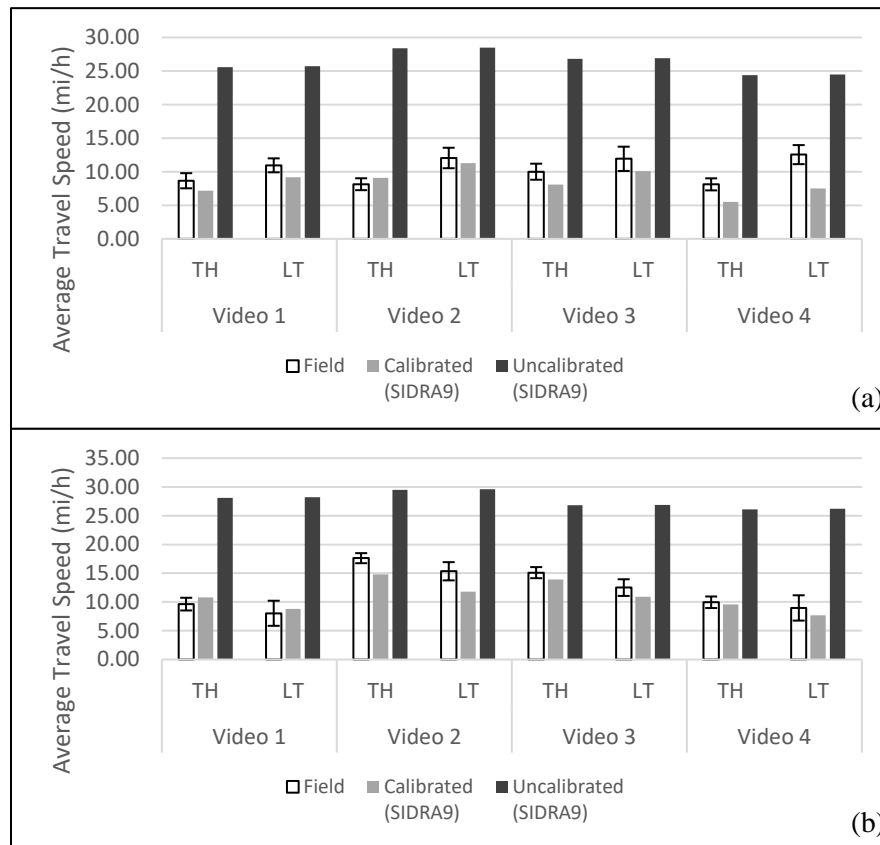


Figure 4-5: SIDRA9 vs Field Average Travel Speeds for (a) SB and (b) EB Approaches

The value of calibrating SIDRA9 is very evident from tracking the average travel speed results above. In the un-calibrated model differences were in the 26-30 mph range, but only within 2-3 mph of the field in the calibrated models. In this particular case, the effect of the coded approach speed is critical, perhaps as important if not more important than the values of the gap acceptance parameters.

Figure 4-6 (a) and (b) shows average travel speed results estimated by the calibrated and un-calibrated TransModeler 5.0 and that measured in the field for SB and EB approaches, respectively. TransModeler does not directly output average travel speed. The average speeds presented here are calculated based on “Time-in-System”, which were estimated as the absolute time difference a vehicle passed the roundabout entrance and exit data collection sensors added in the TransModeler model. Then, average travel speed of each movement is calculated as the distance between the entrance and exit sensors divided by the corresponding time-in-system.

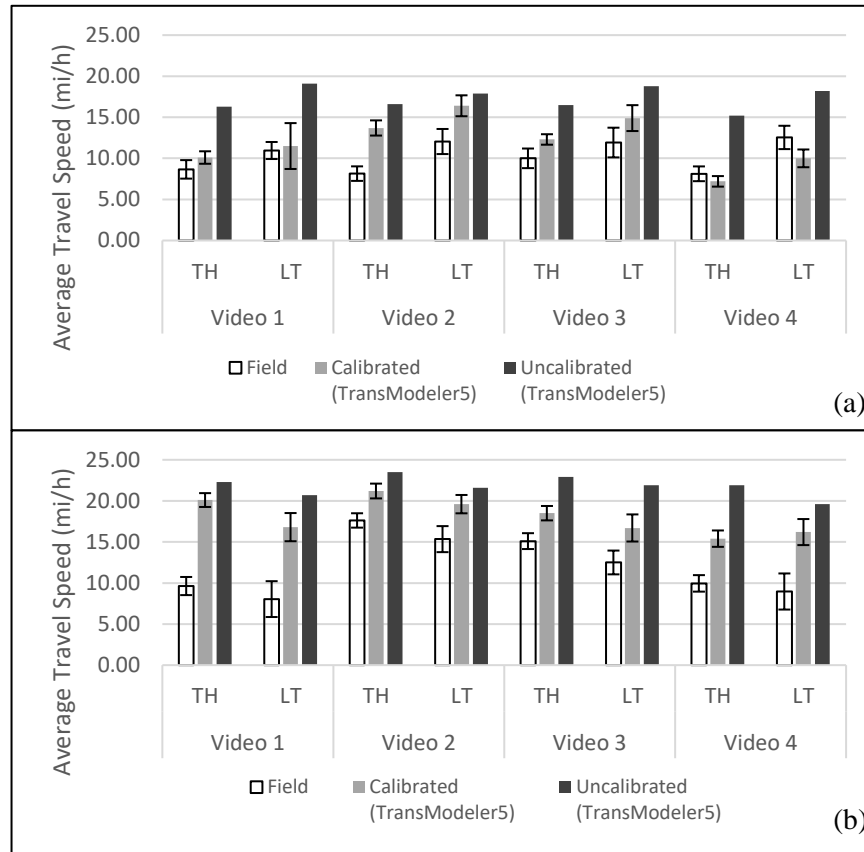


Figure 4-6: TransModeler vs Field Average Travel Speeds for (a) SB and (b) EB Approaches

The average speed plots reveal that there are some visible differences between those field measured and TransModeler simulations with the latter generating speeds that were 3-10 mph higher than their field counterpart. Differences were more pronounced for the EB than the SB approach, possibly as a result of the higher presence of buses on that approach. In all cases, however, the calibrated model still outperformed the un-calibrated model

4.6 Summary and Discussion

This chapter described the challenges of a roundabout model calibration and validation across platforms in a case where sight distance restrictions result in violating many of the “regular” roundabout analytical and microsimulation model assumptions. Chief among those is the inability to observe the true back of queue, making it infeasible to calibrate or validate based on delay or queue length, since the basic assumption of travel at the desired or speed limit is not

valid. This led to the modification of the process to focus on time in the system as our available performance measure. A representative analytical model, SIDRA9 along with a microsimulation model, TransModeler version 5.0 were tested. Calibration included the incorporation of an initial queue to estimate demand, the application of three methods for estimating the approach critical headways and follow up headways, and the setting up of virtual detection stations to estimate time in system and average travel speed. This research, for the first time has developed a new approach intended to determine the distribution of rejected gaps based on TransModeler definition of how critical headways are measured.

Following is a summary of findings from the single lane roundabout analysis

- 1) Calibrated models performed consistently better -- in terms of matching field observations-- than un-calibrated ones regardless of the model used, especially in the presence of measurements taken when queues are present
- 2) It is important that the entry speeds into the model links match that measured in the field, and not be assumed to be close to the free flow speed or speed limit.
- 3) The current SIDRA9 model cannot account for initial queue effects. Consultation with the model developers yielded an approximate solution. The developer intends to enable the effect of an initial queue in future releases of the model
- 4) Related to the previous items, measurements of OD volumes at the yield line will tend to underestimate demand, especially in the presence of queues
- 5) It appears that Trans Modeler uses a single set of buffer times for the entire facility, making it difficult to calibrate separate critical headways for each approach. This required the team to carry out separate runs to properly calibrate the two subject approaches.
- 6) The three analytical methods used for calibrating the critical headway gave very close results within 0.5 seconds of each other
- 7) The results confirmed the appropriateness of the current practice of using SIDRA for modeling roundabout operations.

5 Chapter 5: Coordinated Signalized Intersection

The third site visited in this project was the Oleander Dr. and S. College Rd. coordinated signalized intersection in New Hanover County (34°12'37.4"N; 77°53'12.3"W). It is located approximately 4 miles south-east of the Wilmington International Airport. Speed limits on both the Oleander Dr. and the S. College Rd are 45 mph. Figure 5-1 gives a general view of the intersection.

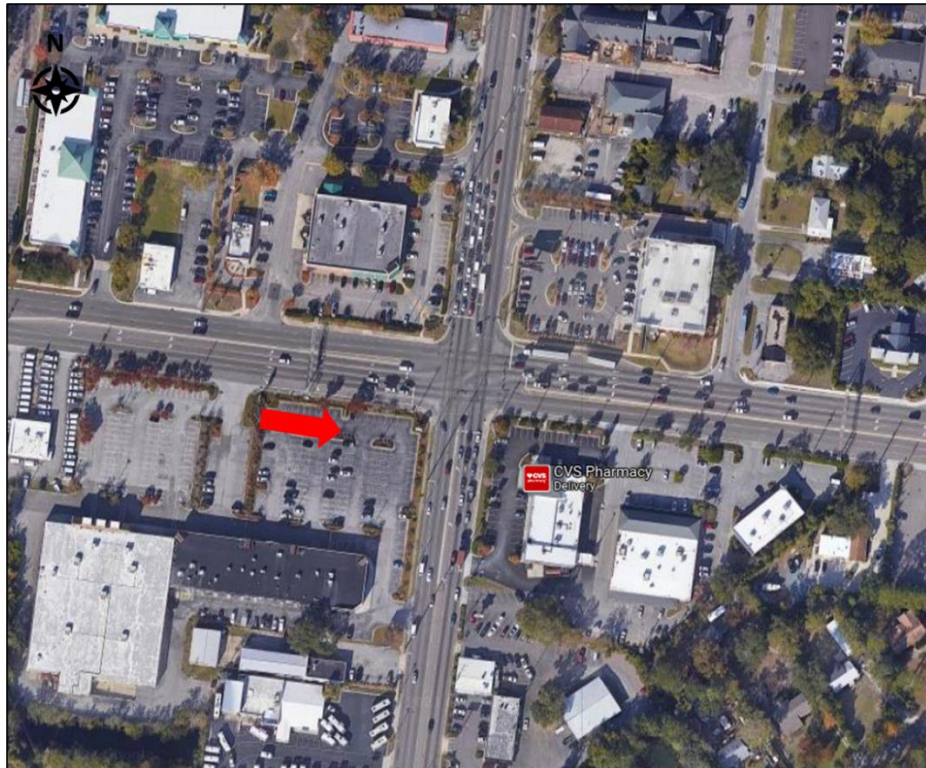


Figure 5-1: Aerial View of Oleander Dr. and S. College Rd. Intersection

5.1 Site Description

The geometric layout of this site is shown in Figure 5-2. Each of the two entry approaches on Oleander Dr. has two through lanes, an exclusive right turn pocket, and two left turn lanes. The north approach of S. College Rd. consists of two through lanes, an exclusive right turn lane, and one left turn lane. The south approach of S. College Rd. consists of one through lane, one shared through and right lane, and one left turn lane. The movements of interest in this study were the EB through and EB left movements on Oleander Dr., as that approach was found to be the most congested one at the intersection.

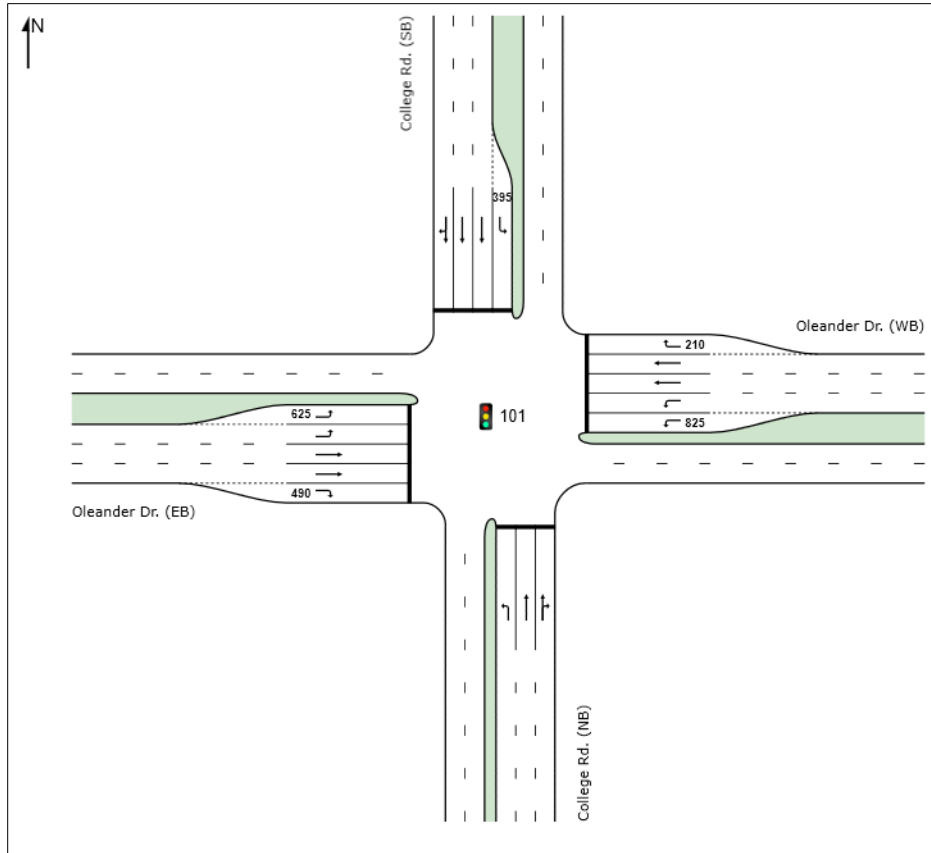


Figure 5-2: Geometric Layout of Oleander Dr. and S. College Rd.

5.2 Data Collection and Extraction Method

5.2.1 Data Collection

Two types of data were collected. The first type was the upstream traffic flow arrival rates, stop bar discharge rates (saturation flow rates during queueing) and discharge flows. The second type was signal-related data including detector placements, phase sequencing, minimum and maximum greens, and gap timer settings.

To collect the traffic flow data, a drone was used. By taking advantage of drone's wide video frame, we could observe simultaneously all traffic movements. The only issue was battery life, which limits the videotaping to only 10-30 contiguous minutes. In this regard, we had to split the peak-hour data collection into multiple drone flights, which resulted in unobserved intervals between flights. For this intersection, fortunately, the drone was connected to a tether system, which provided an additional power source for the drone to operate longer.

Figure 5-3 shows the flight sequence of the drone. For this intersection, the green line depicts the flight sequence of the drone, when connected to a power source through a tether. The drone would take off, hover, and then descend. The pilot would adjust the angle of the drone to enable full coverage of a geo-fenced area. Recording would start when the drone was correctly positioned and stop when recharge was needed.

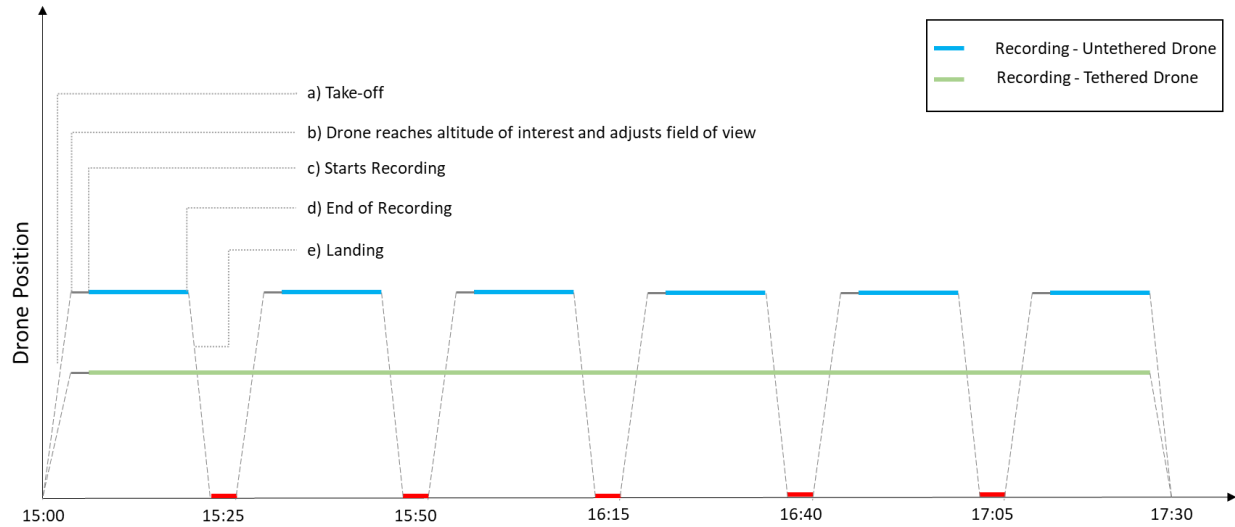


Figure 5-3: Drone's Flight Sequence

Data for the traffic signal came from two sources. The first was the as-built plans, which included the detector placement and use, input suppression and extension, the phase sequencing, and the signal timing parameters. A volume-density signal controller was deployed at this site. The second source was the green time allocations obtained from the operator's "split monitor". It gave green times by movement for each cycle as well as detector inputs and interpretation (use).

Data extraction and reduction applied mostly to the drone data. We used DataFromSky (DFS) to ensure efficient processing, enhanced accuracy, and fine resolution (DataFromSky, 2021). Most importantly, DFS can provide trajectories for every vehicle identified. Moreover, through calibration, latitude and longitude data can be extracted. Besides location, the other outputs include time stamp, speed, and acceleration.

DFS also enables the deployment of detectors anywhere in video. For each detector, it provides vehicle ID, speed and timestamp for every crossing. As such, it is capable of obtaining lane-based travel time from any designated origin to a designated destination for every vehicle that is traced. Figure 5-4 shows a screenshot of the data processed by DFS for this site. Note that the EB vehicles could not be detected beyond a distance of about 1,000 ft. upstream of the stop line. As a result, our modeling efforts focused on EB through and left turning vehicles traveling between the designated upstream and downstream sensors (shown in red) in Figure 5-4.

The location of the upstream sensor was determined based on the system's ability to detect about 61% of the vehicles that are – eventually--- fully detected at the stop line. The other 39% were undetected due to occlusion or small vehicle size in the video. The 61% of the sample could also provide a reasonable representation of delays and travel times during the data collection period.



Figure 5-4: Processed Drone Video for Oleander Dr. and S. College Rd Showing Vehicle ID's and Entry and Exit Sensor Locations for EB-TH and EB-L Movements

5.2.2 Demand Volume Extraction

Traffic demands extracted for the captured video are given by

Table 5-1. The upstream demands are crucial for near- or over-saturated conditions. The initial and final queues as well as queue dynamics must be matched during the duration of observation. If the queues are zero or negligible at both the beginning and end of the study time frame, the stop bar-based flow rates can be used. But if an initial queue exists, or it grows, then the demands tend to exceed the observed discharge rates. During the data collection period, there were initial and final queues presented at the beginning and end of the period. Since the initial queue is the residual demand from a previous analysis period and the final queue is demand not discharged during the analysis period, the demand rate during the study timeframe can be estimated using Equation (1).

$$q = \frac{D - Q_I + Q_E}{T} \quad (1)$$

Where,

q : Adjusted demand volume on approach or movement (veh/h)

Q_I : Initial queue on approach or movement at the start of the analysis period (veh)

Q_E : Final queue on approach or movement at the end of the analysis period (veh)

D : Discharge from stop line on approach or movement (veh)

T : Analysis period duration (hour)

Equation (1) assumes the values on the right-hand side capture all movements that are serviced (lefts, through movements and rights). It is necessary to point out that when there are separate right-turn or left-turn lanes, additional adjustment factor should be applied.

Table 5-1: Demand Volume Estimation at Oleander Dr. and S. College Rd.

Video9	SB			NB			EB			WB			Intersection
T = 768 sec	LT	TH	RT	LT	TH	RT	LT	TH	RT	LT	TH	RT	Total
Traffic counts at Stopline (veh/T)	25	303	58	16	242	13	71	146	41	82	148	15	1160
Flow rate at Stopline (veh/h) *	117	1420	272	75	1134	61	333	684	192	384	694	70	5438
Adj. flow rate (veh/h) **	117	1420	272	75	1134	61	309	652	192	384	694	70	5381

5.2.3 Signal Timing Extraction

Signal-related data were obtained from two sources: the signal plans and the “split monitor reports”. The first indicated the detector placement and signal timing information, including input delays and extensions, the phase sequencing (lead and lag lefts), and the timing values. These data were “reduced” to provide appropriate inputs for both the analytical and simulation models. In the former case, the phase sequence was of the greatest importance. For the simulation model, all these data were employed. The split monitor reports provided green times by movement and cycle lengths as well as detector inputs and actions taken. For the analytical model, these data were used to indicate the appropriate control being employed. For the simulation model, these data were “reduced” to compute distributions in the green times and cycle lengths, to be compared, during validation, with the signal timing-related outputs from the simulation model.

Average green, yellow, and red durations for each phase (used primarily for the analytical models) are shown in Table 5-2. Trans Modeler entered the actual controller settings for this intersection (not shown here). All four left turn movements operated in protected phases.

Table 5-2: Average Phase Duration during Data Collection

Signal Phase	Phase Number							
	1	2	3	4	5	6	7	8
Bound	SBLT	NBT	WBLT	EBT	NBLT	SBT	EBLT	WBT
Avg Greens	12	65	17	32	12	65	15	33
Yellow Clearance	3.0	4.5	3.0	4.2	3.0	4.5	3.0	4.2
Red Clearance	3.7	2.1	3.7	1.9	3.3	2.2	3.8	1.8

5.2.4 Field Performance Measures

For the EB through and left turning vehicles the approach distance was about 800 ft and the exit distances beyond the stop line were 335 ft. and 253 ft. respectively. Field observations related to the EB through, and left movements are shown in Table 5-3.

The observed entry speeds for both movements were found to be 10 mph lower than the posted speed limit at the site. This is mainly due to the fact that there is a closely-spaced upstream intersection that affects the arrivals at the upstream approach where the entry speed is measured. Furthermore, the average travel speed in the system was observed to be very low for

both the movements. This is mainly due to the short green time for the two phases and frequent cycle failures in the case of the left turn phase. Further confirmation can be gleaned from the observed individual through vehicle travel times shown in Figure 5-5. The periodic fluctuation pattern is explained by whether a vehicle was delayed by one or two red signals at the EB stop line. It relates the time spent in the system as a function of their arrival time at the upstream sensor. In Figure 5-5, the average travel time is shown by the red line, while the green line indicates the free-flow travel time (FFTT). Clearly, the average travel time is significantly higher than the free-flow speed, indicating this is a congested approach; this is also supported by the other performance indicators listed in Table 5-3: Field Measurements of Key Movement Performance Measures. The reader can also note that for the EB-TH movement, there is a heavier cluster of points towards the lower values of travel time, which is indicative of a well-coordinated albeit congested approach.

Table 5-3: Field Measurements of Key Movement Performance Measures

		Video
Travel Distance in System (ft.)	EB-TH	1,135
	EB-LT	1,053
Observed Entry Speed (mph)	EB-TH	34.27
	EB-LT	34.27
Observed Negotiating Speed (mph)	EB-TH	33.32
	EB-LT	16.47
Observed Exit Speed (mph)	EB-TH	36.23
	EB-LT	19.65
Average Time-in-System (sec)	EB-TH	73.06
	EB-LT	123.53
Average Travel Speed (mph)	EB-TH	10.6
	EB-LT	5.8

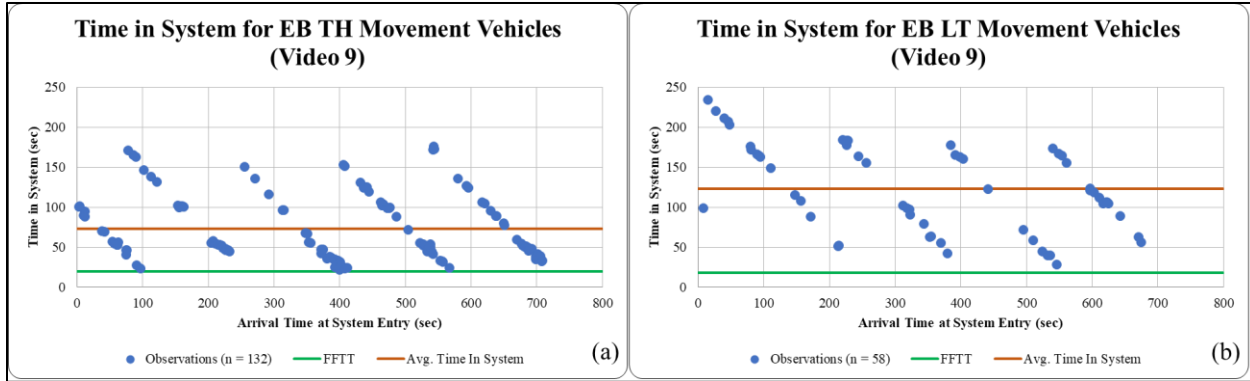


Figure 5-5: Travel Time for EB-TH and EB-LT Vehicles by Arrival Time at Upstream Sensor

5.3 Model Testing and Calibration

The approach of model calibration was to deliver the most accurate input and calibration parameters to all models tested. This includes demand volume levels including any initial queues, signal timing parameters, actual entry speed and saturation flow rate.

Demand levels were reported earlier. The treatment of the initial queue, however, varied between models. SYNCHRO allows users to manually input an initial queue value in a way similar to what HCM6 does, while the current SIDRA model does not support this option. In the latter model, the software technical support recommended the team that this initial queue be converted into an additional demand volume based on its magnitude and duration of observation. In TransModeler, the initial queue was generated during the model warm-up period, after which actual performance measures were collected. This initial queue was also limited to the position of the upstream sensor, which was about 25 vehicles in this case. As mentioned earlier, signal timing information for SYNCHRO and SIDRA was recorded from the ground camera, while Trans-Modeler used the entire actuated control list of parameters to generate the timings.

Saturation flow headways were directly extracted from the DFS processed video by setting a virtual sensor at the stop line for the through and left lanes, and tracking vehicle discharged during the green signals. Table 5-4 below presents a summary of the observed saturation headways and the corresponding saturation flow rates from four video clips collected at the Oleander/College intersection. The calibrated values appear to be much lower than the ideal values cited in the Highway Capacity Manual (1,900 pc/h/pl) for signalized intersections. The input value entered in SIDRA and SYNCHRO was 1,743 veh./hr./lane, which was the measured saturation flow rate for through lanes. For left turn movements, the saturation flow rate was adjusted with the corresponding factor in the analytical models. In combination with the low g/C ratio available for the EB approach, those movements experience a high level of congestion.

Table 5-4: Field Observations of Saturation Flow Rate

Source	Number of Observations	Average Saturation Headway	Saturation Flow Rate (vphpl)
Videos 9 & 10	116	2.08	1,728
Video 11	102	2.14	1,679
Video 12	104	1.97	1,830
Overall	322	2.06	1,743

As pointed out in the previous two chapters, TransModeler uses a Headway Buffer to calibrate saturation flow rate. The team experimented with different values of headway buffer time to generate the appropriate saturation flow rate. For the EB movement at this site, an optimal headway buffer time in Trans Modeler of 1.4 seconds was selected.

5.4 Model Validation

It is important to ensure that the predictions provided by a model are valid. That is, they match or closely approximate the “outputs” observed in the field. We examine this issue in this section. The travel time results for the period are summarized in Table 5-5. Figure 5-6 shows a graphical depiction of the time-in-system for the through and left movements of the EB approach at the intersection. Observations from both the table and the figure reveal that Trans Modeler provides the closest estimate-of-time in system followed by Synchro and SIDRA, respectively. Overall, all three models are able to capture the high travel times observed at the field. However, both analytical models significantly overestimated the time-in-system for the movements at the approach. For the through movement, Synchro overestimated the time-in-system by 26%, whereas SIDRA’s was about 51%. For the left turn movement, both the analytical models overestimated the time in system a little over 50%. However, the micro-simulation model underestimated the time-in-system by about 30% for the left movement. It is important to note that in Trans Modeler, the headway buffer was calibrated for the through movement. Since Trans Modeler employs a global headway buffer value the results indicate that the simulated left-turn saturation flow rate was coded to be higher than the field observed value. Therefore, this tends to result in an underestimated control delay, which eventually leads to a lower time-in-system.

SIDRA’s over-estimation of time-in-system stems from the fact that it does not allow direct input of an initial queue into the model. The conversion of the initial queue to additional demand, as recommended by the technical support, resulted in overestimation of both the uniform and incremental delays as portrayed by Figure 5-7. Observations of Figure 5-7 reveal that SIDRA’s delay components consist of zero initial queue delay (d_3), while it overestimated both the uniform and incremental delays. Moreover, Synchro’s time-in-system include all three components of delay. The initial queue delay seems to be overestimated for the left turn movement of the EB approach by Synchro (or more appropriately from the HCM6 method adopted in Synchro). SIDRA on the other hand gives a higher value of uniform and overflow

delays (d_1 and d_2) due to the increased demand and/or higher v/c ratio. SIDRA's resulting v/c is 0.957 compared to Synchro's 0.83.

Table 5-5: Time in System Comparisons: Field vs. Models for Oleander Dr. EB Movements

Oleander Dr. and S. College Rd. Intersection (Eastbound Approach)		
Source	Average Time in System (sec)	
	TH	LT
Field	73.06	123.53
Synchro	92.35	193.15
SIDRA	110.4	186.3
TransModeler	74.5	95.6

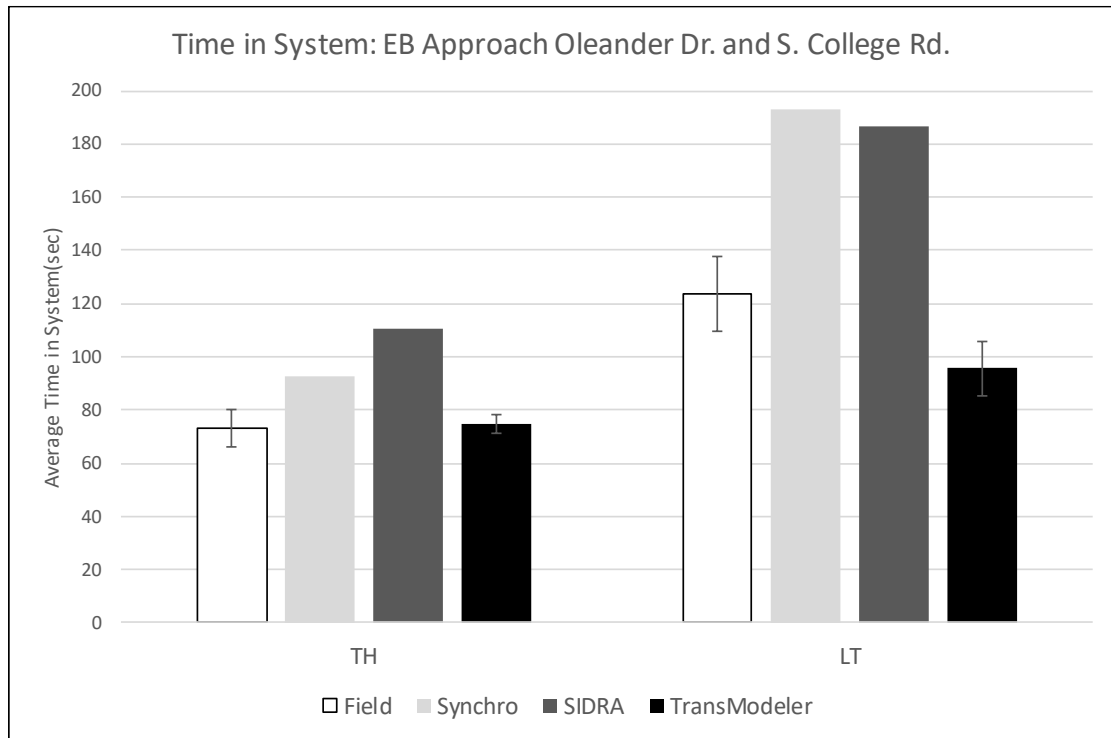


Figure 5-6: Time in System for EB Through at Oleander Dr. and S. College Rd. Intersection

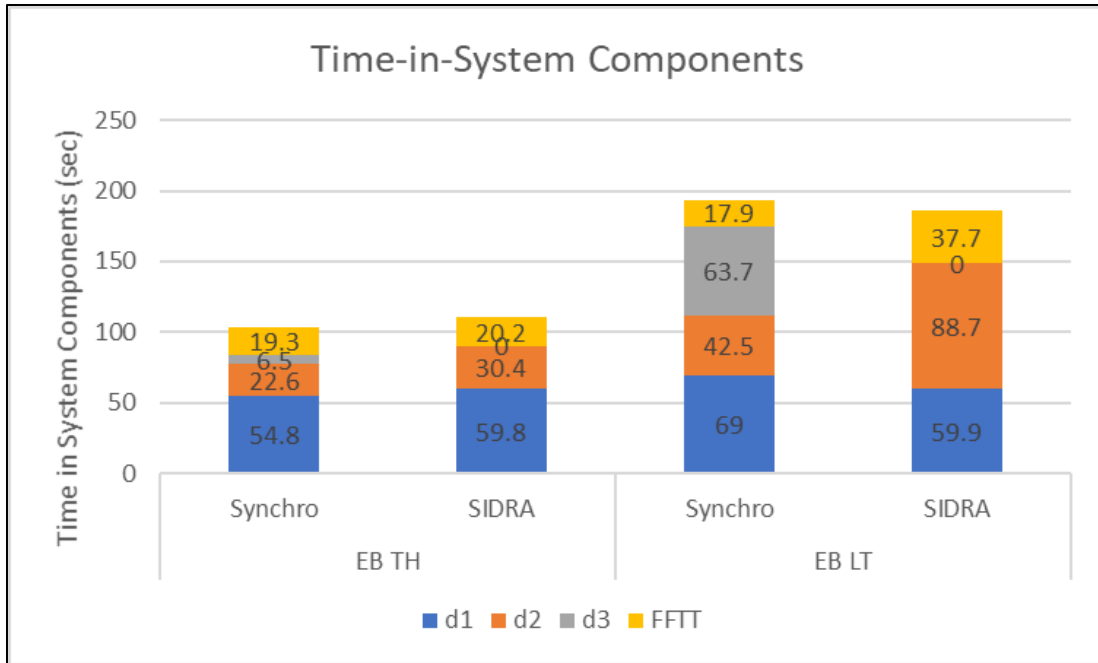


Figure 5-7: Components of time-in-system for EB approach at Oleander Dr. and S. College Rd. intersection

5.5 Summary and Discussion

This chapter presented the model assessment findings for the coordinated intersection located in Wilmington, North Carolina. The traffic light operates as a fully-actuated coordinated signal. Data were collected at the site using a tethered drone and a fixed video camera. Vehicle trajectories were extracted from the collected videos using a third-party vendor’s platform. EB through and left movements were selected for calibration and validation. The employed drone at this site was able to easily capture the position of the back of queue for the approach of interest.

Important measures that were extracted from the field are time in system, vehicle counts, origin-destination matrix, entry and exit speed within the field of view. The following summarizes the lessons learned at this site:

- 1) Automatic data extraction quality degrades as vehicles are away from the drone. The closer the vehicles are to the drone, the higher the chance of being detected and tracked by the processing software. For this site, the upstream virtual gate could detect about 61% of vehicles while the stop bar gate could detect 100% of vehicles.
- 2) Initial and final queues should be incorporated in the demand extraction procedure as they tend to drastically impact the output of models.
- 3) Of the two analytical models, SYNCHRO directly considers the effect of an initial queue while SIDRA cannot account for the presence of initial queue in its Release 9. However, the initial queue is converted to extra demand in SIDRA. This not only resulted in high v/c ratio, but also yielded higher values of uniform and incremental

- delays. On the other hand, SYNCHRO's initial queue delays were modest and comparable to the field observations.
- 4) Trans Modeler initial queue length coding requires an iterative process, where demand volumes are entered, and queue length measured at the end of the model warm up period. The process is repeated until the measured queue length closely match the initial queue in the field.
 - 5) Due to the nature of operations of the traffic signal (very similar to a pre-timed signal due to phase max-outs), the signal timing coding in SYNCHRO and SIDRA were easily achieved. However, Trans Modeler needed a substantial amount of effort to accurately code the signal controller settings.
 - 6) The field saturation flow rates at that site were found to be low compared to the baseline value in the HCM (about 10% lower).
 - 7) The initial queue delays derived from the HCM6 model appear to be generating excessive delays that are not consistent with the field observations.

In general, Trans Modeler was best able to match the time in system in the field, albeit with some overestimation for the through movements. It was followed by SYNCHRO which overestimated the time in system by almost a quarter for the EB-TH and by more than half for the EB-LT. SIDRA had the largest difference (more than 50% for both the through and left turn movements) compared to the field observations. It appears that the main source of overestimation is traced back to SIDRA's inability to explicitly incorporate the effects of an initial queue.

6 Chapter 6: Offset Intersection

This chapter assesses the validity of the three analytical and simulation tools in accurately describing traffic performance at the offset intersection of Capital Blvd. and Highwoods Blvd. on the west, and Westinghouse Blvd. on the East (35.816861, -78.600306). The segment between the two signals is approximately 410 ft. in length, and thus *can* create a spillback situation that may affect the discharge rate for both the EB Through traffic on Capital and SB left turn traffic from Highwoods Blvd. The estimated AADT for Capital Blvd. in this area is over 75,000. Figure 6-1 depicts a screenshot of the site. The two movements under consideration for validation were the EB through movement on Capital between the two intersections, and the SB left turn movement from Highwoods to Capital. It was expected that this first movement would operate at a very good LOS given the available number of lanes, ample green time and very good coordination. Conversely, we expect the LT movement from Highwoods to have lower capacity and encounter a sub-optimal progression offset at the second intersection.



Figure 6-1: Plan View of Offset Intersection at Capital, Highwoods and Westinghouse Blvd

6.1 Site Description

The site geometric layout is shown in Figure 6-2. Note that the exclusive left turn lane on Capital and Westinghouse was not included in the models' codes since this movement (a) did not interfere with either of the two movements selected for evaluation and (b) that LT lane carried very little traffic during the data collection period. The E-W through movement operated from three exclusive and one shared lane, while the SB LT movement had a single exclusive lane. Finally, because of the skew in the LT from Highwoods movement, we expect a slight reduction in its saturation flow rate and capacity. Signal data came from the split monitor and were verified with ground cameras on the key approaches being investigated.

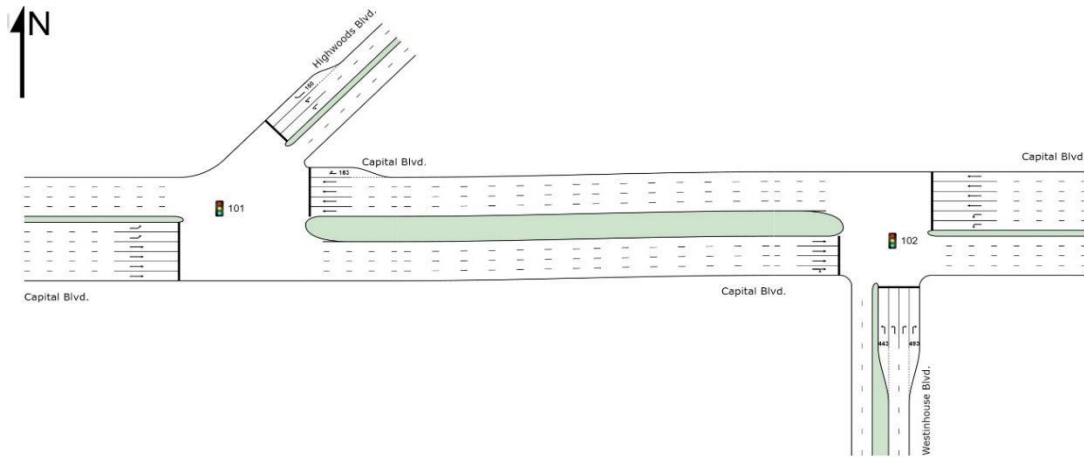


Figure 6-2: Geometric Layout of the Offset Intersection

6.2 Data Collection and Extraction

6.2.1 Data Collection

Similar to the previous sites, data collection was primarily carried out using drone video supplemented with ground cameras. Because of the limited field of view and the need to cover both intersections, the focus was on traffic traversing the short E-W link between the two intersections whether it arrived from the north or the west. However, only a very short segment upstream of the Highwoods intersection could be covered by the drone video. Similar to the previous sites, drone videos were processed through the Data From Sky (DFS) party. The team then used the DFS pixel data to generate the vehicle trajectories in the system. This enabled the team to extract all calibration and validation parameters. Figure 6-3 shows a screenshot of the DFS processed video, along with the location of the virtual sensors (shown in yellow) needed to extract the movement travel times.

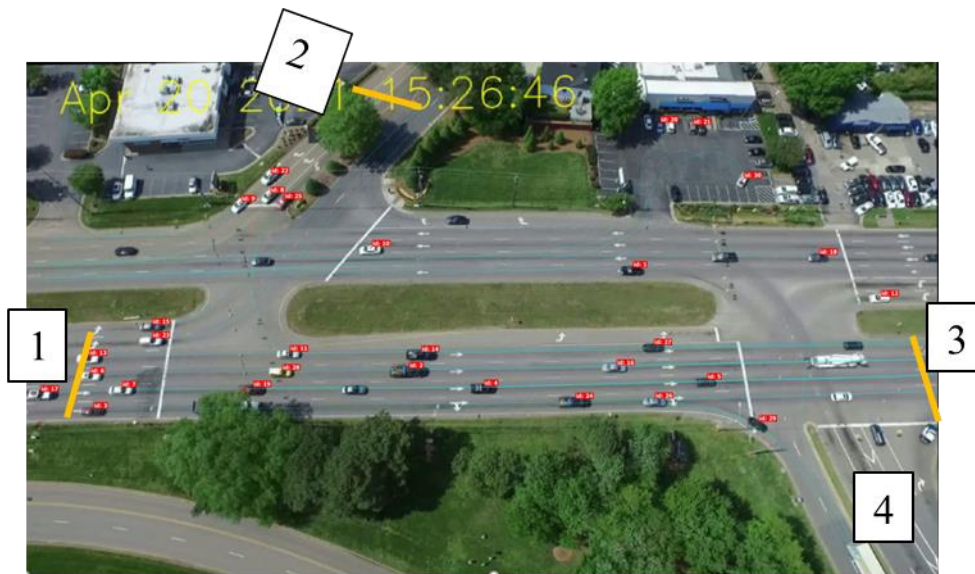


Figure 6-3: DFS Processed Screenshot of Offset Intersection with Vehicle Trajectory IDs, OD Labels and Location of Virtual Sensors

The numbered boxes designate the origins (1, 2) and destination (3, 4) points of the selected movements. Because the processed video data includes individual vehicle trajectories, all calibration and performance statistics are movement or OD based.

6.2.2 Demand Volume Extraction

Demand volumes were extracted directly from the drone video at the two intersections, yielding the turning movements counts shown in Table 6-1. There were no initial queues to speak of at either intersection, so that no additional modification to the demand was needed. The highlighted cells show the selected movements used for model validation purposes.

Table 6-1: Estimated Demand Flow Rates at the Two Offset Intersections

	Capital Blvd and Highwoods Blvd					
Approach	EB		WB		SB	
Movement	LT	TH	TH	RT	LT	RT
Demand Flow Rate (vph)	76	2,662	2,606	126	151	352
	Capital Blvd and Westinghouse Blvd					
Approach	EB		WB		NB	
Movement	TH	RT	LT	TH	LT	RT
Demand Flow Rate (vph)	2,650	201	50	2,681	107	138

In addition, Trans Modeler requires the designation of OD flows for its simulation. These are depicted in Table 6-2 below. The highlighted cells pertain to the movements of interest.

Table 6-2: Origin Destination Hourly Demands at Offset Intersection





Origin (FROM) Destination (TO) Index	To 1	To 2	To 3	To 4
From 1	-	76	2,499	164
From 2	352	-	113	38
From 3	2,580	102	-	50
From 4	74	33	138	-

* Index numbers are shown in Figure 6-3.

6.2.3 Signal Data Extraction

The signal data at both intersections were extracted from the split monitor reports and confirmed by the drone videos upon monitoring the departure times of the different movements at their stop line. The prevailing cycle length during data collection was set at 263 seconds. The EB through movement offset was measured at 13 seconds between the two EB stop lines. The distance

between these two stop lines is about 410 ft. The phasing plan is shown in Figure 6-4. It is clear that while the EB through movement demand is quite high (in excess of 2,650 vph across 4 lanes), it accounts for most of the cycle green time (around 215 seconds in $\Phi 2$). The team does not expect that movement to be problematic unless the field offset were found to be sub-optimal and generating queue spillback within the short inter-intersection spacing. Conversely, the LT movement from Highwoods to Capital receives less than 30 seconds of green in $\Phi 4$.

Capital & Highwoods Blvd (Upstream) Intersection Signal Phase (Cycle= 263 sec)		
$\Phi 2$		$\Phi 4$
		
230 sec		33 sec
$\Phi 6$	$\Phi 5$	
		
190 sec	40 sec	





Capital & Westinghouse Blvd (Downstream) Intersection Signal Phase (Cycle= 263 sec)		
$\Phi 1$	$\Phi 2$	$\Phi 4$
		
13 sec	217 sec	33 sec
$\Phi 6$		
		
230 sec		

Figure 6-4: Signal Phasing Plan at the Offset Intersection

6.2.4 Field Performance Measures

Similar to our selection of MOE's in the previous sites, travel time or time in system between the virtual sensors was the selected validation measure. For EB-TH the sensor distance is 605 ft. and 776 ft. for the SB-L movement. Travel time was extracted for both the EB-TH on Capital and SB-L from Highwoods Blvd. As expected, individual vehicle travel times are highly variable, and will depend on their arrival time at the stop line----- as shown on the X-axis in Figure 6-5 --- (between ODs 1-3 and 2-3). It is important to note that this travel time includes the experienced delay at the two signals on Highwoods and Westinghouse in addition of course to the link(s) travel times. On average, travel time for the EB-TH movement was 15.03 sec, while that for SB-L was 146.8 sec. Due to occlusion by trees and signage, the SB-L travel time

was collected manually from the video, thus the smaller sample size. For comparison purposes, the free flow travel times for those two movements were estimated at 9.2 and 11.8 sec, respectively. The standard error for the mean travel time was 0.7 seconds for the EB-TH movement and 23.1 sec for the SB-L movement. Thus, our original assumption regarding the quality of traffic performance for those two movements appears to be validated by the data.

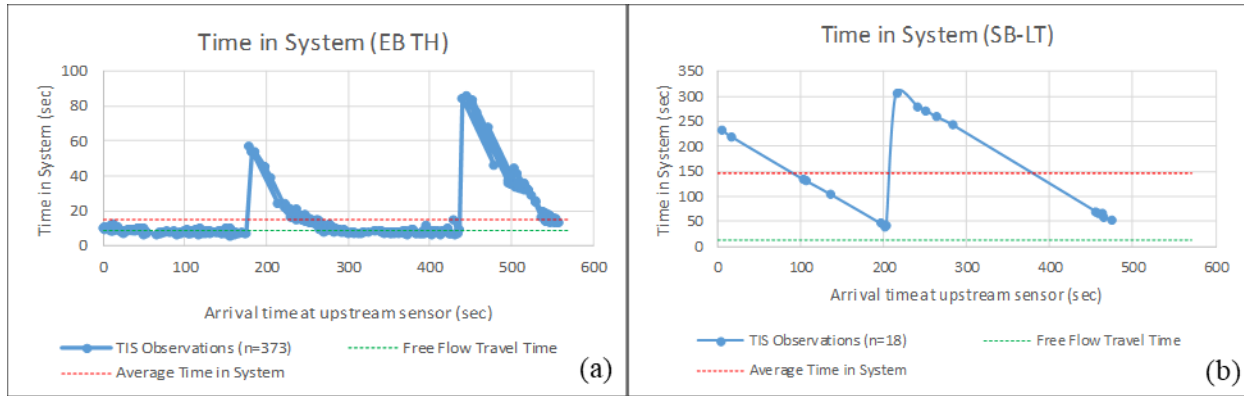


Figure 6-5: Travel Time Profiles for (a) EB-TH and (b) SB-L Movements at Offset Intersection

6.3 Models' Testing and Calibration

As stated earlier, the team's approach to model calibration was to deliver the most accurate input and calibration parameters in all models tested. This includes demand volume levels including any initial queues, signal timing parameters, actual entry speed and saturation flow rates. Demand levels were reported earlier.

Saturation flow headways were directly extracted from the DFS processed video by setting a virtual sensor at the stop line for the EB-through movement on Capital at Westinghouse, and the left turn movement on Highwoods, and tracking the vehicle discharges. Due to the limited field of view as shown in Figure 6-3, while it was possible to measure the discharge at the upstream signal, we could not ascertain whether the vehicles came from a stopped queue, a prerequisite to measuring saturation flow rate. Table 6-3 below gives a summary of the observed saturation headways and resulting saturation flow rates from video period. The calibrated values again appear to be lower than the default values in the Highway Capacity Manual (1,900 pc/h/pl) for signalized intersections. The base saturation flow rate value used in SIDRA and SYNCHRO was 1,700 pc/h/pl which was also adjusted for heavy vehicle and turning movements. The corresponding, calibrated buffer headway in Trans Modeler was 0.6 seconds. Finally, there was no need for adjusting the entry or exit speeds in the models, and those were kept at the prevailing speed limit for both approaches.

Table 6-3: Field Saturation Flow Rates by Movement

Movement	Number of Observations	Observed Avg. Saturation Headway (sec)	Observed Saturation Flow Rate (vphpl.)
SB LT	35	2.1986	1,637
EB TH*	85	2.1154	1,702

*Measured at Capital and Westinghouse

6.4 Model Validation

We first provide a note on the models’ reporting of the performance measures. By coding the approach and exit lengths to be equal to the setback of the upstream and downstream sensors shown in Figure 6-6, SIDRA will directly report the travel between them. SYNCHRO on the other hand does not report travel time, but strictly control delay at the signal. In this case, travel time is estimated as the control delay plus the free flow travel time (based on the field entry speed). TransModeler travel times are computed by setting virtual sensors in the simulation and tracking the vehicles’ time between the two sensors.

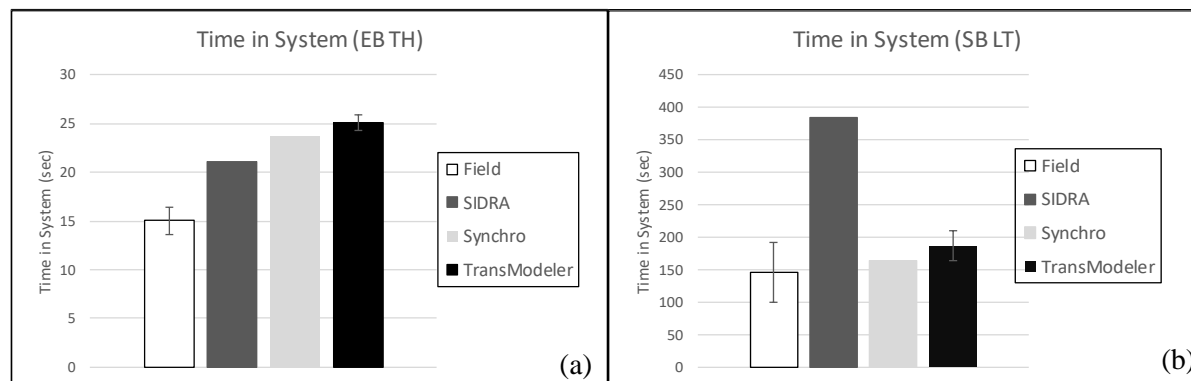


Figure 6-6: Initial Model Validation Results at the Offset Intersection

An *initial* validation of the time in system across models for the two movements is depicted in Figure 6-6. For the EB-TH movement (a), all three models’ predictions were within 10 seconds of the field measurements indicating a LOS in A/B region. However, the SIDRA model appears to severely overestimate the travel time for the SB-L movement (b), while the other two models produced reasonable estimates compared to the field value.

Further exploration of the SIDRA model results revealed that the effective saturation flow rate generated by SIDRA for the SB-L movement dropped to 900 vphpl, causing its v/c to exceed 1.0 by a significant margin and resulting in excessive delay and travel time. Consultation with the model developer indicated that the current model release does not distinguish between a moving or stopped downstream queue. Therefore, the model may predict a blockage of the short link between the two intersections when in fact it may not exist, resulting in a steep drop in the SB-L capacity. This required the team to recalibrate the SIDRA model to the observed

saturation base flow rate of 1,700. Fortunately, SIDRA enables the calibration of a blockage effect on upstream flows through its “Lane Blockage Calibration Factor”. The factor default is 1.0, and the calibrated value yielding the field observed saturation flow was 0.20.

The revised validation figure, post recalibration is depicted in Figure 6-7 below. It is clear that the revised SIDRA travel time is now much closer to both the other two models and the field value, dropping from about 380 sec to 194 sec. Nevertheless, all three models tended to overestimate the field travel time for this particular movement.

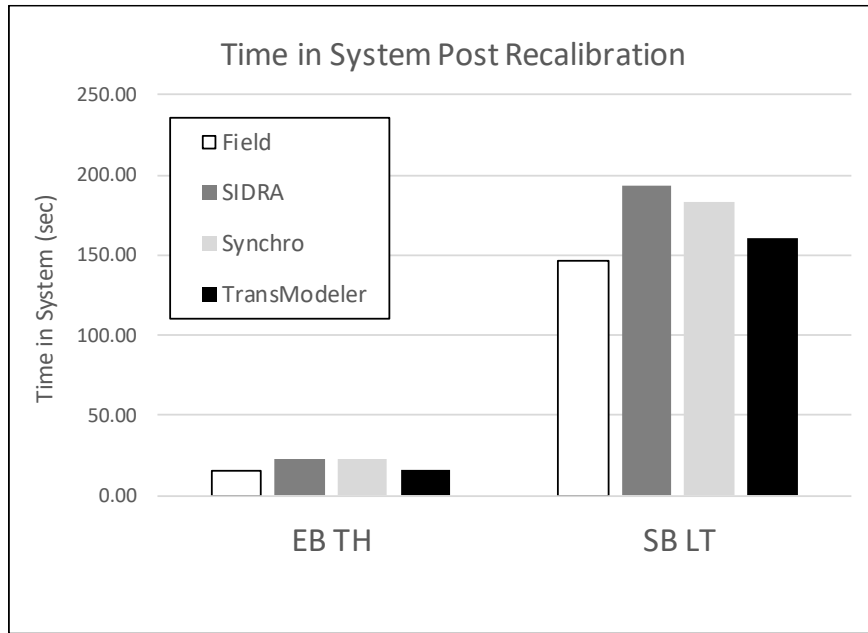


Figure 6-7: Validation Results Post Recalibration of SIDRA Model

6.5 Summary and Discussion

The site covered in this chapter is an offset intersection with spacing between the two intersection stop lines on the main approach slightly above 400 ft. Data collection at that site used drone video supplemented with ground cameras and extracted by a third party vendor, which enabled the team to produce vehicle trajectories within the field of view. The team selected the SB left and EB through movements for calibration and validation. Those movements had very different capacities, both in terms of number of lanes (4 for EB-TH, 2 for SB-L) and fraction of effective green in the cycle (85% for EB-TH, 11% for SB-L). A key aspect of model evaluation at that site was their ability to handles any queues in the short segment, and its impact on the upstream movements through that segment. Similar to the earlier sites, the time in system between key points on both intersections was the selected performance measure.

Key findings and lessons learned at this site follow:

- 1) For sites having multiple intersections, including the offset intersection, travel time comparisons between model predictions and field observations are preferred as they include the effect of both intersections timings and progression quality.

- 2) Field observations of the drone video revealed the presence of a downstream queue for the EB-T movement arriving from Highwoods. That queue – formed by the SB-L movement stopped at Westinghouse, tended to reduce the saturation flow rate to some extent. However, the very high g/C ratio for that movement (0.85) more than compensated for the downstream queuing effect.
- 3) The three models tested were able to replicate the travel time for the EB-TH movement without difficulty. All models predictions were within 10 seconds of the field measured time in system.
- 4) Both Synchro and more so SIDRA tended to overestimate the travel time for the SB-L movement from Highwoods Blvd. Further testing revealed that the SIDRA model cannot adequately differentiate between a static and moving queue on a downstream link. Thus it predicted a downstream blockage that in fact did not materialize. Synchro had some difficulty modeling the queuing impact on the EB-TH movement at Highwoods.
- 5) Using SIDRA's *lane blockage calibration factor*, the team was able to reproduce the SB-L field saturation flow rate and brought SIDRA's prediction of travel time for that movement closer to the field value as well.
- 6) All three models tended to overestimate the SB-L travel time, even after re-calibration. Trans Modeler, however, generated the closest value to the field.
- 7) The delay estimation at sites with multiple intersections appears to be erroneous when using either of the two analytical methods, due to ignoring the platoon structure feeding the downstream approaches. This is explained, and addressed in more details in section 7-5 of the next chapter.

7 Chapter 7: Continuous Flow Intersection

This chapter discusses the models' assessment when applied to a continuous flow intersection (CFI) at the intersection of NC 16 and Mt Holly-Huntersville Rd in Mecklenburg County (35.325745, -80.945210). The 2020 AADTs on NC16 and Mount Holly are estimated at 42,000 and 15,000 respectively. The movements under consideration for validation were the North-Westbound through (labeled WB-TH) and North-Westbound left (WB-L). The two movements are in close proximity to I-485. A portion of their traffic originates from the off-ramp located at exit 16 of the interstate freeway. In addition, through and left movements travel time for the two movements identified earlier were evaluated in the models. Figure 7-1 shows the layout of the intersection.

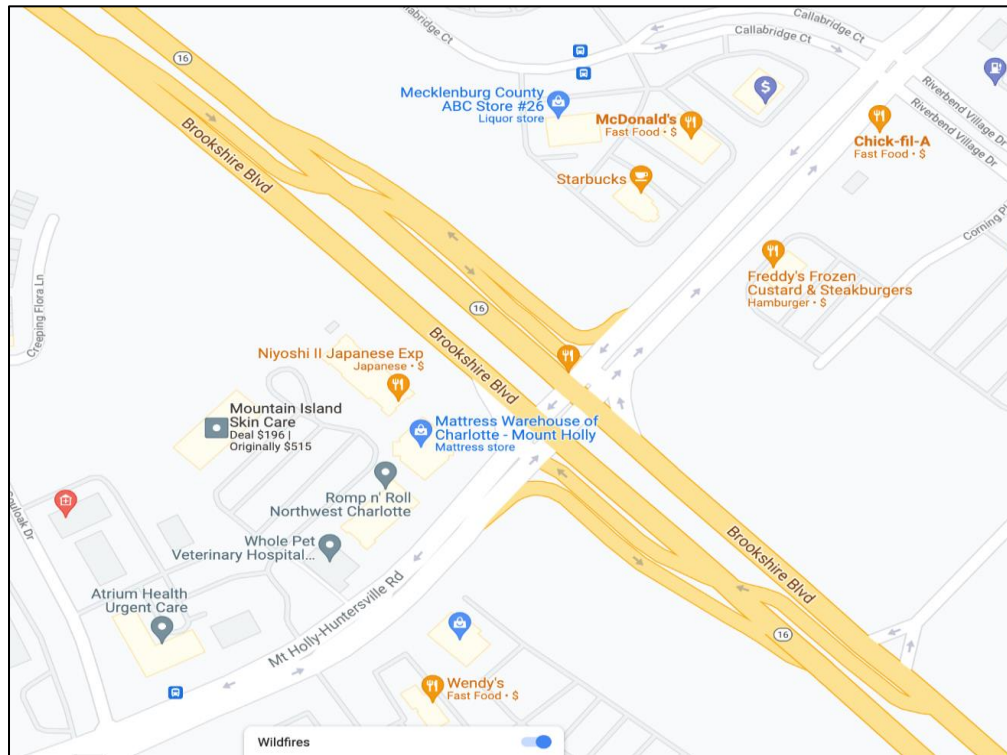


Figure 7-1: Plan view of Continuous Flow Intersection NC 16 and Mt Holly-Huntersville Rd

7.1 Site Description

The site geometric layout is shown in Figure 7-2. It includes three through lanes, an exclusive right turn lane, and two left turn lanes on the WB approach. Similar layout is provided for the EB approach. The left turns are displaced at a distance of about 800 feet from the stop line of the main intersection. The signalized intersections operate in semi actuated coordinated control with a fixed cycle length of 160 seconds, at an offset of 54 seconds between the WB left movement at the supplemental intersection, and the start of the WB through and left turn phase at the main intersection. The speed limit is 55 mph on NC 16 and 45 mph on Mt Holly-Huntersville Rd.

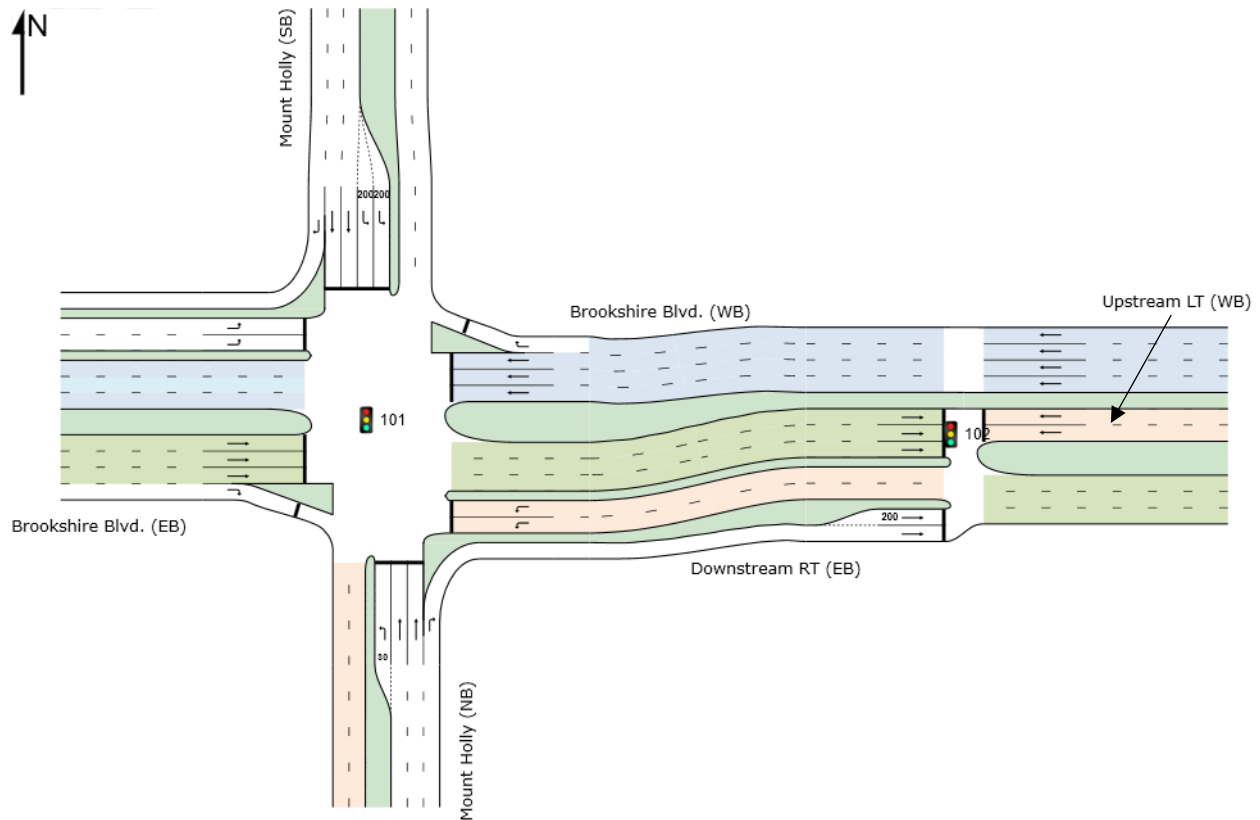


Figure 7-2: Geometric Layout of the CFI at NC 16 and Mt Holly-Huntersville Rd

7.2 Data Collection and Extraction

7.2.1 Data Collection

Similar to the previous sites, data collection at this site was primarily carried out using drone video supplemented with ground cameras. Because of the limited field of view, two drones were deployed to cover the main and supplemental intersections. One focused on the main intersection while the other focused on the displaced left turn at the upstream intersection located about 800 feet on the WB approach. Similar to the previous sites, drone videos were processed through the Data from Sky (DFS) vendor. The team then used the DFS pixel data to generate the vehicle trajectories in the system. This enabled the team to extract all calibration and validation parameters. Figure 7-3 shows a screenshot of the DFS processed video, along with the location of the virtual sensors (shown in red) needed to extract the movement travel times. Travel distances are also indicated in the figure.

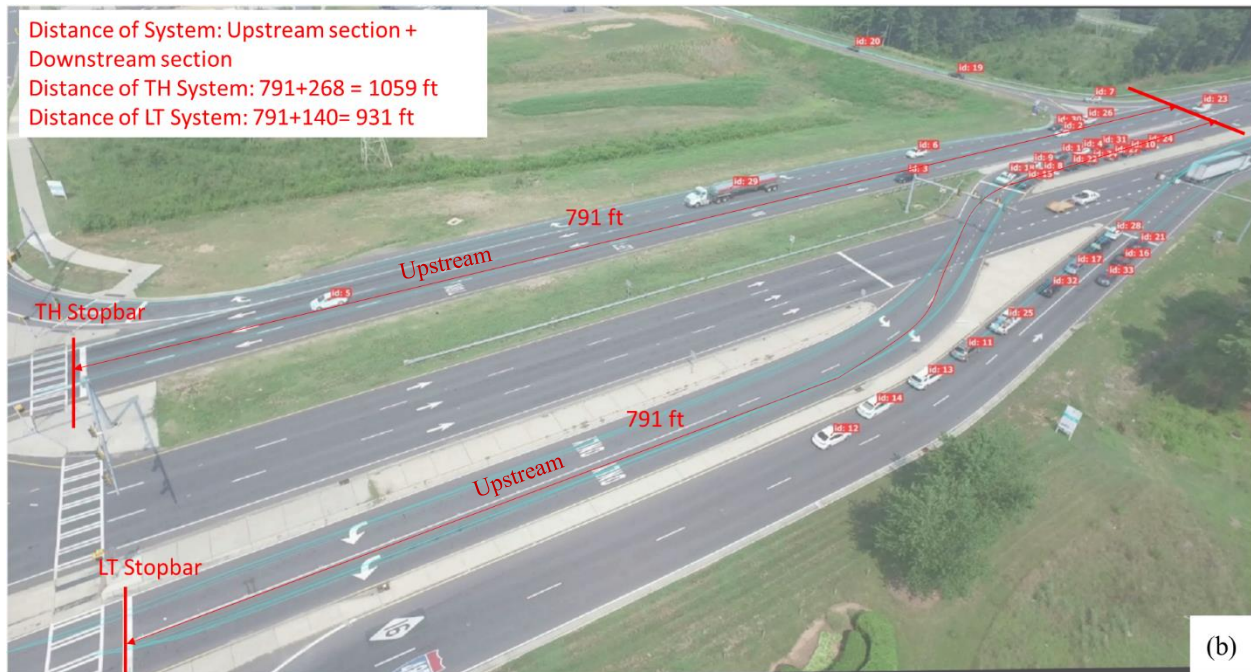
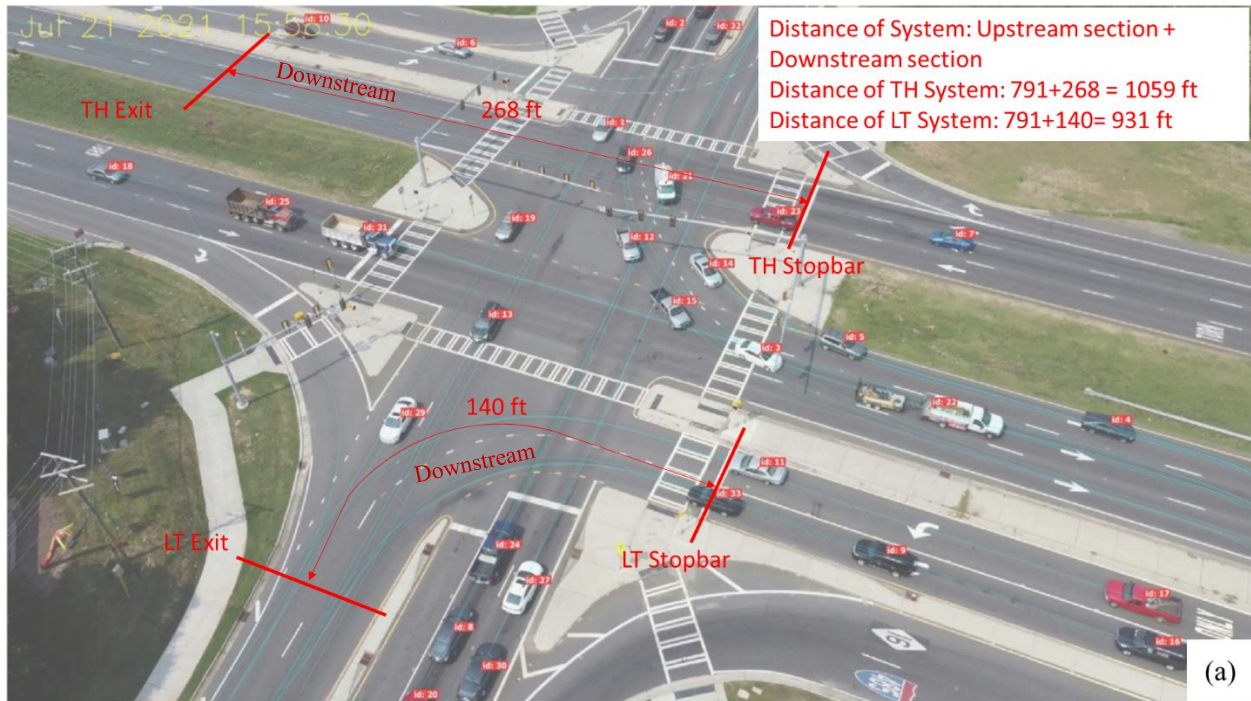


Figure 7-3: DFS Processed Screenshot of a) Main Intersection and b) North Westbound Intersection at NC 16 and Mt Holly-Huntersville Rd along with trajectory IDs and Location of Travel Time Sensors

7.2.2 Demand Volume Extraction

Demand volumes were extracted directly from the drone video at the two intersections, yielding the turning movements counts shown in Table 7-1. There were no significant initial queues at the

start of the data extraction at either intersection, thus no additional modification to demand was needed. The highlighted cells show the selected movements used for model validation.

Table 7-1: Estimated Demand Flow Rate at the Intersection

	WB			EB			NB			SB		
T = 1189 sec (19:49)	LT	TH	RT	LT	TH	RT	LT	TH	RT	LT	TH	RT
Count (veh/T)	59	385	49	44	316	7	7	133	116	95	153	73
Flow Rate (veh/h) *	231	1506	192	133	957	21	21	403	351	288	463	221

7.2.3 Signal Data Extraction

Although split monitor reports were acquired from NCDOT, the team could not use them for the analysis due to issues with Econolite at the crossover intersection. As such, the signal data at both intersections were extracted from ground camera videos. The prevailing cycle length during data collection was 160 seconds. The LT offset between the upstream and the main intersection was 54 seconds. The phasing plan is shown in Figure 7-4 with the highlighted movement depicted in green. It is evident that the through movements on NC 16 receive the majority of the cycle green; much less green time is given to the minor approaches on Mt Holly-Huntersville Rd.

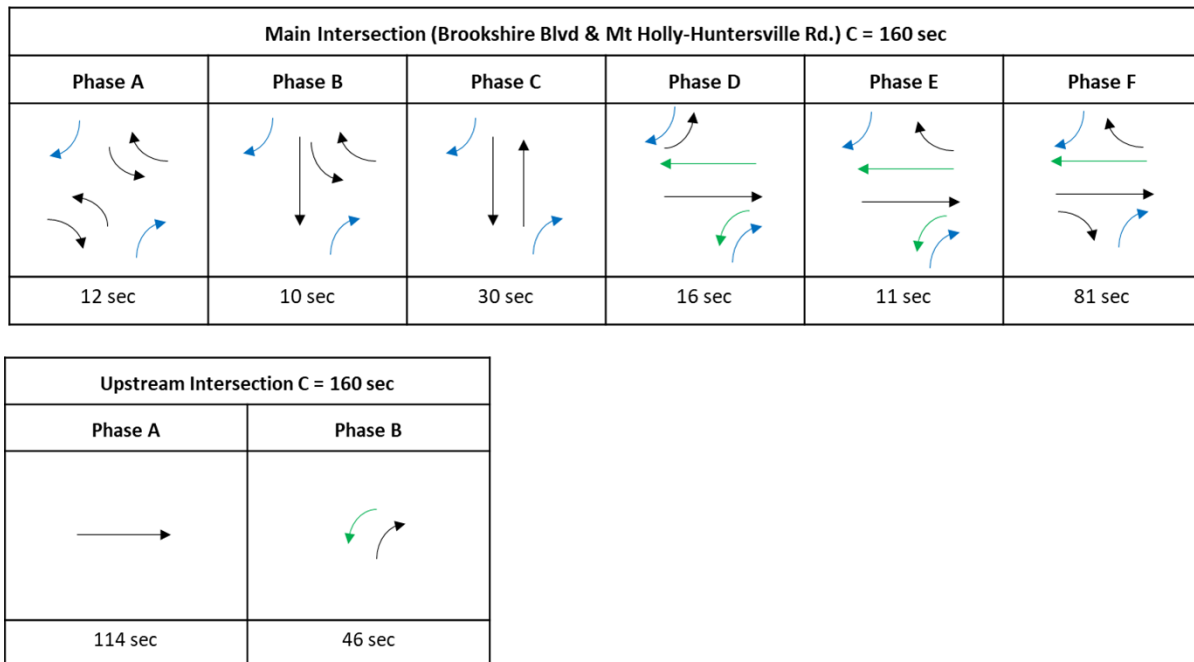


Figure 7-4: Signal Phasing Plan for Main and North Westbound Intersections of CFI

7.2.4 Field Performance Measures

For this site the team used travel time or time in system between virtual sensors as the validation measure. For the WB-TH and WB-L movements the sensor distance is 1,059 ft. and 931 ft., respectively. As was the case for other sites, the individual vehicle travel times are highly variable and directly depend on their arrival time at the stop line as shown in Figure 7-5. Figure 7-5 (a) includes the through delay experienced at the main intersection only, whereas Figure 7-5 (b) includes both delays at the upstream and the main intersection for the left turn movement.

Figure 7-5 (c) and 7-5 (d) includes delays beyond the main intersection stop line, to the exit detector as shown in Figure 7-3 (a). On average, travel time for the WB-TH movement was 32.2 seconds, and 95.3 seconds for the WB-L movement. The left movement travel time reflects the low green time available for that movement. The travel time for the two movements is shown by the dashed red lines. The green dashed lines depict the free flow travel times (about 9.81 seconds for both movements). The standard error for the mean travel time was 1.05 seconds for the WB-TH movement and 5.14 seconds for the WB-L movement. Thus, our original assumption regarding the quality of traffic performance for those two movements is validated by the data.

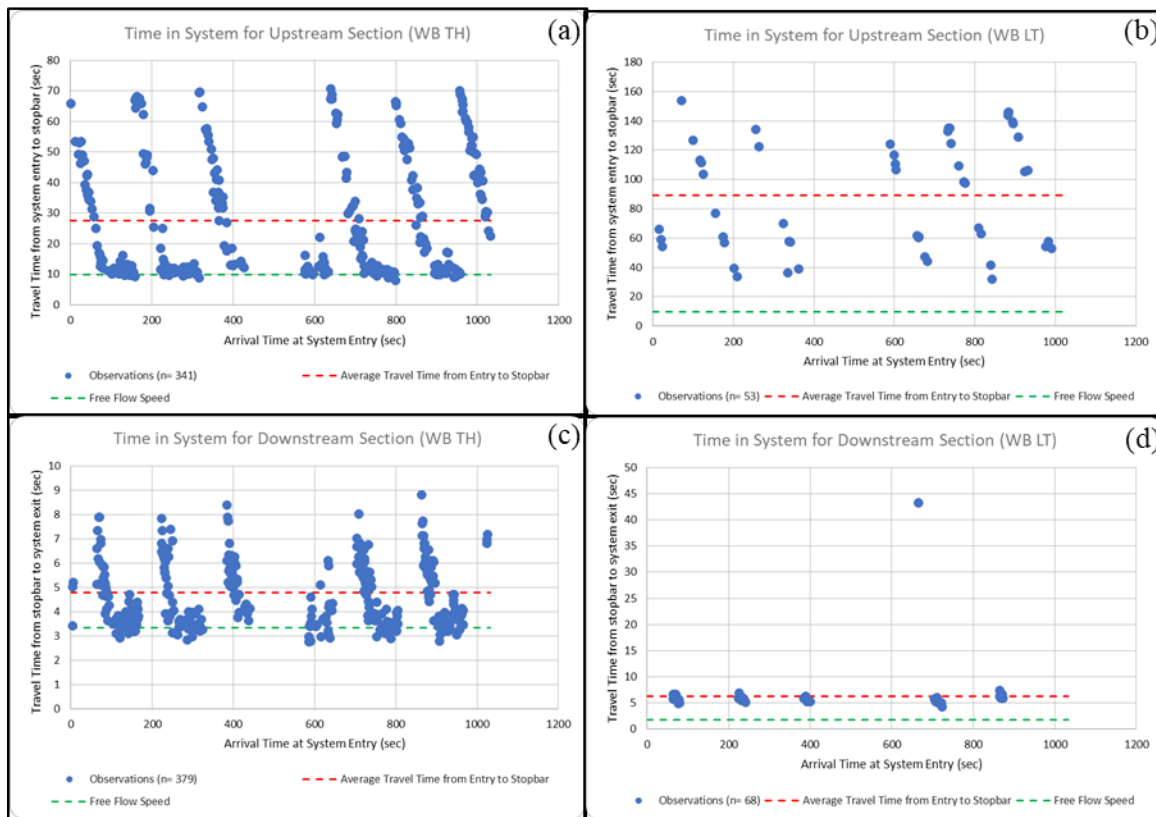


Figure 7-5: Travel Time Profiles for (a) WB TH and (b) WB LT Movements in Upstream Section and for (c) WB TH and (d) WB LT Movements in Downstream Section

7.3 Models' Testing and Calibration

As stated earlier, the team's approach to model calibration was to deliver the most accurate input and calibration parameters in all models tested. This includes demand volume levels including any initial queues, signal timing parameters, actual entry speed and saturation flow rates. Demand levels were reported earlier in the chapter. Saturation flow headways were directly extracted from the DFS processed video by setting a virtual sensor at the stop line for the WB-TH movement on NC16 at the East approach.

The saturation flow rate for the WB-L and WB-TH were found to be 1,698 vphpl and 1,777 vphpl, respectively. The two saturation flow rates were calculated at the main intersection. The left turn queues at the upstream intersection were not long enough for a reliable estimation

of a saturation headway. The corresponding, calibrated buffer headway in Trans Modeler was found to be 0.5 seconds. The entry and exit speeds for this facility needed not be explicitly entered in the model because the observed back of queue was well within the field of view of the drone and in no instance the back of queue exceeded beyond the upstream sensor. As such, the entry speed was coded as 55 mph (speed limit of the approach).

7.4 Model Validation

Travel time estimation mechanics for the three tools is different as mentioned in previous chapters. SIDRA directly reports travel time for the sections modeled. SYNCHRO does not report travel time, but only control delay at the signal. In this case, travel time is estimated as the control delay plus the free flow travel time. TransModeler travel times are computed by setting virtual sensors in the simulation and tracking the vehicles' time between the two sensors.

The validation of the time in system across models for the two movements is depicted in Figure 7-6. For the WB-TH movement, all three models' predictions were within 5 seconds of the field measurements. For the WB-L movement Trans Modeler results were within 5 seconds of the field measurements. However, SYNCHRO and SIDRA results were off by more than 20% of the field measurements in this case. Both models overestimated the time-in-system for this movement due to modeling issues that are discussed in the next section.

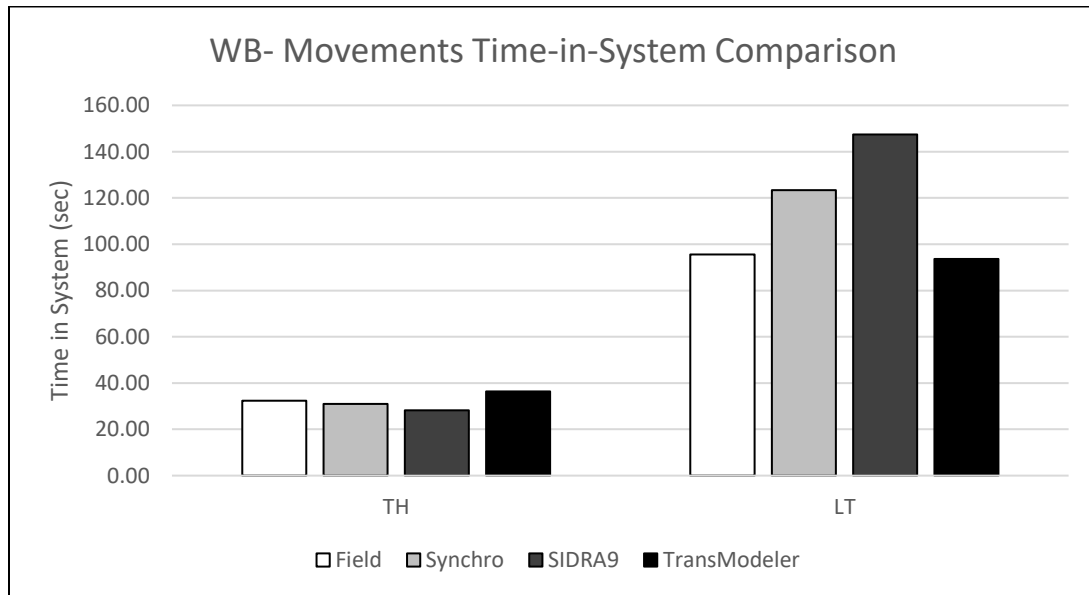


Figure 7-6: Model Validation Results for the two movements on the Westbound Approach

7.5 Addressing the Limitations of Analytical Models at CFI's

It is clear from Figure 7-6 that both Synchro and Sidra tend to overestimate the delay and travel time for the left turn movement at the main intersection. In fact, this result reveals a much more general problem for this class of models. That is, their delay estimation for a platoon of vehicles leaving one intersection and arriving at a downstream intersection during a

portion of the cycle is problematic. The same situation can also be shown to occur at the offset intersection covered in Chapter 6, where the SB-LT movement enters the EB approach on Capital Blvd and Westinghouse. What both analytical models assume is that the upstream flow platoon departs throughout the cycle and merges with other traffic downstream (when applicable). Therefore, both models assume that the LT movement in the CFI will experience a red time of 140 seconds, and a green time of 20 seconds at the main intersection.

In reality the left turn movement at the upstream intersection is blocked from proceeding to the main intersection for most of the cycle, which is about 118 sec of the 160 sec cycle. Only during the remaining green time of 42 seconds is that platoon allowed to proceed downstream. Simply stated, the LT flow rate downstream is literally zero during the 118 seconds and non-zero only during the 42 seconds. Not only that, but how much of the red time that platoon will encounter at the main intersection depends on the green offset between the two left turn signals. In our case, the lead LT vehicle in a cycle will arrive approximately 36 seconds before the main intersection green starts. So, in effect *the 36 seconds is the effective red time* for that movement. The actual main intersection LT green time is 20 seconds, and both Synchro and Sidra assume the actual red time to be $160 - 20 = 140$ sec. That is the primary reason for the rather high predicted delay for that movement by both models.

The solution to this problem is illustrated in Figure 7-7. That figure shows the most likely arrival and departure patterns in the average cycle for the LT movement in the *critical lane* at the main intersection. Field data also showed a high level of lane underutilization observed in the data, with the inner or left lane carrying close to 70% of the overall LT traffic. The flow rate (q) of 0.1714 v/s represents the average arrival flow rate in the critical lane during the 42 sec of upstream green; the departing flow rate (s) of 0.4722 v/s is the observed saturation flow rate of 1,700 pcph/lane. The actual green offset between the two signals is 54 seconds, of which 18 sec constitute the travel time between the two stop lines. Thus, the area bounded between the arrival and departure lines represents the total delay in the average cycle. In addition, there is a maximum number of vehicles that the downstream signal can handle per cycle, which is about 9.4 vehicles (on average) in the critical lane or 13.4 vehicles in both lanes. Should the upstream signal send more than this volume per cycle, the main intersection approach will become oversaturated and queues may develop that could even affect the upstream signal efficiency.

The delay and travel time calculations for the critical and non-critical lanes at the downstream, intersection are depicted in Table 7-2 below. Note that at the bottom of the table the upstream delay and free flow travel time have been added to generate the overall travel time for that movement through the entire intersection.

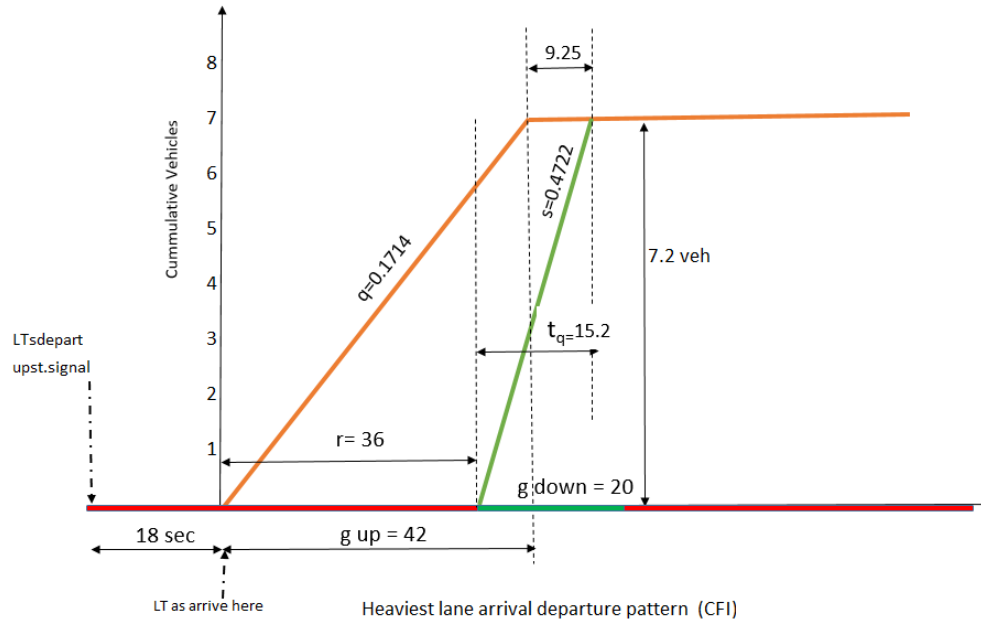


Figure 7-7: Arrival and Departure Flows for the WB-LT Movement Intersection of Brookshire and Mount Holly CFI

Table 7-2: Proposed Travel Time Estimation Method for WB-L Traffic at Main Intersection

Variable	Left Lane	Right Lane	Combined
Hourly volume	162	69	231
Vehicle arrivals per cycle (C= 160 s)	7.2	3.1	10.3
Platoon Length leaving the upstream signal (s)	42	42	42
Departing Flow Rate (v/s) This is the volume /cycle divided by platoon length	0.1714	0.0730	
Saturation flow rate (v/s)	0.4722	0.4722	
Experienced red time at Main Intersection (s)	36	36	
Effective green time at Main Intersection (s)	20	20	
Time to clear the lane queue (s)	15.2	6.6	
Uniform Back of Queue (veh.)	7.2	3.11	
Overall delay per cycle (s)	162.9	55.97	
Uniform delay per vehicle (d ₁)	22.6	18.3	21.32
Lane Capacity (vph)	607	607	
Lane v/c ratio = 7.2/(.4722*20) in left lane	0.76	0.32	
Overflow delay per vehicle (d ₂), (s)	8.79	1.42	6.59
Overall control delay per vehicle (d), (s)	31.4	19.7	27.9
Overall control delay at upstream signal (s)	50.38	46.09	49.1
Free flow Travel time for LT movement (s)			18.3
Total travel time for LT movement (s)			95.3 s

The table above proposes a new and validated method for estimating travel time at a CFI for a LT movement that is stopped at two intersections on a CFI approach. It takes care of the demand starvation at the downstream signal during most of the red phase, and takes into account the effect of the offset on the arrival pattern at the main intersection. For comparison purposes, the field travel time for this movement was measured at 95 sec as shown in Figure 7.5 (b) and 7-5 (d). This is virtually identical to the predicted value by the new method in the above table.

The new method computational details have been shared with the Sidra model developers, and they plan to fully incorporate it in a future version of that software. It may be useful for NCDOT to also be aware of this limitation in their use of Synchro for that purpose. This method was also applied to the SB Left turn movement at the offset intersection at Capital Boulevard and Highwoods Blvd. It resulted in a revised estimated travel time for that movement of 152 seconds, compared to an observed field value of 147 seconds, and (uncorrected) model estimates of 183 sec, 193 sec and 164 sec in Synchro, Sidra, and Trans Modeler, respectively.

Finally, it is clear that the current field offset of 54 sec in the CFI is not optimal for the left turn movement, since 85.7% of the downstream arrivals occur during the red phase as depicted in Figure 7-7. However, when compared to the magnitude of through movement volumes, it makes little difference when the overall delay across all movements is concerned.

7.6 Summary and Discussion

This chapter covered the continuous flow intersection located in Mecklenburg County. The site was recently built to replace a traditional signalized intersection. The left turn movements are displaced 800 ft from the main intersection's stop bar. As opposed to other sites, the data collection at the site used two drones supplemented with two ground cameras. One drone covered the main intersection while the other focused on the left turn movement. DFS was used as the main medium for processing the drone video footage reporting trajectories and other needed input and performance measures. Validation for this intersection focused on the Westbound approach and encompassed two movements – Westbound Through and Westbound Left.

Key findings and lessons learned at this site follow:

- 1) A single drone was not deemed sufficient to capture the operation of the main intersection and its crossovers. As a result, two drones were deployed at the site. One focused on the main intersection while the other focused on the approach of interest and the crossover left turn signal at that approach.
- 2) Drone footage data processing included a manual step to match vehicles observed in the two videos since DFS does not provide an automatic procedure for matching the vehicles in consecutive videos. This step is crucial for accurate estimation of delay and time-in-system for individual vehicles.
- 3) In the absence of split monitor reports for a signalized intersection, fixed video cameras can be used to capture signal splits. Footage from fixed video cameras were used to extract the splits for this site since the split monitor reports provided were defective.

- 4) The measured saturation flow rates were found to be below the current HCM defaults. The saturation flow rate for the WB-TH and WB-L were found to be 1,777 and 1,698, respectively.
- 5) The model predictions for the through movement travel time were all within 5 seconds of the observed field values indicating the utility of both the simulation and analytical model in estimating performance for such low-delay movements.
- 6) Both SIDRA and SYNCHRO tended to overestimate the delay and travel time for the WB-LT movement by over 20%. Trans Modeler on the other hand produced travel times that were again within 5 seconds of the field observations for that movement.
- 7) The team has developed a new approach to estimate delay for the LT movement at CFI's at the main intersection. The method corrects the current faulty assumptions in both SIDRA and SYNCHRO regarding continuous arrivals at the main intersection throughout the cycle. The correction has produced a travel time virtually identical to the field value.
- 8) The new method mentioned in the previous bullet also applies to offset intersections, and in fact to the general case where any minor street traffic that is entering another downstream intersection during a limited time period of the cycle is being evaluated.

8 Chapter 8: Traditional Diamond Interchange

This chapter covers the models' assessment when applied to a traditional Diamond Interchange at the intersection of I-85 and NC-86 in Orange County (36.059035, -79.082474). The estimated AADT for NC86 in that area is about 11,000 with AADTs for the on-ramp and off ramps ranging from 2,700-3,600. The movements under consideration for validation were the SB through and right turn movements at the North intersection of the interchange, along with the WB-L movement originating from the I-85 WB off ramp. In addition, through movement travel time in both directions between the North and South intersections was evaluated in the models. Generally speaking most movements in the interchange operate well below capacity. Figure 8-1 shows the layout of the diamond interchange, along with the 4 origin and destination points used in the analysis.



Figure 8-1: Plan View of Traditional Diamond Interchange at I-85 and NC 86 with Indicated Origin and Destination Labels

8.1 Site Description

The site geometric layout is shown in Figure 8-2. It includes a single shared through and left lane between the intersections, and two approach lanes on either side. Off ramps have dedicated right and left lanes at both intersections as well. The distance between the stop lines on NC86 is about 725 ft., which can accommodate a queue of nearly 27 vehicles in each direction. The signalized intersections operate in semi actuated coordinated control with a fixed cycle length of 90 seconds, at an offset of 31 seconds. Speed limit is 45 mph on NC86 and 55-65 mph on I-85 per NCDOT speed limit map.

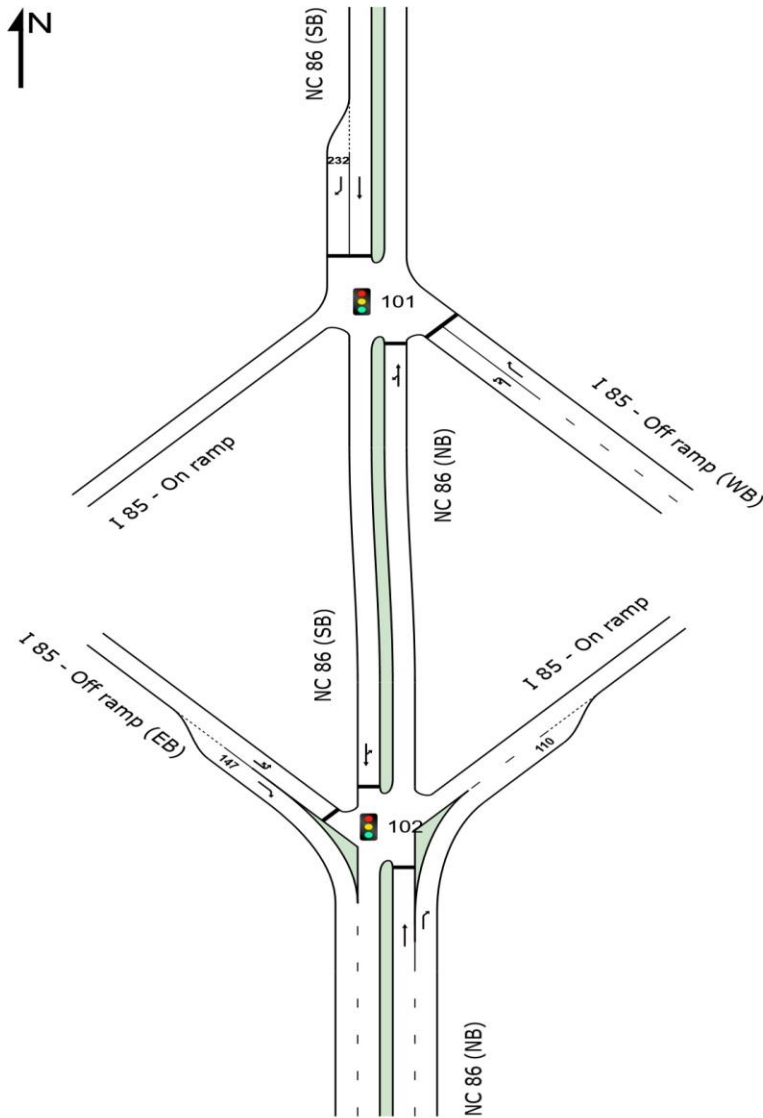


Figure 8-2: Geometric Layout of the I-85 and NC 86 Interchange

8.2 Data Collection and Extraction

8.2.1 Data Collection

Similar to the previous sites, data collection at this site was primarily carried out using drone video supplemented with ground cameras and in this case two Bluetooth units for the purpose of collecting route travel times on NC86. These units were located North and South of the signalized intersections at a distance of 1,822 ft. Because of the limited field of view, drone videos were focused on the three North Intersection movements. Similar to the previous sites, drone videos were processed through the Data from Sky (DFS) party. The team then used the DFS pixel data to generate the vehicle trajectories in the system. This enabled the team to extract all calibration and validation parameters. Figure 8-3 shows a screenshot of the DFS processed video, along with the location of the virtual sensors (shown in red) needed to extract the movement travel times. Travel distances are also indicated in the figure.

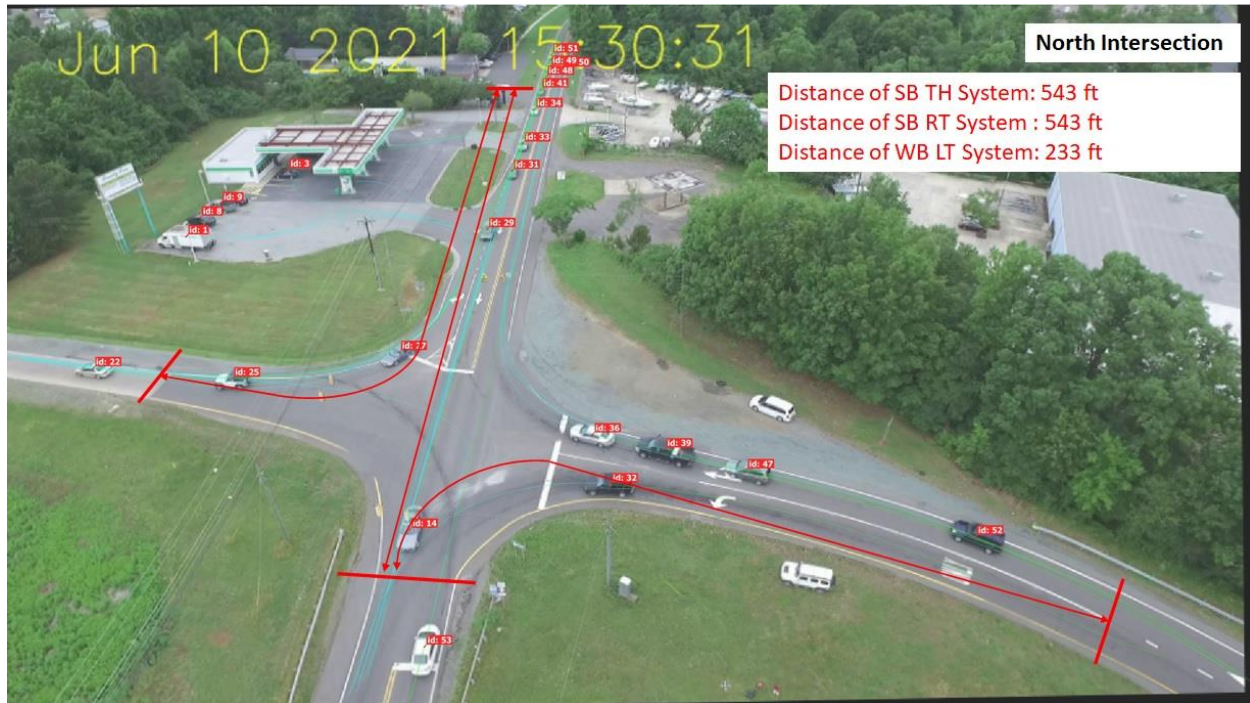


Figure 8-3: DFS Processed Screenshot of the North Intersection on NC86 and I-85 along With Trajectory IDs and Location of Travel Time Sensors

8.2.2 Demand Volume Extraction

Demand volumes were extracted directly from the drone video at the two intersections, yielding the turning movements counts shown in Table 8-1: Estimated Demand Flow Rates at the Two Intersections. There were no initial queues to speak of at either intersection, so that no additional modification to the demand was needed. The highlighted cells show the selected movements used for model validation purposes.

Table 8-1: Estimated Demand Flow Rates at the Two Intersections

	North Intersection (NC 86 & I-85 WB Exit)							South Intersection (NC 86 & I-85 EB Exit)						
	SB		NB		WB			SB		NB		EB		
	TH	RT	LT	TH	LT	TH	RT	LT	TH	TH	RT	LT	TH	RT
Count (vehs)	84	28	54	48	29	0	25	18	94	93	38	7	0	40
Flow rate (veh/h)	400	133	257	229	138	0	119	86	448	443	181	33	0	190

In addition, Trans Modeler requires the designation of OD flows for its simulation. These are depicted in Table 8-2: Origin Destination Hourly Demands at Interchange below. Highlighted cells pertain to the movements of interest.

Table 8-2: Origin Destination Hourly Demands at Interchange

Origin* - Destination*	To 1	2	3	4	Sum
From 1	0	336	64	133	533
2	119	0	138	0	257
3	208	181	0	234	623
4	34	0	190	0	224
Sum	361	517	392	367	1,637

* Index numbers are shown in Figure 8-1.

8.2.3 Signal Data Extraction

The signal data at both intersections were extracted from the split monitor reports and confirmed by the drone and ground camera videos upon monitoring the departure times of the different movements at their stop line. The prevailing cycle length during data collection 90 seconds. The SB through movement offset was measured at 31 seconds between the North and South stop lines, respectively. The phasing plan is shown in Figure 8-4 with the highlighted movements depicted in green. It is clear that while the NS movement receive the majority of the cycle green, less is provided to the off ramp traffic in either direction.

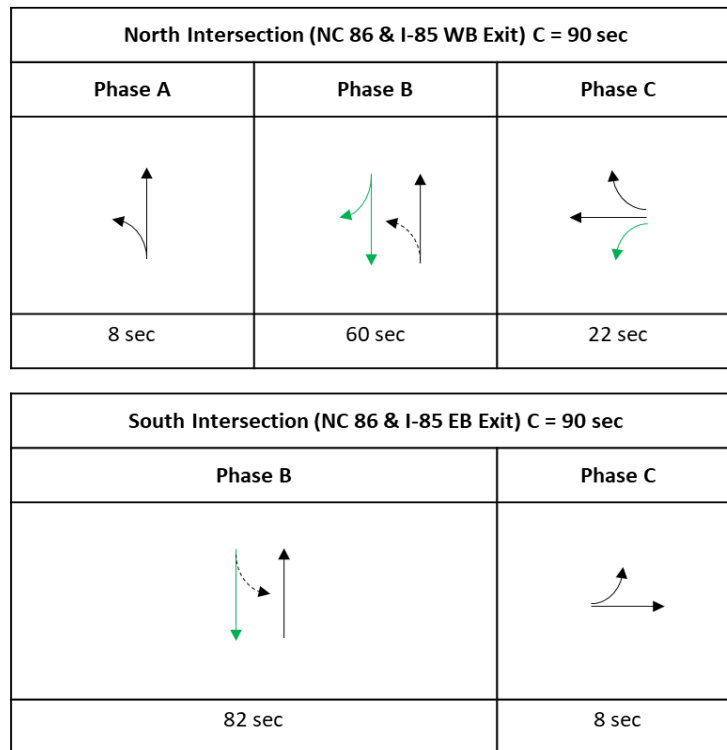


Figure 8-4: Signal Phasing Plan at the Offset Intersection

8.2.4 Field Performance Measures

Similar to our selection of MOE's in the previous sites, travel time or time in system between the virtual sensors was the selected validation measure. For SB-TH and SB-R movements the sensor distance is 543 ft., and 233 ft. for the WB-L movement. As expected, individual vehicle travel times are highly variable, and depend on their arrival time at the stop line----- as shown on the X-axis in Figure 8-5 (a-c). It is important to note that this travel time includes the experienced delay only at the North Intersection. On average, travel time for the SB-TH movement was 25.3 sec and that for the SB-R was 26.5 seconds. The WB-L travel time was 41.9 sec, a reflection of the lower green time available for that movement, per Figure 8-4. For comparison purposes, the free flow travel times for those SB-T and WB-L movements were estimated at 8.23 and 4.54 seconds, respectively. The standard error for the mean travel time was 4.2 seconds for the SB-TH movement and 8.6 sec for the WB-L movement. Thus, our original assumption regarding the quality of traffic performance for those two movements appears to be validated by the data.

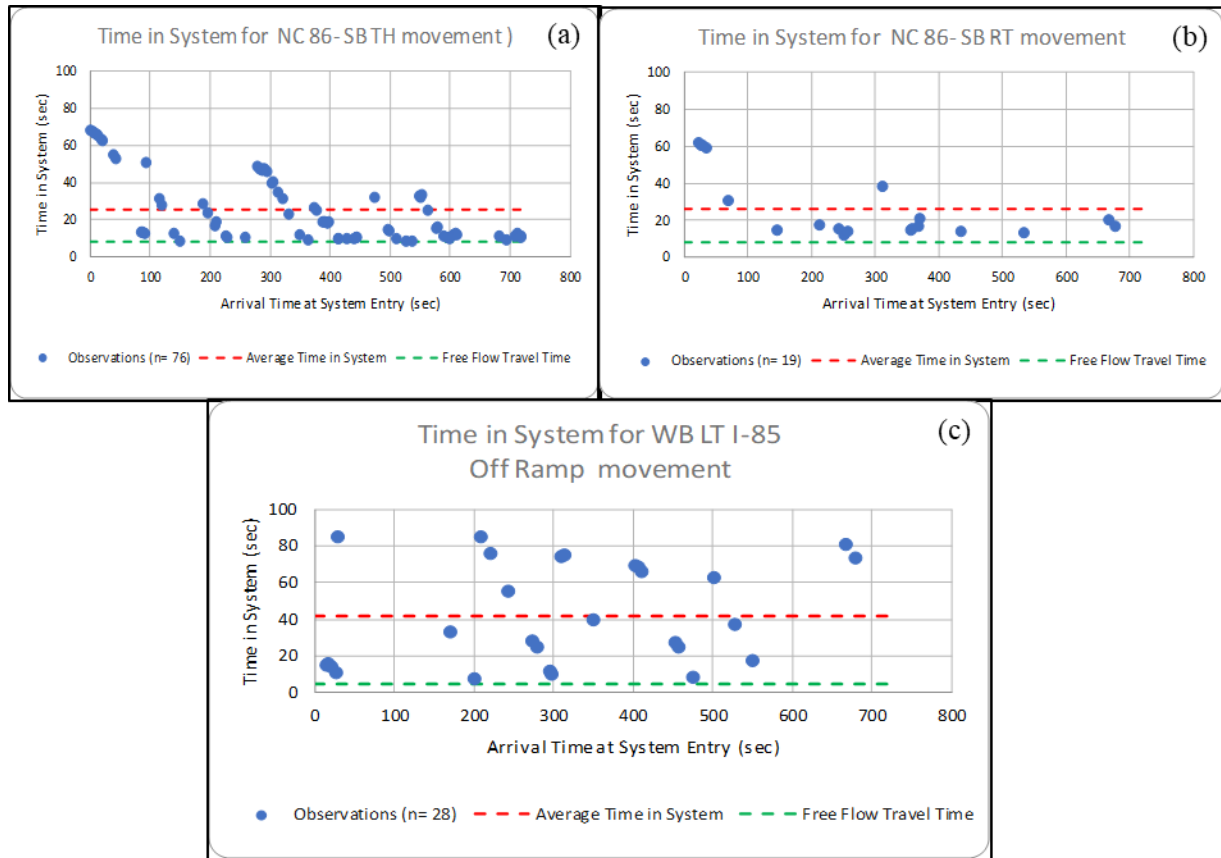


Figure 8-5:: Travel Time Profiles for (a) SB-TH, (b) SB-R and (c) WB-L Movements at the North Intersection

The route travel times measured by the Bluetooth units generated very small samples of travel times due to equipment malfunction. Overall, the units recording only 13 matched travel times in the SB direction and 6 matches in the NB direction. For the purpose of documentation, the average travel time in the SB direction was 64.7 sec, while the corresponding value for the NB route was 72.1 seconds. These values are consistent with the higher NB volume as indicated in Table 8-3: Calibrated Entry, Negotiating and Exit Speeds for Key Movements. In both routes, a minimum travel time of 40 seconds was observed. Interestingly, the average travel times translate into an average speed in the range of 17-19 mph, which includes the effect of delays at both intersections. Similarly, the unstopped vehicle travel time translates into a speed of 32 mph.

8.3 Models’ Testing and Calibration

As stated earlier, the team’s approach to model calibration was to deliver the most accurate input and calibration parameters in all models tested. This includes demand volume levels including any initial queues, signal timing parameters, actual entry speed and saturation flow rates. Demand levels were reported earlier. Saturation flow headways were directly extracted from the DFS processed video by setting a virtual sensor at the stop line for the SB-through movement on NC86 at the North Intersection. Queues were very short on the off ramp to enable the measurement of reliable saturation headways for the LT movement. The calibrated value for the SB-TH movement was found to be 1,528 vph /lane, again a value that is much lower than the default values in the Highway Capacity Manual (1,900 or 1,750 pc/h/pl) for signalized intersections. That value was subsequently adjusted for heavy vehicle and turning movements. The corresponding, calibrated buffer headway in Trans Modeler was 0.6 seconds

Finally, and in order to match the entry and exit speeds on the approaches for the movements of interest, which is an important input into the analytical models, the speeds shown in Table 8-3 were coded in both SIDRA and Synchro models.

Table 8-3: Calibrated Entry, Negotiating and Exit Speeds for Key Movements

Average Speeds		mi/h	ft/s
Upstream	SB-TH	30.3	44.5
	SB-RT	30.3	44.5
	WB-LT	18.0	26.4
Negotiation	SB-TH	18.8	27.6
	SB-RT	5.6	8.2
	WB-LT	8.6	12.5
Downstream	SB-TH	30.3	44.5
	SB-RT	22.6	33.1
	WB-LT	16.0	23.5

8.4 Model Validation

A note on the models’ reporting of the performance measures: by coding the approach and exit lengths to be equal to the setback of the upstream and downstream sensors shown in Table 8-3, SIDRA will directly report the travel between them. SYNCHRO on the other hand

does not report travel time, but strictly control delay at the signal. In this case, travel time is estimated as the control delay plus the free flow travel time (based on the field entry speed also shown in Table 8-3). TransModeler travel times are computed by setting virtual sensors in the simulation and tracking the vehicles' time between the two sensors.

The validation of the time in system across models for the three movements at the North Intersection is depicted in Figure 8-6. For the SB-TH movement (a), all three models' predictions were within 10 seconds of the field measurements indicating a LOS in the A/B region. For the SB-RT, again the models were within 10 seconds of the field value, with Synchro tending to under-predict that travel time. Finally, all three models appear to have correctly captured the operation of the WB-L movement at a higher delay and travel time, again within 10 seconds of the field values.

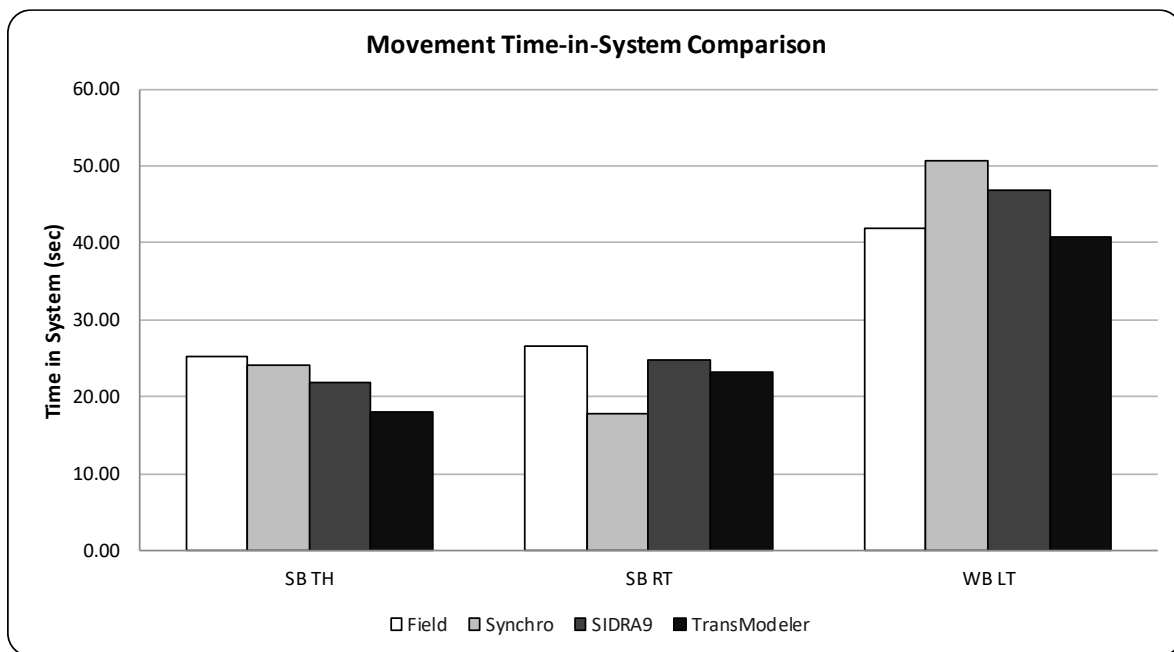


Figure 8-6: Model Validation Results at North Intersection by Turning Movement

Figure 8-7 depicts the route travel times between the three models and the field for both NB-TH and SB-TH movements on NC86 – over a travel distance of about 1,820 ft. In general, all models tended to underestimate the route travel time in both directions, with one exception. It is possible that those estimates may be compromised by coding an inflated value of free flow speeds within the route. The exception was Trans Modeler estimation of the NB-TH travel time, which was within 10 seconds of the field value.

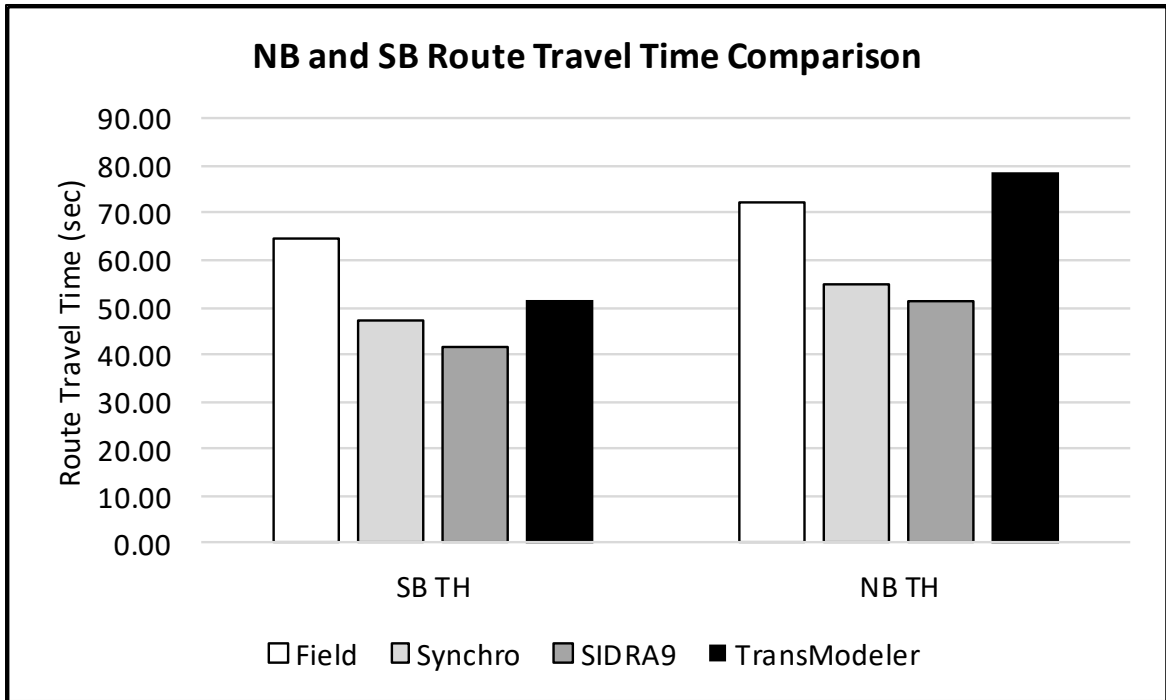


Figure 8-7: Model Validation Results Based on NB and SB Route Travel Time

8.5 Summary and Discussion

The site covered in this chapter is a traditional diamond interchange with spacing between the two intersection stop lines on NC 86 nearing 725 ft. Data collection at that site used drone video supplemented with ground cameras and two blue tooth units. Drone videos extracted by DFS could only fully cover the North Intersection and thus the validation for this site focused on three movements at that location. The Blue Tooth units enables the measurement of through movement travel times both north and south of the two signalized intersections. This particular site operated under virtual free flow conditions, with the critical movement being the LT movement from the off-ramp at the north intersection, which operated at a v/c just below 0.50. The expectation here was that all models should produce valid results within a LOS at most.

Key findings and lessons learned at this site follow:

- 1) The team is consistently measuring field saturation flow rates that are well below the HCM defaults, including at this site (base flow rate of about 1,530). Lack of significant queues on other approaches, during data collection, necessitated the use of a single value for all approaches.
- 2) A second consistent finding is the generally lower values of approach and exit speeds than most analytical models assume. In this site, the speed limit is 45 mph on NC 86, yet most observations of the free flow speed were in the range of 25-35 mph. This implies that field verified approach and exit speeds must be used as additional calibration parameters.

- 3) The blue tooth units experienced difficulties in generating sufficient matches to enable a proper validation of the through vehicle travel time on NC 86 through both intersections. The comparative results with the model predictions should therefore be viewed with caution.
- 4) As suspected, the validated movement system travel time were all within 10 seconds of the observed field values indicating the utility of the analytical approaches in estimating performance for under-saturated flow conditions
- 5) Between the three models, the calibrated Trans Modeler results were closest to the field values, both for the three movements tested and the two route travel times. However, all models performed adequately in terms of characterizing the general LOS at that site (A or B).

9 Chapter 9: Critical Movement Analysis and CAP-X

Critical Movement Analysis uses the observed or forecasted turning movement demands to identify critical volume to capacity ratios for intersections. In intersections with multiple independently controlled zones, each zone is analyzed separately. This approach is commonly used at the preliminary planning and early alternatives analysis phase of project development and requires knowledge of the demand volumes as well as basic intersection geometry.

FHWA has published the CAP-X tool for conducting Critical Movement Analysis which includes many intersection designs with automatic outputs for quick use of the input data. The outputs of CAP-X are the Critical Lane Volume and Volume to Capacity Ratio for each zone. The following subsections document the CAP-X analysis of each analyzed intersection in this research, followed by a summary comparison to the performance measures from the other tools utilized earlier.

Other default values can be modified depending on the agency policy or additional field data. These include the percent of heavy vehicles, future year volume growth, critical lane volume maximums for 2, 3 and 4-phase signals, turning movement adjustment factors for CLV, truck to PCE ratio, and multimodal activity level.

9.1 Isolated Signalized Intersection in Chapter 3

The basic signalized intersection is one of the standard designs included in the CAP-X software. Aside from demand and geometry, no changes to the standard analysis method are needed to complete the analysis. As shown in Figure 9-1, using the hourly demand inputs results in a Volume to Capacity ratio of 0.85 and Critical Lane Volume of 1268. A summary comparison of CAP-X v/c ratios against the model estimates for each case is presented at the end of this chapter

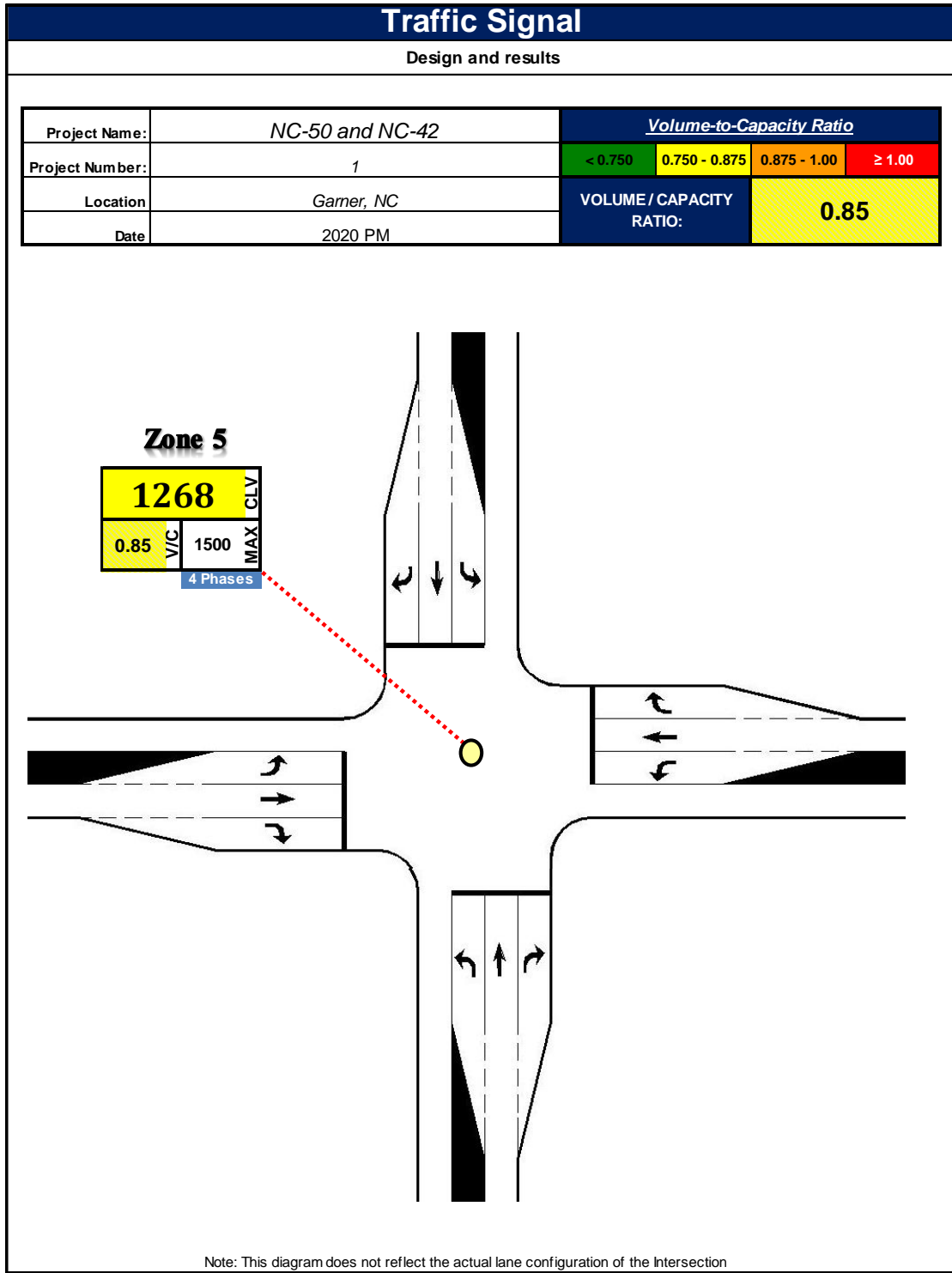


Figure 9-1: Isolated Signalized Intersection CAP-X Outputs

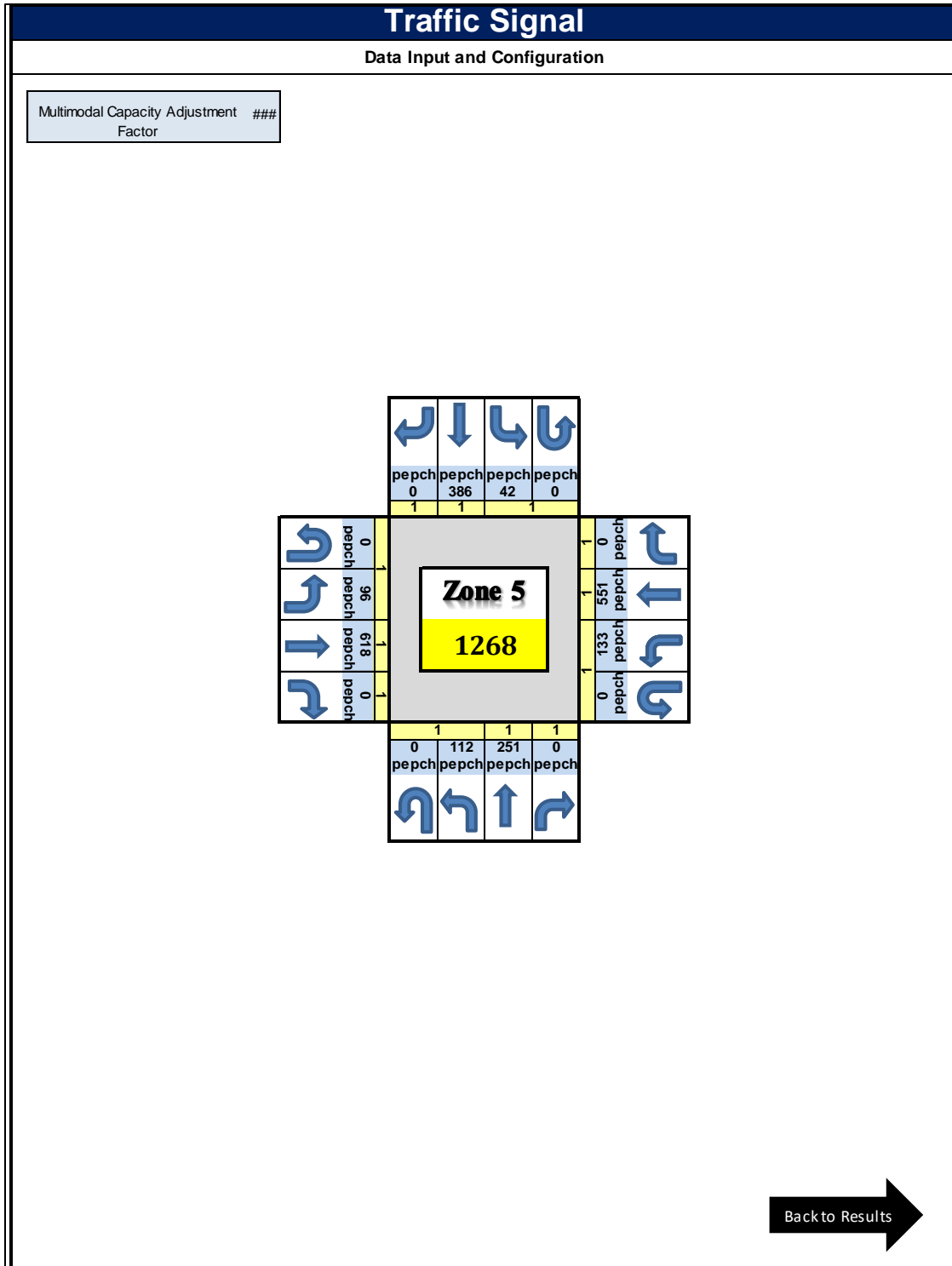


Figure 9-2: Isolated Signalized Intersection CAP-X Inputs

9.2 Single Lane Roundabout in Chapter 4

The Hillsborough St and Pullen Rd roundabout contains a single circulating lane, however three of the four approaches include a right turn channelized lane that bypasses the circulating traffic. This geometry is not directly supported in CAP-X, therefore the two most similar geometries are both used, namely a single lane roundabout and 1x2 roundabout. As seen in Figure 9-3 and Figure 9-5, the maximum V/C for each approach is 0.81 for the single lane roundabout and 0.69 for the 1x2 roundabout. It is likely that the actual design operates more closely to the single lane conditions overall, but with high right turning volumes it may be possible that the channelized lanes remove a high percentage of demand from the merging traffic. Additionally, the three approaches with the highest V/C in the single lane design are also the approaches with the right turn lanes.

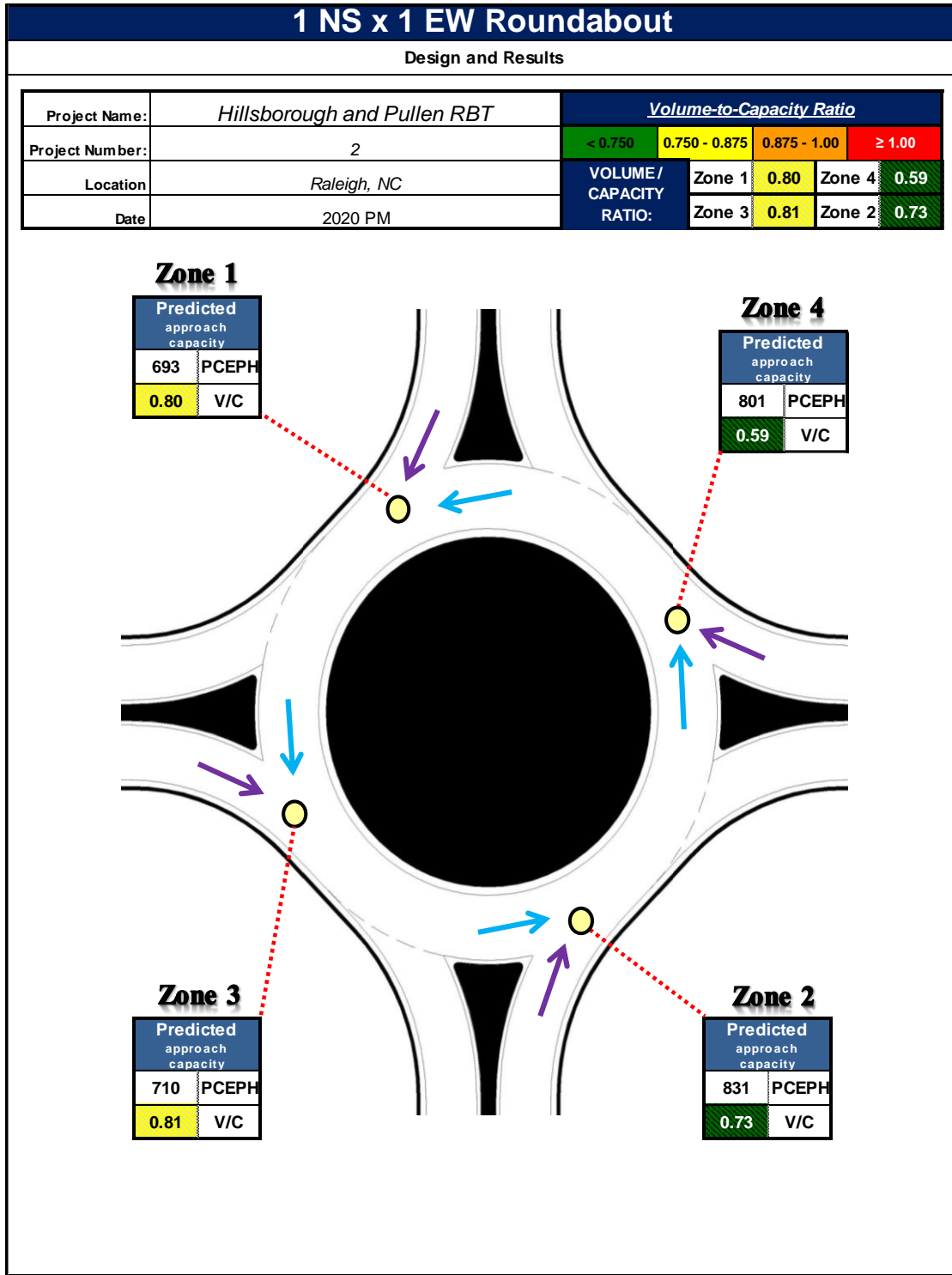


Figure 9-3: Single Lane Roundabout CAP-X Results

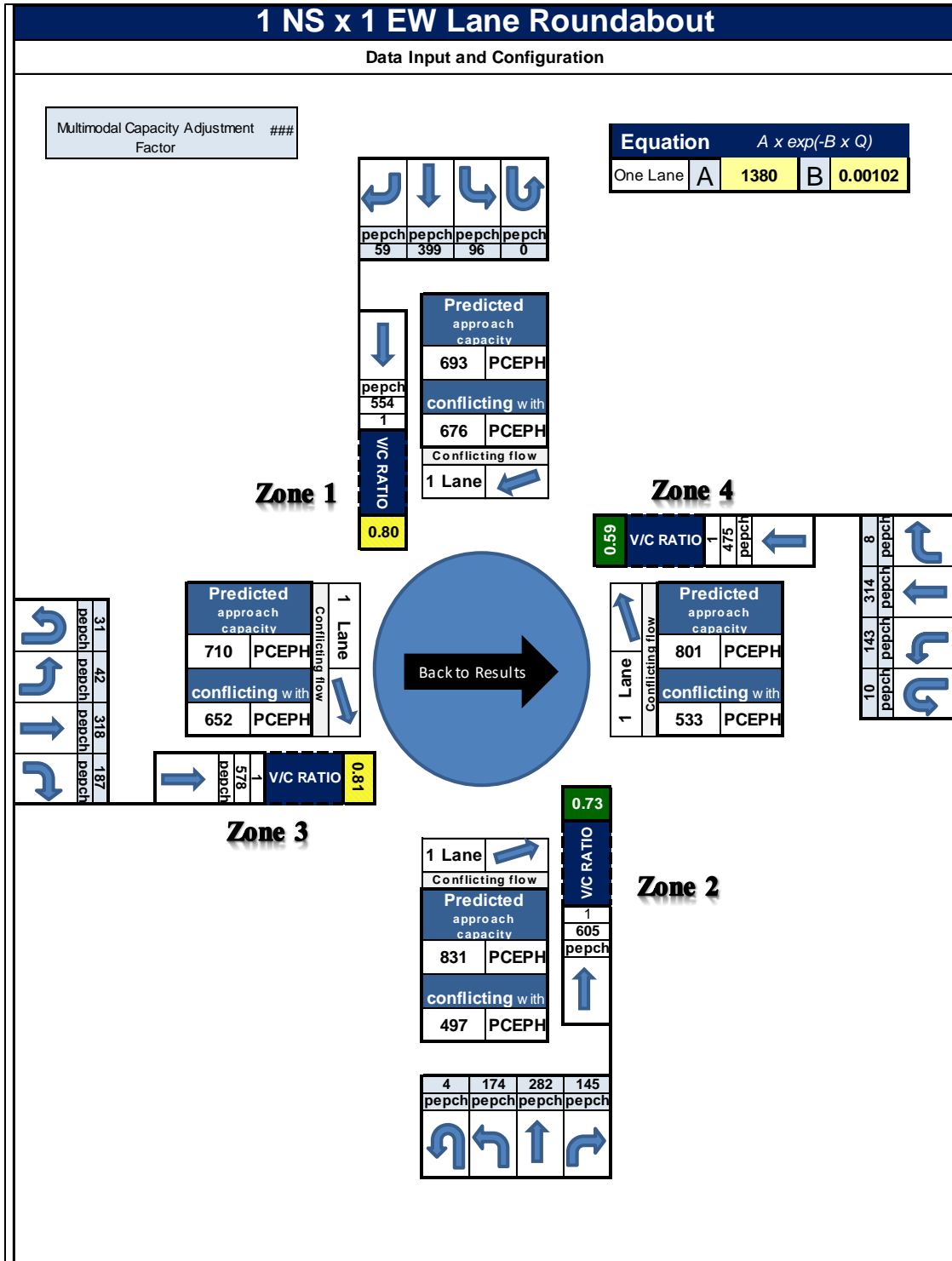


Figure 9-4: Single Lane Roundabout CAP-X Inputs

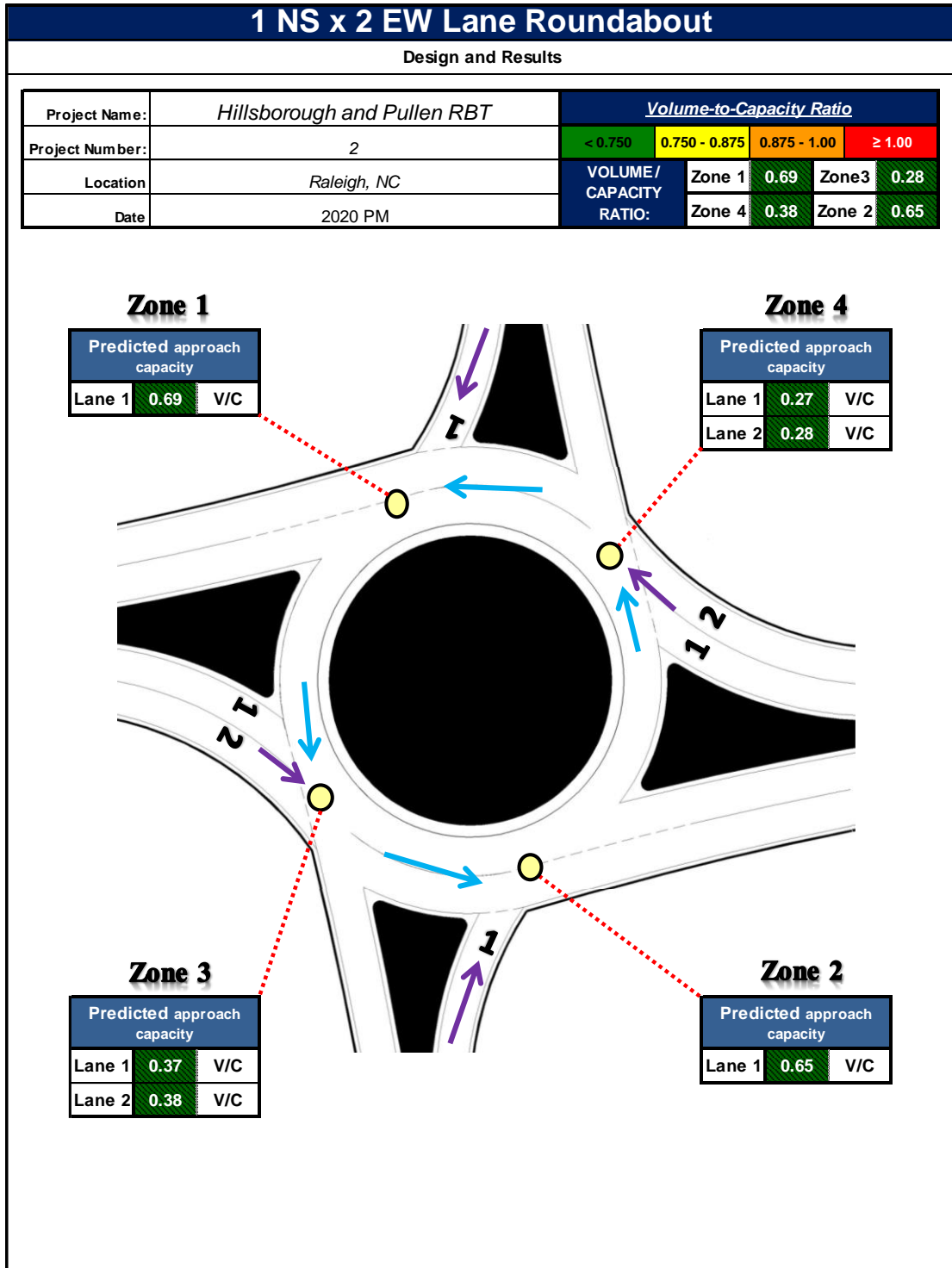


Figure 9-5: 1x2 Roundabout CAP-X Results

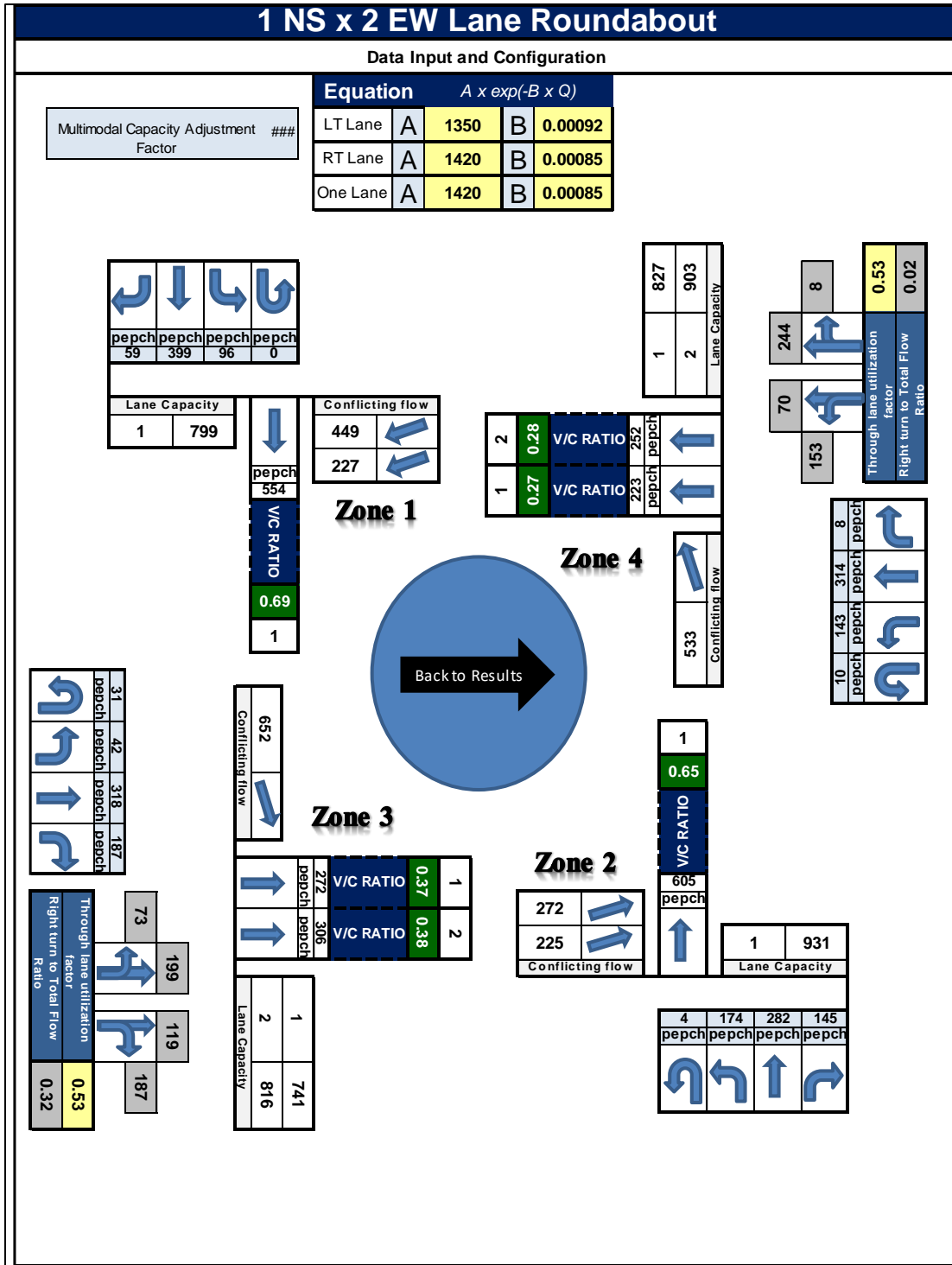


Figure 9-6: 1x2 Roundabout CAP-X Inputs

9.3 Coordinated Signalized Intersection in Chapter 5

Critical Movement Analysis occurs at each intersection zone independently, meaning that a coordinated signal and isolated signal are functionally identical in analysis procedures. At a

planning level analysis, deterministic models such as the Highway Capacity Manual urban streets method may provide additional analysis detail, however in CAP-X the coordination impacts are not directly modeled. Figure 9-7 shows the Oleander Dr & College Rd intersection results in a V/C of 0.85 and CLV of 1280.

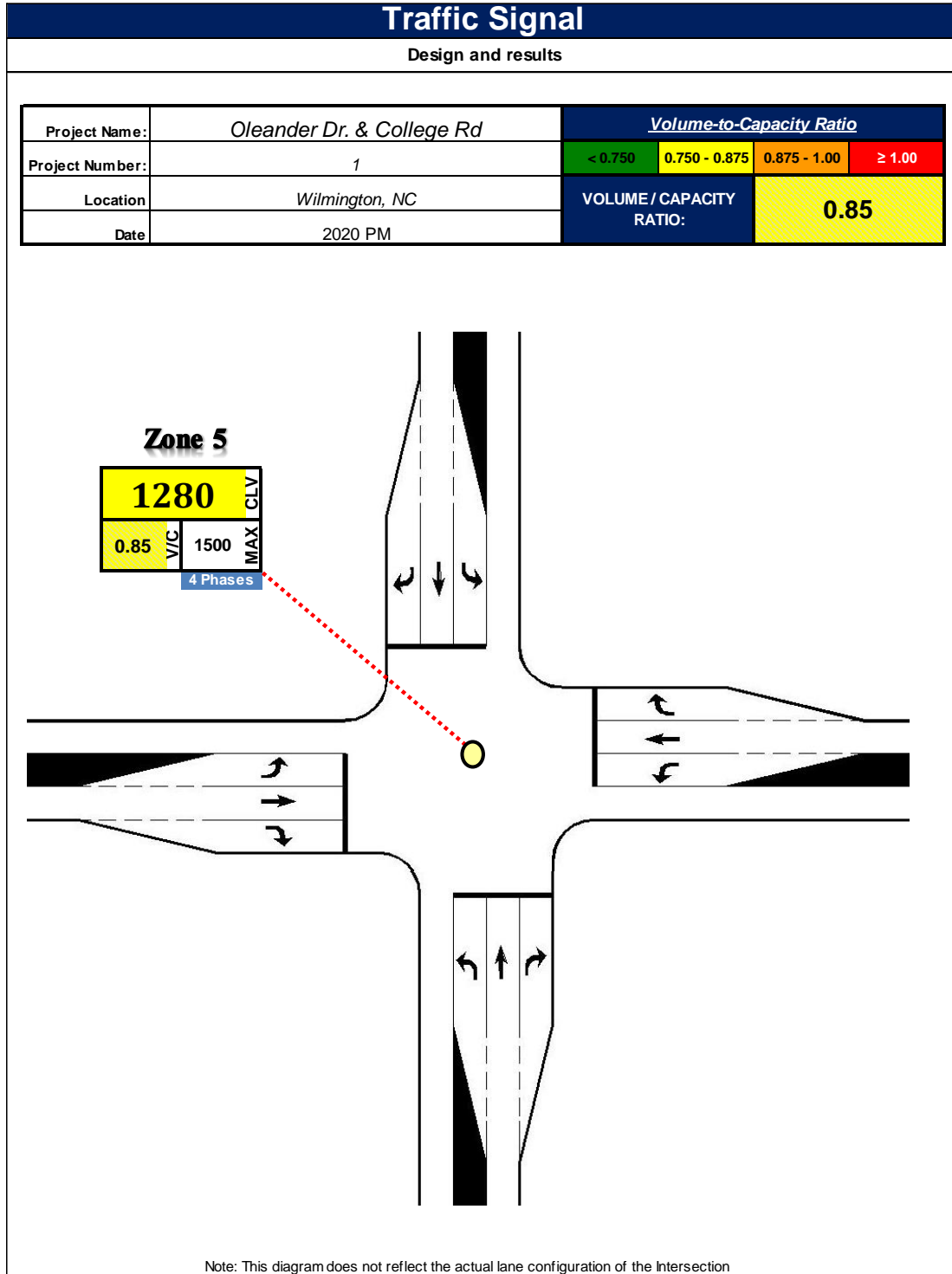


Figure 9-7: Coordinated Signalized Intersection CAP-X Results

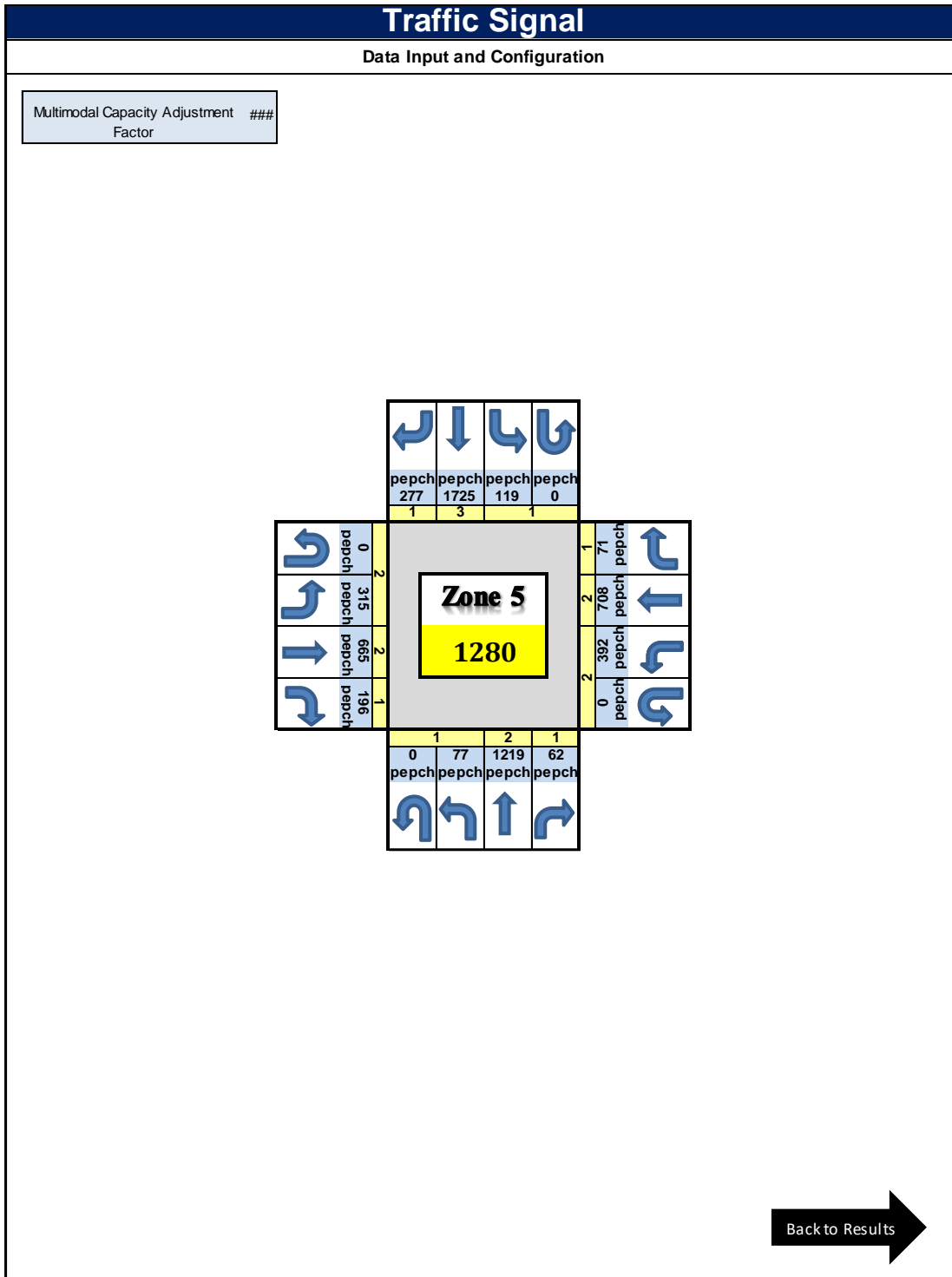


Figure 9-8: Coordinated Signalized Intersection CAP-X Inputs

9.4 Offset Intersection in Chapter 6

Offset intersections are not separately modeled in CAP-X, so each zone must be separately modeled as two signalized T intersections. Figure 9-9 shows that the Capital and Highwoods Blvd intersection has a V/C of 0.5 and CLV of 876, while Figure 9-11 shows the Capital and Westinghouse Blvd intersection has a V/C of 0.47 and CLV of 814. If considered as a single intersection, the worst V/C would be reported for the overall intersection.

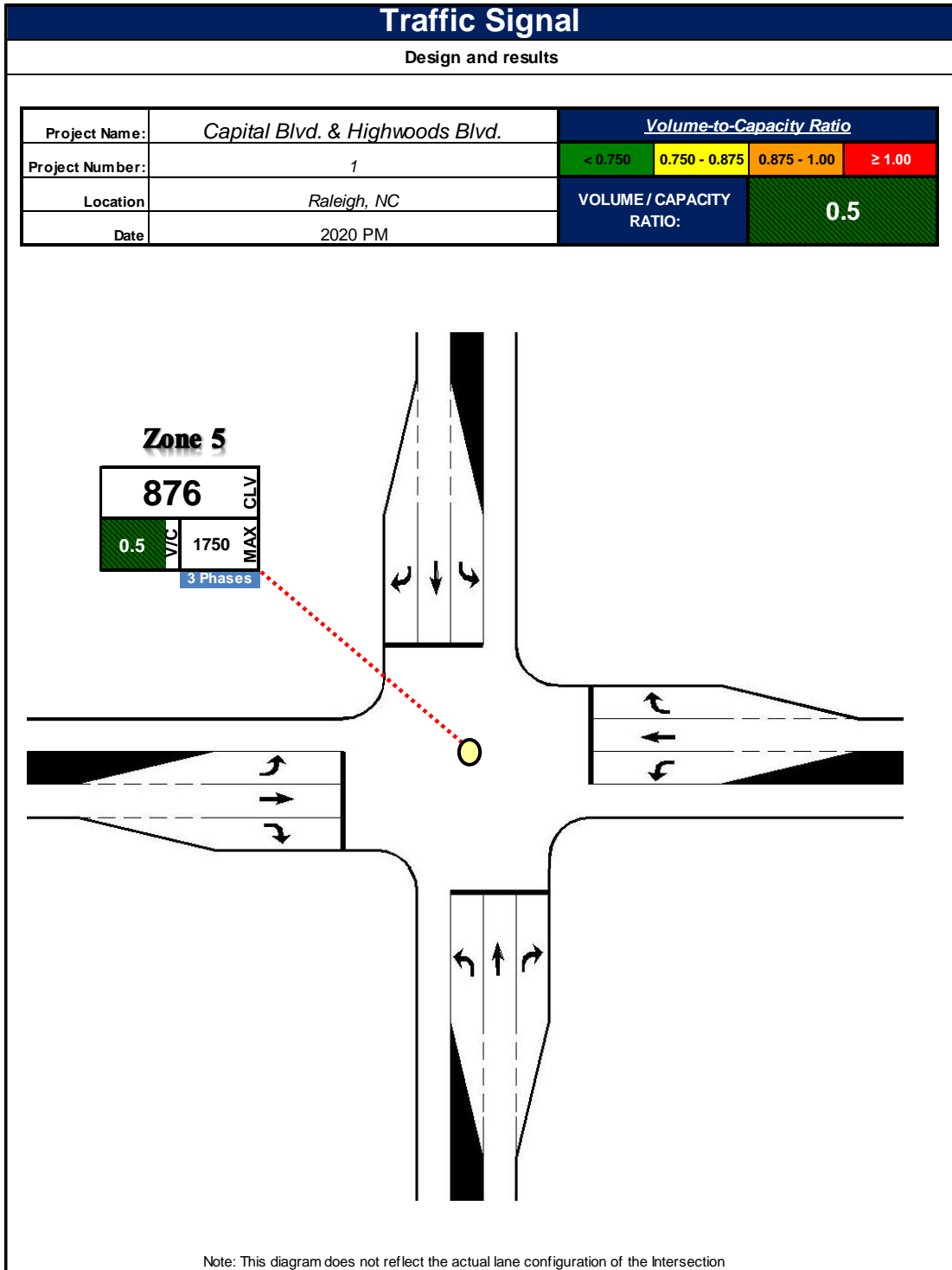


Figure 9-9: Offset Intersection First Zone CAP-X Results

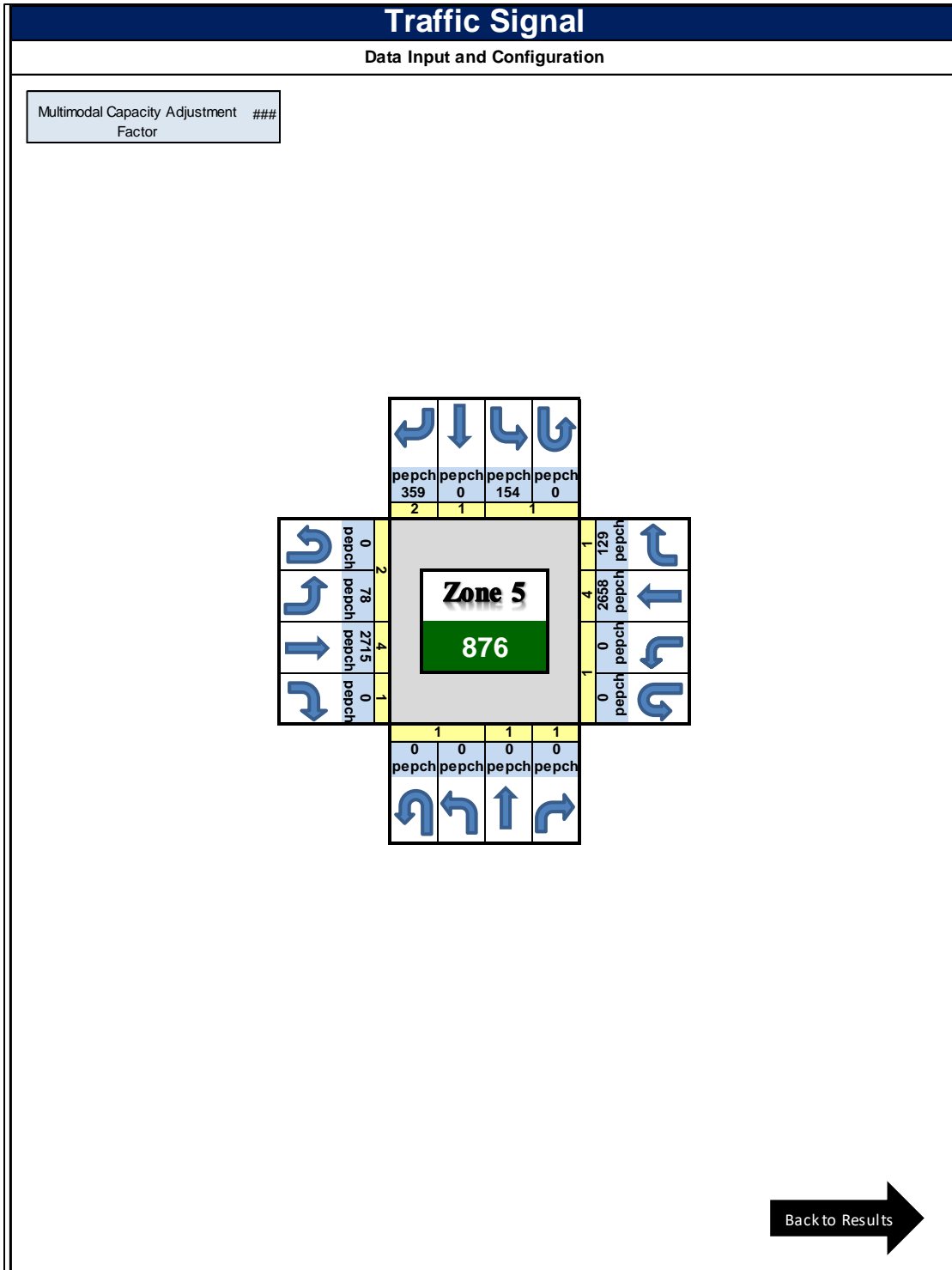


Figure 9-10: Offset Intersection First Zone CAP-X Inputs

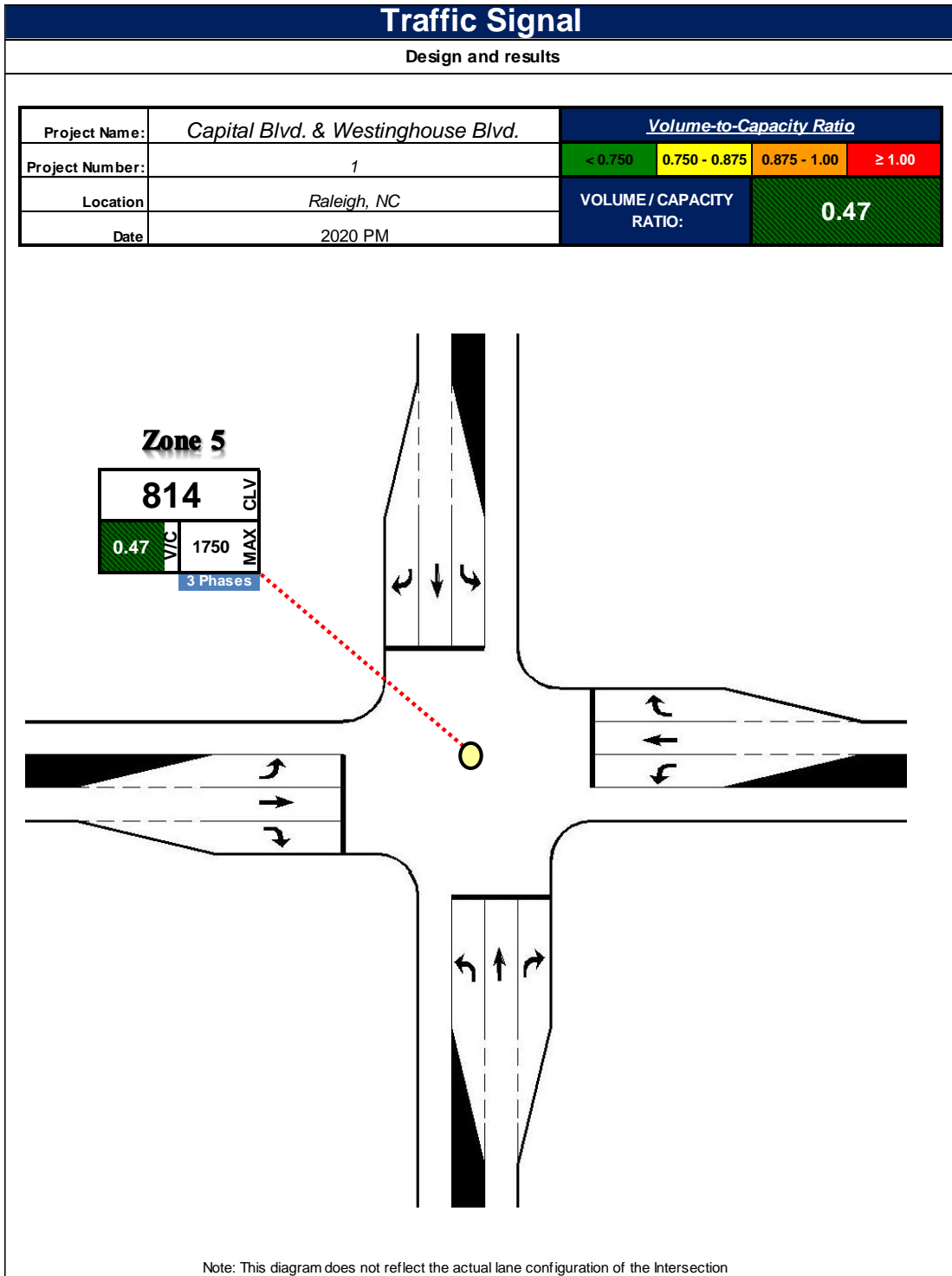


Figure 9-11: Offset Intersection Second Zone CAP-X Results

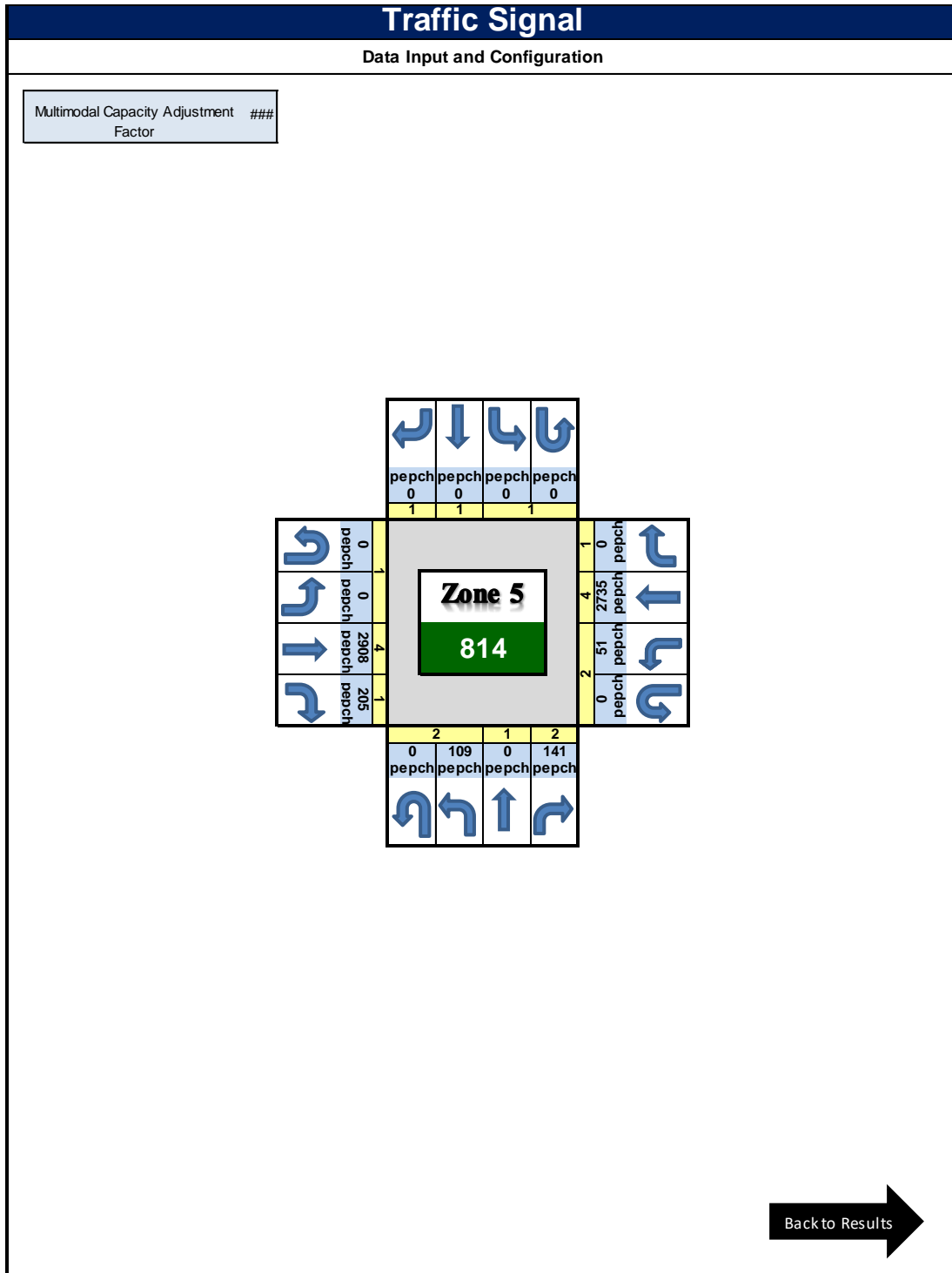


Figure 9-12: Offset Intersection Second Zone CAP-X Inputs

9.5 Continuous Flow Intersection in Chapter 7

The Continuous Flow Intersection is also known as a displaced left turn intersection. A full CFI includes crossover/displaced left turns at all approaches, while a partial will include them at only

certain approaches (usually E-W or N-S). Full, N-S and E-W Displaced Left Turn intersections are included in CAP-X by default. Figure 9-13 shows the results for the Brookshire Blvd. & Mt. Holly-Huntersville Rd. At the CFI, which is summarized for the central intersection has a V/C of 0.7 and CLV of 1,220 vph; the two crossover intersections operate at a V/C of 0.47/0.42 and CLV of 850/759 respectively.

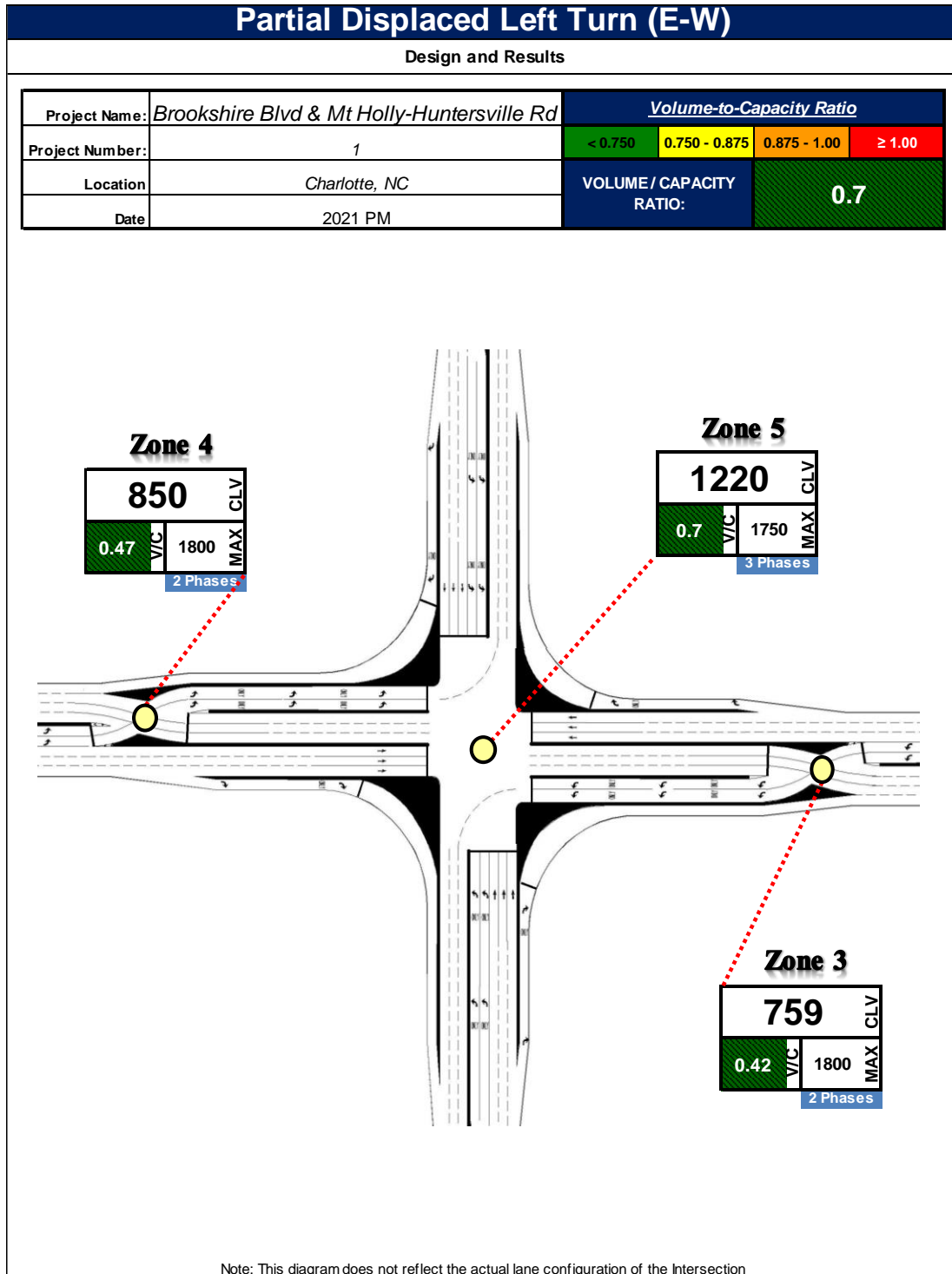


Figure 9-13: Continuous Flow Intersection CAP-X Results

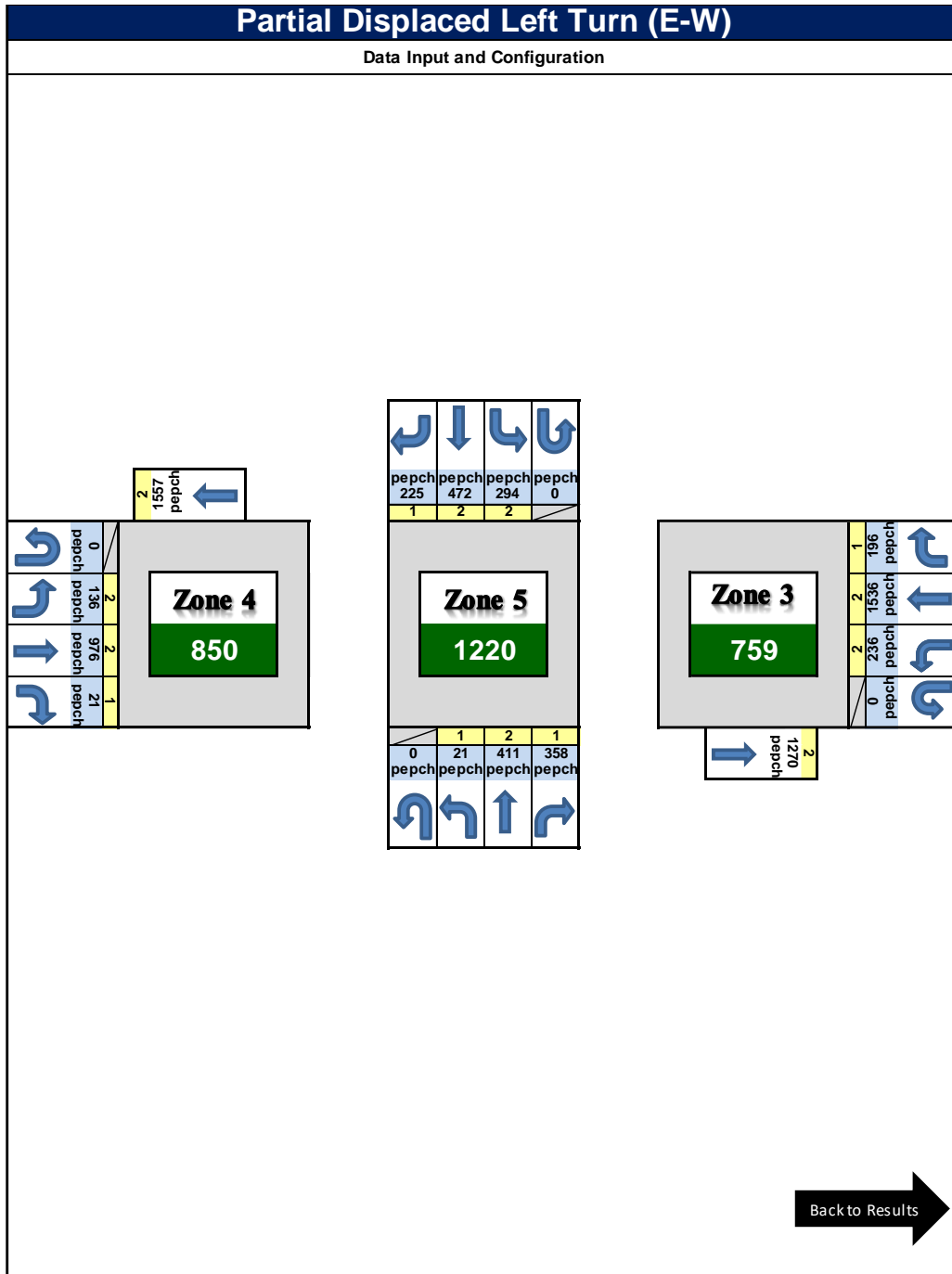


Figure 9-14: Continuous Flow Intersection CAP-X Inputs

9.6 Traditional Diamond Interchange in Chapter 8

Interchange inputs in CAP-X are entered on an Origin-Destination basis, similarly to Trans Modeler. Figure 9-15 shows the Traditional Diamond Interchange results with the northern intersection operating at V/C of 0.46 and CLV of 798, while the southern intersection has a V/C of 0.58 and CLV of 1,016. Overall, the worst intersection would be considered for initial screening of alternatives.

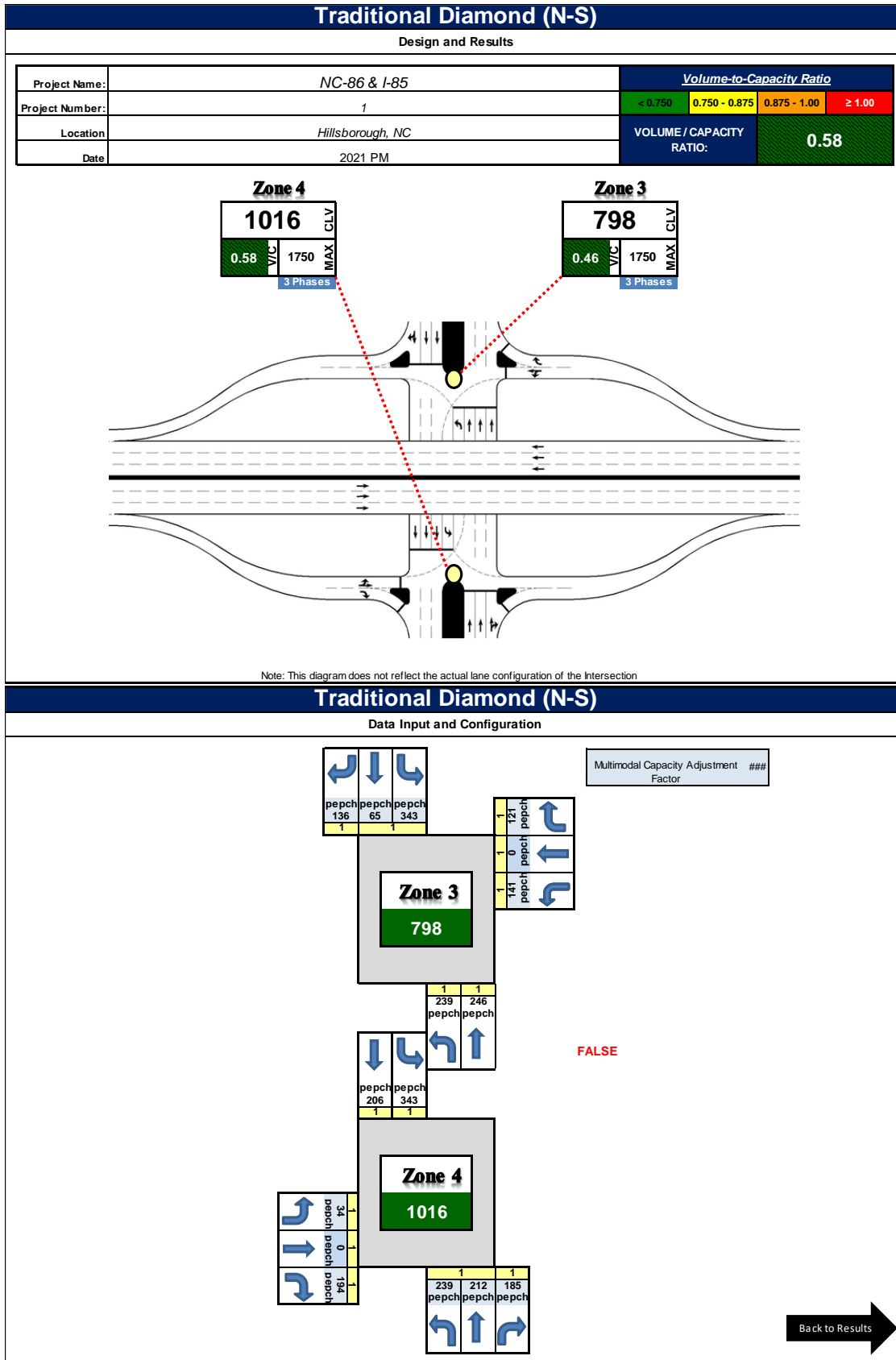


Figure 9-15: Traditional Diamond Interchange CAP-X Inputs and Results

9.7 Summary of Results

Table 9-1 summarizes the CAP-X results for each of the intersections as well as those reported by the other analysis tools. In Synchro and SIDRA, the highest movement delay result is presented, thus the highest delay doesn't mean the highest v/c ratio. If facility consists of more than two intersections, the highest delay among all movements in multiple intersection was presented. In the case of multi-intersection facilities, maximum v/c ratio, network LOS, and overall control delay are presented. In addition, we present the aggregate v/c ratio across all movements on a facility. The highlighted columns are the one that can be compared based on overall performance.

Network LOS is related to Travel time index or Speed efficiency instead of delay in SIDRA. Synchro doesn't provide network LOS. For isolated and coordinated intersection and roundabout, observed initial queue were applied differently. Since initial queue is converted to additional demand and added to original demand, v/c ratio estimated is higher than Synchro. Finally, the table also shows the overall facility average V/C ratio across all sites and models.

Overall, CAP-X results are best compared directly to a worst (critical) movement, however on a screening basis the results are typically used for overall intersection screening which would compare to total delay or LOS from other tools. The isolated intersection results indicate that other tools are predicting more serious delays than a V/C of 0.85 would indicate, which is likely due to initial queue delays these other models include. The roundabout comparison seems to be closer to the 1x2 lane CAP-X model compared to the other tools with good LOS. The coordinated intersection likely shows similar issues as the isolated intersection with LOS E/D results from all other tools.

The offset intersection shows very different results for the worst movement compared to the facility average, however the average results from the other tools seem to compare favorably to the 0.5 V/C from CAP-X. The CFI shows a similar trend to the offset intersection with LOS C from other tools compared to 0.7 V/C from CAP-X. Finally, the traditional Diamond interchange shows a variety of delays in other tools at or under LOS C compared to the CAP-X V/C of 0.58. In general, these results show that while very simplified, the lower CAP-X V/C values correlated very well at the good LOS, while very congested intersections did not always have very high V/C in CAP-X likely due to the other tools ability to capture initial queue delays.

Finally, comparing SYNCHRO, SIDRA and Trans Modeler *at the intersection level* shows that in five of the six sites, their reported LOS was at most within one LOS range of each other. The one exception is the traditional diamond interchange where SIDRA yielded a LOS of A, while SYNCHRO reported LOS B and Trans Modeler a LOS of C. In conclusion, these results indicate that at a planning level, critical lane analysis was successful in identifying relative performance of the designs although the actual operations tend to be more severe in microsimulation and in the field than the CAP-X V/C values indicate.

Table 9-1: CAPX vs. Models Comparison Table- Intersection Level Performance

SITE Identification and (Chapter number)	CAPX V/C***** and CLV	SYNCHRO v/c, LOS, and Control Delay (Worst Delay Movement)	SYNCHRO Avg. v/c, LOS and Control Delay (Facility Average)	SIDRA v/c, LOS, and Control Delay (Worst Delay Movement)	SIDRA Intersection Average v/c, LOS, and Control Delay (Facility Average)	TransModeler LOS and Control Delay (Facility Average)
Isolated Intersection (3)*	0.85 (1268)	0.57/ F/58.7***	0.67/ F/ 82.2	1.447/ F/ 167.4	0.87/ E/ 69.6	F (135.8)
Single Lane Roundabout (4)*	0.81 [1x1] 0.69 [1x2]	0.653/ C/ 17.1	0.53/ B/ 13.3	0.703/ C/ 20.2	0.54/ B/ 13.9	A (9.9)
Coordinated Intersection (5)	0.85 (1280)	0.97/ F/ 175.2	0.86/ E/ 71.6	1.152/ F/ 148.6	0.83/ E/ 66.5	E (57.9)
Offset Intersection (6) *****	0.5 (876)	0.96/ F/ 163.8**	0.52 / B/ 14	0.929/ F/ 167.3**	0.45/ B/ 16.3**	B (17.2)
Continuous Flow Int. (7) *****	0.7 (1220)	0.88/ F/ 91.2	0.48/ C/ 21	0.68/ F/ 86.8	0.44/ C/ 21.2	C (23.8)
Traditional Diamond Int. (8) *****	0.58 (1016)	0.69/ F/ 104.9	0.44/ B/ 12	0.68/ E/ 73.4	0.42/ A/ 8.8	C (30.0)

* For some facilities, multiple videos were recorded. The table shows the most critical delay and LOS

**This value masks a problem, since most of the traffic at the two intersections travel in the EB-TH and WB-TH directions on Capital, and operates with a very high g/C ratio and with good coordination. Travel route from SB Highwoods Blvd. to EB Capital and Westinghouse experiences a very high delay of 167.3 sec (LOS F). However, our research shows that the delay value for SB traffic is over-estimated by a considerable margin.

*** Most of the control delay is due to an initial queue. Thus, the v/c ratio for the movement was relatively low.

**** The overall facility LOS for multi-intersection facilities is based on overall control delay thresholds in the HCM.

***** CAP-X base CLV sum limit is 1800 for 2-phase, 1750 for 3-phase and 1700 for 4-phase signals

10 Chapter 10: Sensitivity Analysis

Sensitivity analysis is a well-known technique for studying cause-and-effect relationships when field data are not available or real-world testing is problematic. However, since the simulation model employed is not likely to be calibrated, technically speaking, it is relative changes that should be the focus, not the actual predicted values. This comment is not intended to detract from the value of doing the analysis, however. If the model can produce reasonable results in well-understood settings, the analyst can assume that the predictions in other settings are valid, too, and provide valuable insights.

There are two sites for which we did not manage to collect new field data because of limitations from COVID. One is the RCI (Reduced Conflict Intersection) on NC-55 in Holly Springs (New Hill Road / Holly Springs Road) and the other is a DDI (diverging diamond interchange) on US-17 in Leland, NC (Village Road / River Road). For both sites, TransModeler datasets were available as well as turning movement volumes and signal plans. Consequently, for these sites, we elected to do sensitivity testing using Synchro and TransModeler, both models currently used in the Congestion Management Group at NCDOT.

For both facilities, we focused on storage capacity-related issues. As design engineers know, ensuring the storage capacity is adequate is always a challenge in any construction project. Part of this dilemma relates to the prediction of future demands; and part of it relates to the way the facility is designed to operate. In the case of an RCI, it is the U-turn crossovers that are often of principle concern. Access to them is from the left-hand lane, and the turning bays must be carved out of the median. The left-turn bays present a similar challenge. For a DDI, it is often the storage capacity on the bridge, between the signals, in both directions. There must be adequate storage for the queue that accumulates, from the upstream through and the left turn movements from the freeway.

For this sensitivity analysis, we selected inputs and parameters that would affect the storage adequacy. We focused on the a) the demands, b) the saturation flow rates, c) the signal timing, specifically, the maximum greens, and d) the offsets. If the demands are higher than expected, the saturation flow rates are low, or the maximum green are low, or the offsets are not good, the storage limits can be reached, in fact, unintentionally.

We elected to vary one factor at a time. We wanted to ensure that we studied the impacts of each factor separately. While compound effects do occur in the field, and they can be studied, the effects of individual factors are then obscured. We did not want to confound our analysis by allowing changes in multiple factors to affect the results simultaneously.

10.1 RCI Analysis

The RCI is in Holly Springs at the intersection of NC-55 and Holly Springs Road / New Hill Road as shown in Figure 10-1. The main street lefts cross the opposing throughs under signal control; and the side street right turns are also signal controlled. The signals are both semi-actuated, coordinated with background cycle lengths of 70 seconds northbound and 140 seconds southbound. The signals are two-phase: the main street throughs are by themselves, and the main street lefts and side street rights are serviced simultaneously. The U-turns upstream and downstream are also signalized. They operate semi-actuated coordinated with cycle lengths of 70 seconds northbound and 140 seconds southbound. Both signals are two phase: main street throughs and then the U-turns. The offsets are 22 seconds northbound and 20 seconds southbound.



*Figure 10-1: Reduced Conflict Intersection / NC-55 & Holly Springs Road / New Hill Road /
35°39'27.86"N / 78°50'54.99"W*

Using both Synchro and TransModeler, we studied the performance of the facility for the following scenarios:

- *Demand:* hold all else constant and study demands that are 20% below and above the base values.

- *Saturation flow rate*: hold all else constant and explore the impacts of having the base saturation flow rates be 200 pc/hr/lane below and above the 1,900 nominal value.
- *Maximum greens*: hold all else constant and test maximum green values that are 20% below the base values and 20% above.
- *Offsets*: hold all else constant and test offsets that are 20% below and above the base value.

10.2 Findings

Our findings start with the saturation flow rates for the various movements. Fundamentally, these values must be the same between the two analysis packages, or it will not be possible for the results to be the same. Also, it is the *output* saturation flow rates from Synchro that must match the *observed* saturation flow rates from TransModeler. That is, in Synchro, the analyst provides a base saturation flow rate (e.g., 1900 pc/hr./ln) and Synchro then applies adjustment factors, consistent with the HCM, to obtain the *prevailing* saturation flow rates, by lane group, used for analysis. These are the values that TransModeler must match. The saturation flow rates in TransModeler are *not* an input. Rather it is the driver behavior parameters that *cause* the saturation flow rates. In addition, TransModeler provides a buffer time distribution and a parameter marker feature, so that saturation flow rates can be adjusted, globally (buffer time) and locally by approach (parameter markers). In the analyses that follow, both features were used.

Table 10-1 shows the per lane saturation flow rates by movement for both Synchro and TransModeler at the RCI. As can be seen, the *output* saturation flow rates computed by Synchro vary by movement, with most of them being about the same value (e.g., around 1700 pcp/hpl under the 1900 pcp/hpl base value) while two of them, for the EBR-W (EastBound Right movement at the West Intersection) and the WBR-E, are substantially different, around 1,400 pcp/hpl. To match these values, we took two actions. First, we adjusted the buffer time distribution, which applies universally, and adjusted it so the *output* saturation flow rates, in general, were about 1700 pcp/hpl. Then, we added parameter markers to the EBR-W and the WBR-E movements, which in this case, very fortunately, are also approaches, so we could create saturation flow rates that closely matched those from Synchro (1,333 versus 1387 for the EBR-W and 1,406 versus 1,421 for the WBR-E).

Table 10-1: Saturation Flow Rates Per Lane / NC-55 & Holly Springs Road / New Hill Road

		Saturation Flow Rates (veh/h/ln)																							
		Synchro - Sat. Flow output										TransModeler - Sat. Flow output													
		New Hill (W)			North U-Turn			Holly Springs (E)				South U-Turn		New Hill (W)			North U-Turn			Holly Springs (E)				South U-Turn	
		3	6	3	3	6	2	7	7	2	7	3	6	3	3	6	2	7	7	2	7				
Base	NBL-W	SBT-W	EBR-W	UT-N	SBT-N	NBT-E	SBL-E	WBR-E	NBT-S	UT-S	NBL-W	SBT-W	EBR-W	UT-N	SBT-N	NBT-E	SBL-E	WBR-E	NBT-S	UT-S					
Sat Flow	1700	1536	1576	1241	1559	1560	1584	1575	1272	1560	1559	1506	1583	1481	1270	1565	1552	1534	1364	1552	1281				
	1900	1717	1761	1387	1743	1743	1770	1761	1421	1743	1743	1690	1731	1565	1333	1698	1690	1756	1406	1659	1324				
	2100	1882	1946	1533	1926	1927	1956	1946	1571	1927	1926	1756	1856	1629	1395	1827	1884	1846	1463	1739	1469				

While it's possible to look at Table 10-1 and spot the differences, it's easier to compute the differences and provide a separate table. The result is in Table 10-2. Each cell in the matrix

shows the difference between the TransModeler and Synchro values (TM-S); where the value is negative if the TransModeler value is smaller. The row at the bottom shows the root-mean-square differences between the values in the columns. That is

$$RMS\Delta = \sqrt{\frac{1}{N} \sum_i (TM_i - S_i)^2}$$

where: $RMS\Delta$ is the numerical value shown, i is the index to the observations (here, there are three in each column, so $i = 1, 2, 3$, N is the number of difference observations (which is 3), TM_i is the TransModeler value and S_i is the Synchro value. While using this root-mean-square metric may not be the first idea that comes to mind for the reader, it has significant advantages: a) all the differences are converted to positive values and b) the larger differences receive greater emphasis than the smaller ones.

Table 10-2: Differences in the Saturation Flow Rates / TransModeler versus Synchro / NC-55 & Holly Springs Road / New Hill Road

		Differences in Saturation Flow Rates (TM-Synchro)									
		New Hill (W)			North U-Turn		Holly Springs (E)			South U-Turn (S)	
		3	6	3	3	6	2	7	7	2	7
		NBL-W	SBT-W	EBR-W	UT-N	SBT-N	NBT-E	SBL-E	WBR-E	NBT-S	UT-S
Sat Flow	1700	-30.0	7.5	240.5	-289.0	5.5	-31.5	-41.0	92.5	-7.5	-278.0
	1900	-26.4	-30.2	178.7	-409.2	-44.9	-79.4	-4.9	-14.8	-83.5	-419.5
	2100	-126.0	-90.0	96.5	-530.5	-99.5	-72.0	-100.0	-108.0	-187.5	-456.5
RMSΔ		38.2	27.5	90.9	210.6	31.6	32.2	31.2	41.3	59.3	196.1

The most striking differences in Table 10-2 pertain to the U-turns, for both the northern and southern U-turn intersections. This is because of a limitation in Synchro. It does not have a specific adjustment factor for U-turns, even though such adjustments exist in the HCM release 6. Thus, when we specified the U-turn movements, we categorized them as left turn moves; which means Synchro used the left turn adjustment factor (which is 0.95). TransModeler, on the other hand, is accounting for the impact of the turn geometry on the rates at which vehicles can cross the stop-bar; and that is manifest in a significantly lower saturation flow rate (which, intuitively, is defensible). The take-away is this: for intersections where U-turns are allowed, but inconsequential, this shortcoming is likely not a problem; but for a setting like this RCI, where the U-Turns are the only turning movement occurring, that weakness has a clear impact. A possible solution is to override the LT adjustment factor in Synchro with a smaller adjustment when modeling a heavy U-turn movement.

Next, we examined the signal timings. As with the saturation flow rates, in Synchro, the timing values are *inputs*, with the caveat that Synchro does make minor adjustments if the signal is actuated. For TransModeler, the signal timings are *outputs* as well, *but* they are created by the signal’s responses to the actuations based on the timing inputs provided (e.g., the volume-density parameters plus the placement of the detectors and the adjustments to the detector inputs affected by the detector input processing, like delays and extensions). Table 10-3 shows the displayed greens for each movement. By displayed green, we mean the average seconds of green per cycle given to the vehicles on a given approach.

Table 10-3: Displayed Greens by Scenario / NC-55 & Holly Springs Road / New Hill Road

		Displayed Green (sec) / Cycle W&N = 140 / Cycle E&S = 70																							
		Synchro										TransModeler													
		New Hill (W)			North U-Turn			Holly Springs (E)				South U-Turn		New Hill (W)			North U-Turn			Holly Springs (E)				South U-Turn	
		3	6	3	3	6	2	7	7	2	7	3	6	3	3	6	2	7	7	2	7				
		NBL-W	SBT-W	EBR-W	UT-N	SBT-N	NBT-E	SBL-E	WBR-E	NBT-S	UT-S	NBL-W	SBT-W	EBR-W	UT-N	SBT-N	NBT-E	SBL-E	WBR-E	NBT-S	UT-S				
Demand	-20%	40.7	85.4	40.7	14	113.2	38.3	17.7	17.7	47.8	9	38.3	87.7	38.3	15.2	111.7	40.3	15.8	15.8	72.4	13.7				
	0%	43	83.1	43	15	112.2	36.1	19.9	19.9	45.4	11.4	42.8	83.5	42.8	19.2	108.1	37.9	18.1	18.1	49.9	12.7				
	20%	43	83.1	43	16.5	110.7	35	21	21	43.7	13.1	43.3	82.8	43.3	21.1	106.3	36.5	19.6	19.6	47.1	12.6				
Sat Flow	1700	43	83.1	43	15.7	111.5	35.1	20.9	20.9	44.7	12.1	42.3	83.8	42.3	19.5	107.8	37.3	18.7	18.7	48.6	12.6				
	1900	43	83.1	43	15	112.2	36.1	19.9	19.9	45.4	11.4	42.8	83.5	42.8	19.2	108.1	37.9	18.1	18.1	49.9	12.7				
	2100	44.4	81.7	44.4	14.5	112.7	37	19	19	46.1	10.7	42.6	83.5	42.6	19.1	108.1	38.1	18	18	54.6	13.1				
Max Green	-20%	33	65.1	33	14.3	84.9	26.7	15.3	15.3	33.2	9.6	33	65.2	33	15.7	83.6	27.6	14.4	14.4	54.6	9.9				
	0%	43	83.1	43	15	112.2	36.1	19.9	19.9	45.4	11.4	42.8	83.5	42.8	19.2	108.1	37.9	18.1	18.1	49.9	12.7				
	20%	53	101.1	53	16.2	139	45.8	24.2	24.2	58.1	12.7	52.2	101.9	52.2	22.3	132.9	48.3	21.7	21.7	68.4	15.7				
Offset	-20%	43	83.1	43	15	112.2	36.1	19.9	19.9	45.4	11.4	42.6	83.9	42.6	19	108.4	37.5	18.5	18.5	55.9	13.7				
	0%	43	83.1	43	15	112.2	36.1	19.9	19.9	45.4	11.4	42.8	83.5	42.8	19.2	108.1	37.9	18.1	18.1	49.9	12.7				
	20%	43	83.1	43	15	112.2	36.1	19.9	19.9	45.4	11.4	43.3	83	43.3	18.9	108.1	37.7	18.5	18.5	47.3	12.2				

To ensure that the annotations in the table are clear, for the scenarios, the demands explored are 20% below and above the base case values. The saturation flow rates are 1700, 1900, and 2100 pc/hr/lane (pcphpl). The maximum green values are 20% below and above the base case values, and the same is true for the offsets. The results for all four signals are shown. From left to right: a) the New Hill intersection on the west side, b) its associated U-turn intersection to the north, c) the Holly Springs intersection on the east side and d) the associated upstream U-Turn intersection to the south. The annotations for the turning movements are: NBL-W (northbound left for the western main intersection), SBT-W (the southbound throughs), and EBR-W (the eastbound rights); UT-N (the U-turns at the associated U-turn intersection to the north and SBT-N (the southbound throughs); NBT-E (the northbound throughs on the eastern intersection, SBL-E (the southbound lefts), and WBR-E (the westbound rights); and NBT-S (the northbound throughs at the southern U-turn) and SBL-S (the southbound U-Turns).

Table 10-4 presents the numerical differences between the values. As can be seen, the values are nearly identical except for the NBT-S for the -20% demand scenario where TransModeler is providing significantly more green time than Synchro.

Table 10-4: Differences in Displayed Greens / TransModeler versus Synchro / NC-55 & Holly Springs Road / New Hill Road

		Difference in Displayed Green (TM-Synchro)									
		New Hill (W)			North U-Turn		Holly Springs (E)			South U-Turn (S)	
		3	6	3	3	6	2	7	7	2	7
		NBL-W	SBT-W	EBR-W	UT-N	SBT-N	NBT-E	SBL-E	WBR-E	NBT-S	UT-S
Demand	-20%	-2.4	2.3	-2.4	1.2	-1.5	2	-1.9	-1.9	24.6	4.7
	0%	-0.2	0.4	-0.2	4.2	-4.1	1.8	-1.8	-1.8	4.5	1.3
	20%	0.3	-0.3	0.3	4.6	-4.4	1.5	-1.4	-1.4	3.4	-0.5
Sat Flow	1700	-0.7	0.7	-0.7	3.8	-3.7	2.2	-2.2	-2.2	3.9	0.5
	1900	-0.2	0.4	-0.2	4.2	-4.1	1.8	-1.8	-1.8	4.5	1.3
	2100	-1.8	1.8	-1.8	4.6	-4.6	1.1	-1	-1	8.5	2.4
Max Green	-20%	0	0.1	0	1.4	-1.3	0.9	-0.9	-0.9	3.5	0.3
	0%	-0.2	0.4	-0.2	4.2	-4.1	1.8	-1.8	-1.8	4.5	1.3
	20%	-0.8	0.8	-0.8	6.1	-6.1	2.5	-2.5	-2.5	10.3	3
Offset	-20%	-0.4	0.8	-0.4	4	-3.8	1.4	-1.4	-1.4	10.5	2.3
	0%	-0.2	0.4	-0.2	4.2	-4.1	1.8	-1.8	-1.8	4.5	1.3
	20%	0.3	-0.1	0.3	3.9	-4.1	1.6	-1.4	-1.4	1.9	0.8
	RMSΔ	0.9	1.0	0.9	4.1	4.0	1.8	1.7	1.7	9.2	2.0

The next set of values we checked are the V/C ratios: the movement-specific flow rates divided by the movement-specific capacities (the saturation flow rates multiplied by the fraction of average green time to the cycle length). Tables 10-5 and 1-06 show the V/C ratios for both Synchro and TransModeler and the differences between them.

Table 10-5: V/C Ratios by Scenario / NC-55 & Holly Springs Road / New Hill Road

		V/C ratios																											
		Synchro										TransModeler																	
		New Hill (W)			North U-Turn			Holly Springs (E)				South U-Turn				New Hill (W)			North U-Turn			Holly Springs (E)				South U-Turn			
		3	6	3	3	6	2	7	7	2	7	3	6	3	3	6	2	7	7	2	7	3	6	3	3	6	2	7	7
		NBL-W	SBT-W	EBR-W	UT-N	SBT-N	NBT-E	SBL-E	WBR-E	NBT-S	UT-S	NBL-W	SBT-W	EBR-W	UT-N	SBT-N	NBT-E	SBL-E	WBR-E	NBT-S	UT-S								
Demand	-20%	0.25	0.75	0.97	0.57	0.70	0.56	0.81	0.50	0.55	0.71	0.25	0.69	0.84	0.63	0.67	0.51	0.84	0.52	0.46	0.79								
	0%	0.30	0.97	1.15	0.66	0.88	0.74	0.90	0.56	0.72	0.70	0.28	0.90	0.94	0.62	0.86	0.68	0.92	0.57	0.60	0.76								
	20%	0.36	1.16	1.38	0.72	1.07	0.92	1.03	0.63	0.90	0.73	0.33	1.09	1.12	0.68	1.05	0.85	1.02	0.63	0.76	0.92								
Sat Flow	1700	0.33	1.08	1.29	0.71	0.99	0.85	0.96	0.59	0.82	0.73	0.31	0.99	1.00	0.65	0.94	0.74	1.05	0.59	0.64	0.78								
	1900	0.30	0.97	1.15	0.66	0.88	0.74	0.90	0.56	0.72	0.70	0.28	0.90	0.94	0.62	0.86	0.68	0.92	0.57	0.60	0.76								
	2100	0.26	0.89	1.01	0.62	0.79	0.65	0.86	0.53	0.64	0.67	0.27	0.84	0.91	0.60	0.80	0.61	0.88	0.55	0.60	0.77								
Max Green	-20%	0.31	0.99	1.20	0.55	0.93	0.80	0.94	0.58	0.79	0.66	0.29	0.92	0.98	0.61	0.89	0.75	0.92	0.57	0.65	0.78								
	0%	0.30	0.97	1.15	0.66	0.88	0.74	0.90	0.56	0.72	0.70	0.28	0.90	0.94	0.62	0.86	0.68	0.92	0.57	0.60	0.76								
	20%	0.29	0.95	1.12	0.73	0.85	0.70	0.89	0.55	0.68	0.75	0.27	0.89	0.93	0.64	0.84	0.64	0.92	0.57	0.52	0.74								
Offset	-20%	0.30	0.97	1.15	0.66	0.88	0.74	0.90	0.56	0.72	0.70	0.28	0.90	0.95	0.63	0.86	0.69	0.90	0.56	0.63	0.83								
	0%	0.30	0.97	1.15	0.66	0.88	0.74	0.90	0.56	0.72	0.70	0.28	0.90	0.94	0.62	0.86	0.68	0.92	0.57	0.60	0.76								
	20%	0.30	0.97	1.15	0.66	0.88	0.74	0.90	0.56	0.72	0.70	0.28	0.91	0.93	0.63	0.86	0.68	0.90	0.56	0.63	0.79								

The most striking differences are for the EBR-W and NBT-S movements. TransModeler produces significantly lower V/C ratios than Synchro. Our explanation is that TransModeler processes the arriving vehicles in a more efficient way than Synchro assumes happens.

Tables 10-7 and 10-8 show the “maximum” queue length predictions for Synchro and TransModeler and the differences between them. These are expressed in terms of number of vehicles per lane in both models.

Table 10-6: Differences in V/C Ratios / TransModeler versus Synchro / NC-55 & Holly Springs Road / New Hill Road

		Differences in V/C Ratios (TM-Synchro)										
		New Hill (W)			North U-Turn			Holly Springs (E)			South U-Turn (S)	
		3	6	3	3	6	2	7	7	2	7	
		NBL-W	SBT-W	EBR-W	UT-N	SBT-N	NBT-E	SBL-E	WBR-E	NBT-S	UT-S	
Demand	-20%	0.00	-0.07	-0.13	0.06	-0.03	-0.05	0.03	0.02	-0.08	0.09	
	0%	-0.02	-0.07	-0.21	-0.04	-0.02	-0.06	0.01	0.01	-0.13	0.06	
	20%	-0.03	-0.07	-0.26	-0.04	-0.02	-0.07	-0.01	0.00	-0.14	0.19	
Sat Flow	1700	-0.02	-0.10	-0.29	-0.05	-0.05	-0.11	0.09	-0.01	-0.18	0.05	
	1900	-0.02	-0.07	-0.21	-0.04	-0.02	-0.06	0.01	0.01	-0.13	0.06	
	2100	0.01	-0.05	-0.10	-0.02	0.01	-0.05	0.02	0.02	-0.04	0.09	
Max Green	-20%	-0.02	-0.06	-0.22	0.05	-0.04	-0.05	-0.02	-0.01	-0.14	0.12	
	0%	-0.02	-0.07	-0.21	-0.04	-0.02	-0.06	0.01	0.01	-0.13	0.06	
	20%	-0.01	-0.07	-0.19	-0.09	-0.01	-0.06	0.03	0.02	-0.16	-0.01	
Offset	-20%	-0.02	-0.07	-0.20	-0.03	-0.02	-0.05	-0.01	0.00	-0.09	0.14	
	0%	-0.02	-0.07	-0.21	-0.04	-0.02	-0.06	0.01	0.01	-0.13	0.06	
	20%	-0.02	-0.06	-0.22	-0.03	-0.02	-0.06	-0.01	0.00	-0.09	0.09	
	RMSΔ	0.02	0.07	0.21	0.05	0.03	0.06	0.03	0.01	0.12	0.10	

Table 10-7: “Maximum” Queue Length / NC-55 & Holly Springs Road / New Hill Road

		"Maximum" Queues (veh/lane)																											
		Synchro - 95th Percentile *										TransModeler - Maximum																	
		New Hill (W)			North U-Turn			Holly Springs (E)				South U-Turn				New Hill (W)			North U-Turn			Holly Springs (E)				South U-Turn			
		3	6	3	3	6	2	7	7	2	7	3	6	3	3	6	2	7	3	6	3	3	6	2	7				
		NBL-W	SBT-W	EBR-W	UT-N	SBT-N	NBT-E	SBL-E	WBR-E	NBT-S	UT-S	NBL-W	SBT-W	EBR-W	UT-N	SBT-N	NBT-E	SBL-E	WBR-E	NBT-S	UT-S								
Demand	-20%	4.5	27.8	19.6	4.7	16.3	8.5	9.6	3.4	7.9	2.3	3.9	9.9	11.4	4.9	7.0	3.6	8.7	3.9	3.8	7.7								
	0%	4.9	44.2	29.0	5.3	36.1	8.2	12.5	4.9	13.5	2.7	4.6	11.9	34.5	5.6	14.4	4.4	9.3	8.2	4.9	8.8								
	20%	4.8	49.6	37.7	5.6	69.3	12.1	12.7	6.0	23.4	2.9	5.0	12.6	46.4	6.5	24.7	5.1	9.3	4.7	6.1	9.2								
Sat Flow	1700	4.4	44.4	31.0	4.7	55.2	9.2	11.3	5.0	18.9	2.3	4.6	11.0	37.8	4.9	17.3	4.8	8.3	4.3	4.5	7.4								
	1900	4.9	44.2	29.0	5.3	36.1	8.2	12.5	4.9	13.5	2.7	4.6	11.9	34.5	5.6	14.4	4.4	9.3	8.2	4.9	8.8								
	2100	5.0	33.2	27.0	5.4	27.0	9.0	15.3	4.7	11.5	3.1	4.7	12.1	21.0	5.1	10.3	6.1	9.7	4.4	4.9	8.5								
Max Green	-20%	3.1	36.2	24.4	4.5	36.9	6.2	9.9	4.0	11.8	2.4	4.0	10.2	39.8	3.9	15	3.7	7.7	3.5	4.3	6.6								
	0%	4.9	44.2	29.0	5.3	36.1	8.2	12.5	4.9	13.5	2.7	4.6	11.9	34.5	5.6	14.4	4.4	9.3	8.2	4.9	8.8								
	20%	6.7	47.2	33.5	5.8	37.7	11.9	15.4	5.6	14.0	3.4	5.6	13.8	25.2	6.9	18.3	5.6	10.2	4.6	5.8	10.9								
Offset	-20%	4.4	44.2	29.0	5.0	36.1	7.4	12.5	4.9	13.5	2.4	4.0	12.7	28.1	6.0	15.1	5.1	8.6	4.3	4.8	9.1								
	0%	4.9	44.2	29.0	5.3	36.1	8.2	12.5	4.9	13.5	2.7	4.6	11.9	34.5	5.6	14.4	4.4	9.3	8.2	4.9	8.8								
	20%	5.4	44.2	29.0	5.6	36.1	10.6	12.5	4.9	13.5	3.0	4.6	12.1	29.3	4.9	16.9	5.4	9.0	4.3	5.1	8.5								

Table 10-8: Differences in “Maximum” Queue Length / NC-55 & Holly Springs Road / New Hill Road

		Differences in "Maximum" Queues (TM-Synchro)											
		New Hill (W)			North U-Turn			Holly Springs (E)				South U-Turn (S)	
		3	6	3	3	6	2	7	7	2	7	2	7
		NBL-W	SBT-W	EBR-W	UT-N	SBT-N	NBT-E	SBL-E	WBR-E	NBT-S	UT-S		
Demand	-20%	-0.6	-17.9	-8.2	0.2	-9.3	-4.9	-0.9	0.5	-4.1	5.4		
	0%	-0.3	-32.3	5.5	0.3	-21.7	-3.8	-3.2	3.3	-8.6	6.1		
	20%	0.2	-37.0	8.7	0.9	-44.6	-7.0	-3.4	-1.3	-17.3	6.3		
Sat Flow	1700	0.2	-33.4	6.8	0.2	-37.9	-4.4	-3.0	-0.7	-14.4	5.1		
	1900	-0.3	-32.3	5.5	0.3	-21.7	-3.8	-3.2	3.3	-8.6	6.1		
	2100	-0.3	-21.1	-6.0	-0.3	-16.7	-2.9	-5.6	-0.3	-6.6	5.4		
Max Green	-20%	0.9	-26.0	15.4	-0.6	-21.9	-2.5	-2.2	-0.5	-7.5	4.2		
	0%	-0.3	-32.3	5.5	0.3	-21.7	-3.8	-3.2	3.3	-8.6	6.1		
	20%	-1.1	-33.4	-8.3	1.1	-19.4	-6.3	-5.2	-1.0	-8.2	7.5		
Offset	-20%	-0.4	-31.5	-0.9	1.0	-21.0	-2.3	-3.9	-0.6	-8.7	6.7		
	0%	-0.3	-32.3	5.5	0.3	-21.7	-3.8	-3.2	3.3	-8.6	6.1		
	20%	-0.8	-32.1	0.3	-0.7	-19.2	-5.2	-3.5	-0.6	-8.4	5.5		
	RMSΔ	0.6	30.6	7.4	0.6	24.7	4.4	3.6	2.0	9.7	5.9		
	# Lanes	2	2	2	2	2	2	1	2	2	2		

In a few instances, like the SBT-W at New Hill and the SBT-N at the northern U-Turn intersection, TransModeler predicts significantly smaller values than does Synchro. It is important to remember that the Synchro values are 95th percentile queue lengths and the TransModeler values are maximum queue lengths. So, the numbers are not quite comparable; the maximums should be higher than the 95th percentile values, but, since the results are from two different analysis tools, there is no guarantee that such a relationship will hold. Importantly, we also note that when the V/C ratio exceeds 1.0, Synchro uses a different queue estimation formula, which sometimes lead to generating 95th percentile values that are lower than the average queue length. The 95th and maximum queue lengths are important and interesting, but the underlying question is, are the models suggesting that the storage limits are being reached.

Tables 10-9 and 10-10 show the storage capacity utilization results by movement. To cut down on “%” clutter noise, the values are shown as decimals. That means a value like “0.57” should be interpreted as 57% utilization of the storage capacity.

There are some interesting trends. The movement that uses a significant percentage of the storage capacity is the southbound left turn at the Holly Springs Road intersection (SBL-E). Synchro and TransModeler agree that this is a problematic movement. The one where they disagree is the south U-turn at the southern intersection. And that difference can be traced to the difference in the saturation flow rates, where TransModeler is perceiving it is a much lower value than Synchro predicts. Table 10-10 shows the differences in the percent queue utilization

values. Consistent with the comments above, the two movements where the differences are largest are the SBL-E and UT-S.

Table 10-9: Queue Capacity Utilization / NC-55 & Holly Springs Road / New Hill Road

		Queue storage %																							
		Synchro									TransModeler														
		New Hill (W)			North U-Turn			Holly Springs (E)			South U-Turn			New Hill (W)			North U-Turn			Holly Springs (E)			South U-Turn		
		3	6	3	3	6	2	7	7	2	7	3	6	3	3	6	2	7	7	2	7				
		NBL-W	SBT-W	EBR-W	UT-N	SBT-N	NBT-E	SBL-E	WBR-E	NBT-S	UT-S	NBL-W	SBT-W	EBR-W	UT-N	SBT-N	NBT-E	SBL-E	WBR-E	NBT-S	UT-S				
Storage length (veh)		20.6	NA	NA	26.32	NA	NA	21.92	NA	NA	31.16	20.6	NA	NA	26.32	NA	NA	21.92	NA	NA	31.16				
Demand	-20%	0.22	NA	NA	0.18	NA	NA	0.44	NA	NA	0.07	0.19	NA	NA	0.19	NA	NA	0.40	NA	NA	0.25				
	0%	0.24	NA	NA	0.20	NA	NA	0.57	NA	NA	0.09	0.22	NA	NA	0.21	NA	NA	0.42	NA	NA	0.28				
	20%	0.23	NA	NA	0.21	NA	NA	0.58	NA	NA	0.09	0.24	NA	NA	0.25	NA	NA	0.42	NA	NA	0.30				
Sat Flow	1700	0.22	NA	NA	0.18	NA	NA	0.52	NA	NA	0.07	0.22	NA	NA	0.19	NA	NA	0.38	NA	NA	0.24				
	1900	0.24	NA	NA	0.20	NA	NA	0.57	NA	NA	0.09	0.22	NA	NA	0.21	NA	NA	0.42	NA	NA	0.28				
	2100	0.24	NA	NA	0.21	NA	NA	0.70	NA	NA	0.10	0.23	NA	NA	0.19	NA	NA	0.44	NA	NA	0.27				
Max Green	-20%	0.15	NA	NA	0.17	NA	NA	0.45	NA	NA	0.08	0.19	NA	NA	0.15	NA	NA	0.35	NA	NA	0.21				
	0%	0.24	NA	NA	0.20	NA	NA	0.57	NA	NA	0.09	0.22	NA	NA	0.21	NA	NA	0.42	NA	NA	0.28				
	20%	0.32	NA	NA	0.22	NA	NA	0.70	NA	NA	0.11	0.27	NA	NA	0.26	NA	NA	0.47	NA	NA	0.35				
Offset	-20%	0.21	NA	NA	0.19	NA	NA	0.57	NA	NA	0.08	0.19	NA	NA	0.23	NA	NA	0.39	NA	NA	0.29				
	0%	0.24	NA	NA	0.20	NA	NA	0.57	NA	NA	0.09	0.22	NA	NA	0.21	NA	NA	0.42	NA	NA	0.28				
	20%	0.26	NA	NA	0.21	NA	NA	0.57	NA	NA	0.09	0.22	NA	NA	0.19	NA	NA	0.41	NA	NA	0.27				

Table 10-10: Differences in Queue Capacity Utilization / NC-55 & Holly Springs Rd / New Hill Rd

		Differences in %Queue Storage (TM-Synchro)											
		New Hill (W)			North U-Turn			Holly Springs (E)			South U-Turn (S)		
		3	6	3	3	6	2	7	7	2	7		
		NBL-W	SBT-W	EBR-W	UT-N	SBT-N	NBT-E	SBL-E	WBR-E	NBT-S	UT-S		
Demand	-20%	0.000			0.0000			0.000			0.000		
	0%	-0.028			0.0068			-0.041			0.173		
	20%	-0.016			0.0106			-0.145			0.195		
Sat Flow	1700	0.008			0.0342			-0.156			0.203		
	1900	0.008			0.0068			-0.138			0.163		
	2100	-0.016			0.0106			-0.145			0.195		
Max Green	-20%	-0.017			-0.0114			-0.255			0.173		
	0%	0.043			-0.0236			-0.101			0.134		
	20%	-0.016			0.0106			-0.145			0.195		
Offset	-20%	-0.052			0.0433			-0.237			0.242		
	0%	-0.019			0.0365			-0.177			0.214		
	20%	-0.016			0.0106			-0.145			0.195		
	RMSΔ	0.024			0.022			0.156			0.183		

Tables 10-11 and 10-12 present the average delays. Here, for the SBT-W and EBR-W at New Hill, we see the impacts of the differences in the V/C ratios. The delay predictions by Synchro are much higher than those for TransModeler. Which one is “right” requires field data, which we do not have, but a take-away is that Synchro is being more pessimistic about the performance of that movement than is TransModeler. This may reflect the fact that Synchro is making assumptions, analytically about the behavior of the traffic on that approach, while TransModeler is simulating that behavior. The other notable difference is the UT-S at the southern U-Turn intersection where TransModeler is predicting much larger delays than Synchro. Again, this is tied to the significant difference in saturation flow rates predicted by the two analyses.

The NBL-W at New Hill and the EBR-W movements are serviced in the same phase. The difference in their delay is reflective of the much higher v/c ratio for the EBR-W movement, which exceeded 1.0 in most Synchro scenarios. A similar trend can be seen in the TransModeler runs, although Synchro generated slightly higher delays in both cases. The largest differences in delays between models were observed for the SBT-W and UT-S movements. In both cases, Synchro generated delays that were, on average, more than 30 seconds per vehicle than TransModeler. While in some cases, delay differences between movements and across models

can be traced back to saturation flow or green time allocation differences, the evidence from this RCI analysis begins to point to a systematic overestimation of delays in Synchro, particularly for movements across multiple intersections. This phenomenon may be due in part to ignoring the platoon structure effects in its formulation as explained in Chapter 7. .

Table 10-11: Average Delay Sensitivities / NC-55 & Holly Springs Road / New Hill Road

		Average Delays (sec/veh)																					
		Synchro										TransModeler											
		New Hill (W)			North U-Turn			Holly Springs (E)				South U-Turn		New Hill (W)			North U-Turn		Holly Springs (E)			South U-Turn	
		3	6	3	3	6	2	7	7	2	7	3	6	3	3	6	2	7	7	2	7		
		NBL-W	SBT-W	EBR-W	UT-N	SBT-N	NBT-E	SBL-E	WBR-E	NBT-S	UT-S	NBL-W	SBT-W	EBR-W	UT-N	SBT-N	NBT-E	SBL-E	WBR-E	NBT-S	UT-S		
Demand	-20%	34.4	22.3	63.9	51.8	7.6	11.4	32.6	16.5	7	20.9	48.1	11.1	44.3	66.1	5.2	6.2	40.1	21.8	4.4	59.7		
	0%	33	32.1	114.2	62	14.8	13.7	45.5	20.3	11	25.5	51.2	12.6	113.8	66.9	16.5	6.4	42.5	20.1	6.2	63.9		
	20%	31.5	98.9	202.7	65.6	57.3	18.6	55.7	21.7	19.8	26.5	53.1	15.5	179.5	69.9	96.9	7.3	43.3	19.6	7.9	63.9		
Sat Flow	1700	32.3	66	164.7	63.4	30.8	16.4	48.3	20.8	15.3	24.9	50.5	13.5	149.7	73.2	59.2	9.8	42.1	19.8	6.9	55.3		
	1900	33	32.1	114.2	62	14.8	13.7	45.5	20.3	11	25.5	51.2	12.6	113.8	66.9	16.5	6.4	42.5	20.1	6.2	63.9		
	2100	33.1	27.7	72.3	65.2	10	12.5	38.5	20	9	27.3	46.7	11.2	67.5	57.4	8.7	10.5	38.1	20.2	5.8	52.7		
Max Green	-20%	23.1	30	122.2	52.8	19.7	12	46	17	13.1	21.2	44.3	11.5	133.1	19.3	15.8	5.7	37.7	16.7	5.8	45.6		
	0%	33	32.1	114.2	62	14.8	13.7	45.5	20.3	11	25.5	51.2	12.6	113.8	66.9	16.5	6.4	42.5	20.1	6.2	63.9		
	20%	45	36.4	112.8	73.8	13	15.9	47.5	23.7	9.9	30.6	56.1	14.4	86.2	85	21.5	7.4	48.7	24.8	6.6	79		
Offset	-20%	30.2	31.9	114.2	59.1	14.8	13	47.1	20.3	11	25	44.7	14.1	101.5	77.8	17	7.2	40	19.9	6.2	66.7		
	0%	33	32.1	114.2	62	14.8	13.7	45.5	20.3	11	25.5	51.2	12.6	113.8	66.9	16.5	6.4	42.5	20.1	6.2	63.9		
	20%	36.2	32.3	114.2	65.8	14.8	16.4	44.1	20.3	11	26	48.6	12.4	103.6	57.6	17.9	10	39.5	20.1	6.2	54		

Table 10-12: Differences in Average Delays / NC-55 & Holly Springs Road / New Hill Road

		Differences in Average Delays (TM-Synchro)									
		New Hill (W)			North U-Turn		Holly Springs (E)			South U-Turn (S)	
		3	6	3	3	6	2	7	7	2	7
		NBL-W	SBT-W	EBR-W	UT-N	SBT-N	NBT-E	SBL-E	WBR-E	NBT-S	UT-S
Demand	-20%	13.7	-11.2	-19.6	14.3	-2.4	-5.2	7.5	5.3	-2.6	38.8
	0%	18.2	-19.5	-0.4	4.9	1.7	-7.3	-3	-0.2	-4.8	38.4
	20%	21.6	-83.4	-23.2	4.3	39.6	-11.3	-12.4	-2.1	-11.9	37.4
Sat Flow	1700	18.2	-52.5	-15	9.8	28.4	-6.6	-6.2	-1	-8.4	30.4
	1900	18.2	-19.5	-0.4	4.9	1.7	-7.3	-3	-0.2	-4.8	38.4
	2100	13.6	-16.5	-4.8	-7.8	-1.3	-2	-0.4	0.2	-3.2	25.4
Max Green	-20%	21.2	-18.5	10.9	-33.5	-3.9	-6.3	-8.3	-0.3	-7.3	24.4
	0%	18.2	-19.5	-0.4	4.9	1.7	-7.3	-3	-0.2	-4.8	38.4
	20%	11.1	-22	-26.6	11.2	8.5	-8.5	1.2	1.1	-3.3	48.4
Offset	-20%	14.5	-17.8	-12.7	18.7	2.2	-5.8	-7.1	-0.4	-4.8	41.7
	0%	18.2	-19.5	-0.4	4.9	1.7	-7.3	-3	-0.2	-4.8	38.4
	20%	12.4	-19.9	-10.6	-8.2	3.1	-6.4	-4.6	-0.2	-4.8	28
	RMSΔ	16.9	33.1	13.8	13.4	14.4	7.1	6.0	1.7	6.0	36.3

10.3 DDI Analysis

The DDI we studied is located on US-17 (which is also US-74 and US-76) at the interchange with Village Road, NE in Leland, NC just west of Wilmington, NC. An aerial view of the facility is shown in Figure 10-2.



Figure 10-2: Aerial View of the Diverging Diamond Interchange on US-17 (and US-74 and US-76) at Village Road / River Road in Leland, NC

The facility has two lanes in each direction on Village Road. Except for the westbound exit from US-17, the ramps are all one lane wide. The westbound exit starts as being two lanes wide and then expands to four, two right-turn lanes and two left-turn lanes. The signals are both two phase: entering throughs followed by exiting throughs in conjunction with the freeway left turns. The offset between the signals has the westbound green on the northwest signal start 6 seconds before the westbound green for the southeastern signal. While queue spillback on the freeway exit ramps might prove to be a problem, we chose to focus on queue storage between the signals on Village Road.

We studied the performance of the facility in Synchro and TransModeler for these scenarios:

- *Demand*: hold all else constant, test demands that are 20% below & above base values.
- *Saturation flow rate*: hold all else constant and vary the saturation flow rate 200 pc/hr/lane below and above the nominal value of 1900 pc/hr/lane.
- *Signal timing*: hold all else constant and examine maximum greens that are 20% below and 20% above the nominal values
- *Offsets*: hold all else constant and examine offsets that are 10 seconds below and 10 seconds higher than the nominal values.

10.4 Findings

Our findings start with the signal timing outputs, the displayed greens for the various movements. If the demand inputs are the same for both Synchro and TransModeler (which they are) and the (adjusted) saturation flow rates are about the same (which they are; and in Synchro they are an input, while in TransModeler, they are an output), then the next important detail to

check is the signal timing. If the average amount of green time per cycle by Synchro (an input) is different from that provided by TransModeler (an output, from the actuated timing inputs), then the results from the two models will be different. Table 10-13 shows the average displayed greens (seconds) for each scenario considered (the rows) and for each movement (the columns) for Synchro on the left and TransModeler on the right.

Table 10-13: Displayed Greens by Scenario / US-17 at Village Road / River Road

		Displayed Green (sec)												
		Synchro						TransModeler						
		Northwest Intersection			Southeast Intersection			Northwest Intersection			Southeast Intersection			
		WB-TH	EB-TH	SB-LT	WB-TH	EB-TH	NB-LT	WB-TH	EB-TH	SB-LT	WB-TH	EB-TH	NB-LT	Cycle
Demand	-20%	33.3	30.4	17.0	11.6	49.8	29.6	21.9	37.9	16.1	17.1	49.3	34.4	75
	0%	35.4	28.3	19.6	13.0	48.4	25.3	22.1	37.7	16.3	17.1	49.3	34.3	75
	20%	37.0	26.7	23.5	14.5	46.9	22.8	22.2	37.6	16.3	17.7	50.7	35.6	75
Sat Flow	1700	37.2	26.5	22.9	13.8	47.6	24.5	22.1	37.7	16.3	15.1	46.3	31.3	75
	1900	35.4	28.3	19.6	13.0	48.4	25.3	22.1	37.7	16.3	17.1	49.3	34.3	75
	2100	34.6	29.1	18.3	12.2	49.2	26.6	22.1	37.7	16.3	17.7	50.6	35.6	75
Max Green	-20%	30.4	18.3	17.2	11.5	34.9	16.5	26.5	42.3	20.1	23.6	52.7	37.8	60
	0%	35.4	28.3	19.6	13.0	48.4	25.3	22.1	37.7	16.3	17.1	49.3	34.3	75
	20%	41.4	37.3	23.2	14.5	61.9	36.1	27.1	47.8	21.1	15.4	61.0	46.0	90
Offset	-10	35.4	28.3	19.6	13.0	48.4	25.3	22.4	37.4	16.6	15.7	47.3	32.3	75
	0	35.4	28.3	19.6	13.0	48.4	25.3	22.1	37.7	16.3	17.1	49.3	34.3	75
	10	35.4	28.3	19.6	13.0	48.4	25.3	22.1	37.7	16.3	15.8	47.3	32.3	75
	RMSA							12.9	11.5	3.8	5.0	5.3	10.4	

To ensure that the annotations in the table are clear, the demands explored were 20% below and above the base case values. The maximum green values were 20% below and above the base case values, and the offsets were 10 seconds shorter and longer (*not* percentage changes). The results for both signals. From left to right the movements are: a) WB-TH (westbound throughs) at the northwest intersection, b) EB-TH (eastbound throughs at the northwest intersection), c) SB-LT (southbound left turns at the northwest intersection), d) WB-TH (westbound throughs at the southeast intersection), e) EB-TH (eastbound throughs at the southeast intersection, and f) NB-LT (northbound left turns at the southeast intersection).

Comparing the values in the columns among the scenarios it is apparent that the signal timings are somewhat different in both the northwest and southeast intersections. For the northwest intersection, TransModeler gives the EB-TH more green time and the WB-TH, less. For the southeast one, the WB-TH and the NB-LT are allocated more green time in TransModeler than Synchro. These differences should be manifest in the metrics.

Of course, Synchro is “computing” values analytically while TransModeler is “generating” them through simulation, so TransModeler is responding to the arriving traffic patterns in a way that Synchro is not anticipating or perceiving

The next values to check are the V/C ratios: the movement-specific flow rates divided by the movement-specific capacities (the saturation flow rates multiplied by the percentage of green time provided per cycle). Table 10-14 shows the V/C ratios for both Synchro and TransModeler.

Table 10-14: V/C Ratios by Scenario / US-17 at Village Road / River Road

		v/c ratio											
		Synchro						TransModeler					
		Northwest Intersection			Southeast Intersection			Northwest Intersection			Southeast Intersection		
		WB-TH	EB-TH	SB-LT	WB-TH	EB-TH	NB-LT	WB-TH	EB-TH	SB-LT	WB-TH	EB-TH	NB-LT
Demand	-20%	0.28	0.27	0.76	0.57	0.36	0.35	0.37	0.18	0.69	0.33	0.31	0.26
	0%	0.33	0.36	0.83	0.64	0.46	0.51	0.46	0.22	0.85	0.42	0.39	0.33
	20%	0.38	0.46	0.83	0.69	0.57	0.68	0.55	0.27	1.02	0.49	0.45	0.38
Sat Flow	1700	0.36	0.43	0.79	0.67	0.52	0.59	0.52	0.37	0.95	0.53	0.46	0.20
	1900	0.33	0.36	0.83	0.64	0.46	0.51	0.46	0.22	0.85	0.42	0.39	0.33
	2100	0.31	0.32	0.80	0.62	0.41	0.44	0.42	0.30	0.77	0.37	0.34	0.14
Max Green	-20%	0.31	0.45	0.75	0.58	0.51	0.62	0.44	0.34	0.78	0.34	0.41	0.17
	0%	0.33	0.36	0.83	0.64	0.46	0.51	0.46	0.22	0.85	0.42	0.39	0.33
	20%	0.34	0.33	0.84	0.69	0.43	0.43	0.45	0.32	0.79	0.56	0.37	0.15
Offset	-10	0.33	0.36	0.83	0.64	0.46	0.51	0.46	0.22	0.83	0.46	0.40	0.35
	0	0.33	0.36	0.83	0.64	0.46	0.51	0.46	0.22	0.85	0.42	0.39	0.33
	10	0.33	0.36	0.83	0.64	0.46	0.51	0.46	0.22	0.85	0.45	0.40	0.35
	RMSΔ							0.1	-0.1	0.0	-0.2	-0.1	-0.2

In this case, while the V/C ratios are similar, there are some notable differences. For the northwest intersection, both Synchro and TransModeler yielded similar V/C ratios for the SB-LT, but for the WB-TH and EB-TH, Synchro has about the same V/C ratios while TransModeler consistently has a higher V/C ratio for the WB-TH. At the southeast intersection, Synchro and TransModeler agree about the V/C ratios for the EB-TH, but for both the WB-TH and NB-LT, Synchro always has higher values, perhaps due to a difference in saturation flow rates.

Table 10-15 shows the queue length predictions for Synchro on the left and TransModeler on the right. Most notably, TransModeler predicts significantly larger queues for the off-ramp SB-LT at the northwest intersection, while Synchro predicts larger queues for the EB-TH at the southeast intersection.

Table 10-15: Queue Length Sensitivities / US-17 at Village Road / River Road

		Queues (veh/lane)											
		Synchro 95th Percentile						TransModeler - Maximum					
		Northwest Intersection			Southeast Intersection			Northwest Intersection			Southeast Intersection		
		WB-TH	EB-TH	SB-LT	WB-TH	EB-TH	NB-LT	WB-TH	EB-TH	SB-LT	WB-TH	EB-TH	NB-LT
Demand	-20%	2.3	3.7	7.1	4.3	8.4	6.6	3.0	2.1	3.6	3.1	2.0	1
	0%	3.2	4.2	11.2	5.1	10.2	8.2	3.0	2.3	6.7	3.6	2.1	2.6
	20%	8.5	4.5	14.5	5.8	15.3	9.2	3.0	2.4	35.9	3.9	2.1	3.5
Sat Flow	1700	6.0	4.1	12.1	5.0	12.9	8.0	3.0	2.3	6.3	3.6	2.0	2.3
	1900	3.2	4.2	11.2	5.1	10.2	8.2	3.0	2.3	6.7	3.6	2.1	2.6
	2100	1.0	4.4	9.1	5.1	10.2	8.2	3.0	2.3	6.6	3.6	2.0	2.8
Max Green	-20%	3.8	3.3	10.1	4.0	10.8	6.3	3.0	2.3	6.1	3.5	2.0	2.7
	0%	3.2	4.2	11.2	5.1	10.2	8.2	3.0	2.3	6.7	3.6	2.1	2.6
	20%	1.9	5.1	10.8	6.1	12.0	9.9	3.0	2.1	5.2	3.5	2.0	1.9
Offset	-10	4.1	4.2	11.2	5.1	10.6	8.2	2.9	2.1	6.1	3.7	2.1	2.4
	0	3.2	4.2	11.2	5.1	10.2	8.2	3.0	2.3	6.7	3.6	2.1	2.6
	10	3.7	4.2	11.2	5.1	13.2	8.2	3.0	2.5	5.8	3.7	2.0	2.7
	RMSΔ							2.0	2.0	7.6	1.6	9.3	5.7
	# Lanes	2	3	2	2	2	1	2	3	2	2	2	1

There are also some standout anomalies, highlighted in deep red by the conditional formatting, where the queue lengths are much larger than the others for the same movement. As

before, we do need to recall that the Synchro values are 95th percentile queue lengths and the TransModeler results are maximum queue lengths. So, the values are not quite comparable; and the maximums should be higher than the 95th percentile values, but, since the results are from two different analysis methodologies, there is no guarantee that such a relationship will hold. Nevertheless, the TransModeler prediction of a 36 vehicle queue for the SB-LT movement is strikingly at odds with all other estimates across both models. The reader should recall that the v/c ratio for that movement was the only one exceeding 1.0 across models and scenarios.

The 95th and maximum queue lengths are important and interesting, but the underlying question is, are the models suggesting that the storage capacity limits are being reached. Table 10-16 shows the storage capacity utilization by movement. To cut down on “%” clutter noise, the values are shown as decimals. That means “0.71” should be interpreted as 71% utilization of the storage capacity. There is one striking difference. At the southeast intersection, Synchro predicts the 95th percentile queues for the EB-TH movement taking up up 39-71% of the available storage capacity while TransModeler predicts the maximum queue length reaches only 9% of the queue capacity. This is consistent with the earlier finding that TransModeler v/c ratios tended to be lower (and the green times higher) both of which will affect the estimation of queues and delays for that movement compared to Synchro. No such problems were encountered for the WB-TH movement at the Northwest intersection.

Table 10-16: Queue Capacity Utilization / US-17 at Village Road / River Road

		Queue Storage %											
		Synchro						TransModeler					
		Northwest Intersection			Southeast Intersection			Northwest Intersection			Southeast Intersection		
		WB-TH	EB-TH	SB-LT	WB-TH	EB-TH	NB-LT	WB-TH	EB-TH	SB-LT	WB-TH	EB-TH	NB-LT
Storage length (veh)		21.68	NA	NA	NA	21.68	NA	21.68	NA	NA	NA	21.68	NA
Demand	-20%	0.11	NA	NA	NA	0.39	NA	0.14	NA	NA	NA	0.09	NA
	0%	0.15	NA	NA	NA	0.47	NA	0.14	NA	NA	NA	0.09	NA
	20%	0.39	NA	NA	NA	0.71	NA	0.14	NA	NA	NA	0.09	NA
Sat Flow	1700	0.28	NA	NA	NA	0.60	NA	0.14	NA	NA	NA	0.09	NA
	1900	0.15	NA	NA	NA	0.47	NA	0.14	NA	NA	NA	0.09	NA
	2100	0.04	NA	NA	NA	0.47	NA	0.14	NA	NA	NA	0.09	NA
Max Green	-20%	0.18	NA	NA	NA	0.50	NA	0.14	NA	NA	NA	0.09	NA
	0%	0.15	NA	NA	NA	0.47	NA	0.14	NA	NA	NA	0.09	NA
	20%	0.09	NA	NA	NA	0.56	NA	0.14	NA	NA	NA	0.09	NA
Offset	-10	0.19	NA	NA	NA	0.49	NA	0.13	NA	NA	NA	0.09	NA
	0	0.15	NA	NA	NA	0.47	NA	0.14	NA	NA	NA	0.09	NA
	10	0.17	NA	NA	NA	0.61	NA	0.14	NA	NA	NA	0.09	NA
RMSΔ								0.09	NA	NA	NA	0.40	NA

Finally, Table 10-17 presents the trends in the average control delays. Here, for the northwest intersection, the pattern between the movements is similar for Synchro and TransModeler, although Synchro predicts larger values, consistent with the generally higher v/c ratios. For the southeast intersection, the same is true except that Synchro’s predictions of the delays for the EB-TH are two-to-three times those of TransModeler.

Table 10-17: Average Delay Sensitivities / US-17 at Village Road / River Road

		Average Delays (sec/veh)											
		Synchro						TransModeler					
		Northwest Intersection			Southeast Intersection			Northwest Intersection			Southeast Intersection		
		WB-TH	EB-TH	SB-LT	WB-TH	EB-TH	NB-LT	WB-TH	EB-TH	SB-LT	WB-TH	EB-TH	NB-LT
Demand	-20%	18.7	16.0	33.5	33.6	14.3	19.8	13.7	8.3	21.4	23.4	5.8	14.5
	0%	13.8	17.6	35.8	33.6	14.4	25.3	12.2	8.1	20.1	23.6	4.9	14.9
	20%	9.9	18.9	35.0	33.1	16.1	30.7	10.7	8.0	20.8	23.5	4.3	14.5
Sat Flow	1700	11.5	15.8	32.8	34.1	16.5	27.8	11.7	8.1	20.3	23.8	4.6	14.9
	1900	13.8	17.6	35.8	33.6	14.4	25.3	12.2	8.1	20.1	23.6	4.9	14.9
	2100	14.3	16.9	33.6	33.3	13.0	22.9	12.4	8.5	20.0	23.7	4.9	15.1
Max Green	-20%	12.8	17.4	27.9	25.4	15.6	25.5	14.1	9.1	19.8	22.8	3.8	16.6
	0%	13.8	17.6	35.8	33.6	14.4	25.3	12.2	8.1	20.1	23.6	4.9	14.9
	20%	10.8	18.8	40.7	41.9	12.9	24.7	14.2	8.9	19.9	28.0	4.2	12.0
Offset	-10	5.5	17.6	35.8	33.6	7.6	25.3	12.3	8.4	19.7	23.6	4.0	15.2
	0	13.8	17.6	35.8	33.6	14.4	25.3	12.2	8.1	20.1	23.6	4.9	14.9
	10	14.6	17.6	35.8	33.6	18.2	25.3	14.2	8.4	20.1	23.7	4.4	14.5
	RMSΔ							2.9	9.2	14.9	10.0	10.0	10.8

10.5 Summary and Conclusions

This chapter has demonstrated that sensitivity analysis can be used to examine trends in a variety of performance metrics under varying operating conditions. Overall, Synchro and TransModeler predict similar performance trends (i.e. the relative congestion across movements), although Synchro has the tendency to produce higher delays and queues, on average, than does TransModeler. One way to explain this is through a macro analysis. For example, across all 120 scenarios tested in the RCI, TransModeler generated lower v/c ratios than Synchro in 72% of the cases. For the DDI it was an identical 71% of the 72 scenarios. We find that there are noticeable differences, not in the distribution of green time with some exceptions, which is encouraging, but in the “maximum” queue lengths and in the delays. Our perception is that this is because Synchro is analytical and TransModeler is simulation-based. That does not necessarily mean Synchro is better; but it does mean that TransModeler is sensitive to nuances that Synchro cannot “see”. The bottom line, from NCDOT’s perspective, is that either tool can be used if applied carefully and thoughtfully and the information produced will be helpful and meaningful.

We learned a few interesting details about doing side-by-side analysis using Synchro and TransModeler. One is that it is important to ensure that the saturation flow rates match; and *not* the base values, but the actual values that are used to control the discharge rate for each movement. In Synchro, these are values derived from adjusting a base value (e.g., 1900 pcphpl) to capture the effects of the various adjustment factors. In TransModeler, they are an outcome of the driver behavior parameter specifications combined with buffer time distributions, either the one that applies globally or the ones that apply locally due to the parameter marker values. And setting these buffer time distributions is an “observe and adjust” process where you must statistically analyze the saturation headways obtained in the i^{th} iteration and then specify the

distribution to be tested in the $i+1^{st}$ iteration, until the saturation headway distribution lies in an acceptable range of values. It can be done; it is time consuming, and it is critically important.

Another interesting detail is that Synchro has difficulty dealing with U-Turn movements. There isn't an adjustment factor specifically for U-Turns that allows the saturation flow rate to be downward adjusted to capture the effects of the restrictive geometry associated with those turns. In contrast, TransModeler is "designed" to account for the impacts on vehicle movement created by restrictive geometries, so it produces saturation flow rates, for example, for the U-Turns, that accounts for the difficulty of making those movements. (This also reinforces our comment that adjusting the buffer times and parameter marker values is somewhat challenging and iterative, because the saturation flow rates reflect the compound effects of the intersection geometry and the buffer time / parameter marker values employed.)

We also learned that Synchro has a peculiar way of computing the 95th percentile queue length when the V/C ratio is greater than 1.0. Of course, the capacity is exceeded. A standing queue will exist, and it will dissipate only when the demand drops below capacity. However, Synchro does not ask for when that will happen. It simply endeavors to compute the 95th percentile queue length by assuming that the overload condition will exist only for two cycles. That is, it uses an analysis "period" of two cycles to estimate the length of the 95th percentile queue. Because it does this, as the Synchro guidance indicates, it is possible that the 95th percentile queue length estimate may be *shorter* than the 50th percentile (average) queue length estimate. It is very important that this nuance is understood so that analysts are not either misled by the 95th percentile queue length estimates and/or that they misunderstand the relationship between the 95th and 50th percentile queue length estimates when the V/C ratio exceeds 1.0.

In Synchro, alternative or any facilities with multiple intersections can be modeled as separate facilities (HCM option) or as a network. In the former case, the user must enter an arrival type or a progression factor to account for the effect of coordination. Also, since the intersections are dealt with separately, the model does not report a movement based travel times. In the network case, after signal optimization, Synchro actually generates the movements' progression factors based on the optimized (or input) green times and offsets. In either case, movement based OD's are not reported, only intersection level delays are. For Trans Modeler, on the other hand, if the analyst sets up the model "correctly", such overall times-in-system can be observed "easily" because it is possible to focus on reports of the travel times for each OD-pair.

11 Chapter 11 Summary, Conclusions and Guidance

11.1 Summary and Conclusions

This report summarizes the findings of a research project aimed at assessing the accuracy of both analytical and microsimulation tools in describing the operational performance of a variety of intersection and interchange types. The three tools evaluated in this study were SYNCHRO10, SIDRA9 and TransModeler5. The original, Pre-Covid intent was to cover 10 congested interrupted flow facilities in the field. The revised scope reduced the field effort to six sites, with an additional two sites being examined via a sensitivity analysis to variations in demand volumes, capacity and signal control conditions.

The team carried out all fieldwork using high-resolution videos taken from one or two drones at a height of 200-400 ft., supplemented with ground-based cameras and Bluetooth units as needed. Video data was then post-processed via a third-party vendor, Data From Sky (DFS). The processed videos enabled the team to generate individual vehicle ID's and subsequently produce multiple performance measures at the point, segment, and facility levels.

In addition to the general conclusions that follow, the team was able to identify two critical problems and generated solutions for them. The first problem relates to the calibration, in TransModeler, of critical headway parameters like saturation headways at signal-controlled intersections and critical gap values at roundabouts. The research team developed an innovative field approach for estimating the saturation headways and the accepted and rejected headways so that TransModeler could be correctly calibrated. The second issue was in identifying and finding a solution to deal with a major deficiency in both SYNCHRO and SIDRA regarding delay estimates for sites with multiple intersections such as CFIs, DDIs, RCIs and Offset intersections. The current methods in both models tend to severely overestimate delays because they ignore the platooning structure of the departing vehicles at the upstream intersection (s) and the effect of signal offset will have on delays. In effect, both the uniform and random delay terms tend to be overestimated in those cases. The reader can find a detailed explanation of both these contributions in Chapters 4 and 7, respectively. The following bullets summarize the general study findings from both the data collection, data extraction and model validation.

1. The research for the first time generated what we believe is the highest quality input data for model calibration and validation, using count and speed data that are based on vehicle trajectory tracing for vehicles approaching, within and departing each facility by employing Unmanned Aerial Vehicles.
2. The research followed a very rigorous definition of what is meant by model calibration and validation. Calibration was limited to specifying the correct geometry and controls, like estimating driver behavior parameters such as saturation flow rates and gap acceptance (or capacity), along with various vehicle attributes.
3. The research also, perhaps for the first time, included calibration of the signal timing specifications. We deemed this important because otherwise, the amount of green time provided by the simulation model could be significantly different from that provided in the field. If this were true, the V/C ratios would be different, and as a result, the delays

and queue lengths would be very different. We first checked that the signal data inputs were correct when compared to the signal plans, like detector locations, detector modifications of the vehicle inputs, like delays and extensions, and the signal timing values. Then, we compared the observed distributions of green times by movement, from split monitor reports and/or the videos, with the distributions of green times produced by the simulation model. In a few instances, the two were different, and this proved traceable to differences in the maximum green times. The signal plans showed values that were different from those in the split monitor reports. Adjusting the maximum greens in the simulation model fixed this problem.

4. We treated validation as the process of comparing the selected performance measure(s) captured in the field against the three models' predictions of the same. The team warns that calibrating a model by trying to match its *performance measures against the field values* is highly inadvisable, and will result in model overfitting and poor transferability to other sites or conditions.
5. Regardless of the facility being analyzed, all model validation work focused on one or two movements at one approach, where the most comprehensive coverage using drones, ground cameras and (some time) Bluetooth units were available.
6. In general, for congested signalized intersections and interchanges, the effect of varying the green and cycle lengths to model actuated control was not necessary, as in most of the cases most actuated phases tended to max out as opposed to gapping out.
7. The team encountered some difficulties extracting appropriate data for model calibration and validation when the back of the queue persisted beyond the field of view, even for drones operating at 300-400 ft. heights. Demand in this case should be estimated taking into account the initial and final queue at the start and end of each data collection period.
8. In the 3 models tested in this project, the initial queue input was addressed in different ways. In SYNCHRO the initial queue can be entered as separate input; in SIDRA9 the vendor recommended that it be converted into additional demand; and finally in TransModeler5 the initial queue is calibrated by adjusting the warm up period demand.
9. Image processing tools are hindered by the same problem in item 5, which requires the analysis to focus on *performance data that are within the field of view only*. This was done by setting upstream and downstream *virtual* detectors, sometimes within the queue itself as was done for the site in Chapter 3.
10. In cases where the field of view is limited, the demand and entry speeds must be calibrated with field values. In addition, the various distances covered within those detectors including the approach, the negotiation and exit are also field-measured and entered as inputs into the models.
11. As the result of focusing on performance in the field of view at some sites, the most appropriate performance measure by which to validate the various models was the *travel time between the entry and exit virtual sensors*, which in some cases can no longer assume vehicles arriving or departing at the cruise speed.
12. During this research, the team generated a new method for calibrating the critical headway in the TransModeler microsimulation model. The method is described in the

roundabout Chapter 3 and was found to yield more accurate performance measures, compared to the default value used by NCDOT.

13. As stated earlier, the team identified limitations in both SIDRA and SYNCHRO when it comes to modeling offset and continuous flow intersections. This is based on an erroneous assumption that traffic arrives throughout the cycle from an upstream signal, which is not the case. Analytical models overestimate those delays by a significant margin, even if in much of the cycle no arrivals from the source movement take place. An analytical solution has been proposed in this research which has generated closer values to the field observations. Details of that approach are described in Chapter 7.
14. The SIDRA model enables the user to modulate the effect of a downstream blockage through a blocking factor that varies from zero to 1.0, with 1.0 implying full blockage and zero no blockage. This parameter was calibrated to produce the saturation flow rate of an upstream signal in the presence of a downstream queue at the offset intersection.
15. In general, both analytical models tested in this study, namely SIDRA9 and SYNCHRO tended to generate similar outcomes in terms of predicted performance measures. SIDRA holds some advantages in terms of the detailed outputs and visuals generated compared to SYNCHRO, and its ability to do a lane-by-lane analysis that allows for varying lane utilization. This facility was very useful in the cases of the continuous flow intersection and the offset intersection.
16. Calibration, arguably the most important step in any simulation modeling effort, suffers from a lack of simultaneously-collected data. Unmanned aerial vehicles are formidable tools for generating calibration and validation datasets both for analytical and simulation platforms. This research is a testament to those capabilities of UAVs

An overall summary of the model assessment across all sites and validated movements is shown in Table 11-1 below. It shows that the analytical models tended to overstate the field travel times, due primarily to several effects: (a) presence of an initial queue, (b) larger overflow delays than observed in the field, (c) ignoring the upstream platoon structure pattern at a downstream signal. Trans Modeler on the other hand yielded slightly lower travel times but performed better under the studied conditions in most sites.

Table 11-1: Summary of Model Assessment Results

Site Name with Field Data Collection	Movement Tested / Validated	Field Travel Time (s)	SYNCHRO Travel Time (s)	SIDRA Travel Time (s)	TransModeler Travel Time (s)
NC-50 and NC-42 (Video 2)	SB-T	163	322	233	141
	SB-R	158	323	235	108
Pullen-Stinson Roundabout* (*Video 3 ONLY- in mph)	SB-T (SB-L)	10 (12.5)*	UNTESTED	8 (10.5)*	14 (15)*
	EB-T (EB-L)	15(13)*	UNTESTED	14(11)*	18 (16.5)*
College Rd. and Oleander St.	EB-T	73	92	110	74
	EB-L	123	193	186	96
Highwoods @ Capital Blvd**	SB-L	150	180**	190**	160
Capital @ Westinghouse	EB-T	18	20	19	16
CFI Brookshire /Mt Holly**	WB-L	94	123**	148**	91
	WB-T	33	32	30	38
NC 86 @ I-85	SB-T	25	24	22	19
	SB-R	28	18	25	24
	WB-L	41	50	48	41

Red values indicate higher travel times than the field, green indicate lower travel times than the field

* The values reported in these two rows (only) are average travel speeds (mph) not travel times.

** Based on the corrected approach described in Chapter 7, the proposed analytical approach generated travel times that were much closer to the field values in those two cases.

Next the following conclusions can be drawn from the sensitivity analysis described in Chapter 10 of this report. First, conclusions based on the Synchro model results are given.

1. In Synchro, the control delay is strongly affected by the progression factor. The value of the actuated green time output is automatically estimated in the tool as well as demand and saturation flow rate.
2. Back of queue estimation in Synchro is calculated with one of two formulas. For $v/c < 1$ the back of queue is calculated assuming uniform arrivals and departures excluding vehicles experiencing less than 6 seconds of delay. Under oversaturated conditions, the maximum queue length after two cycles is reported as the back of queue. In estimating the 50th and 95th queues, this approach is valid. However, a distinguishing factor between the two formulas is whether metered flow from an upstream signal is considered or not. The 50th percentile queue is computed without considering upstream metering. Conversely, demand flow is restricted by upstream capacity if the upstream v/c exceeds

- 1.0, but only when computing the 95th percentile queue. This had led to the generation of longer 50th percentile queues than 95th percentiles in some scenarios.
3. For the tested DDI the team found that control delay for the SB-LT movement at the NW intersection and the WB-TH movement at the SE intersection were not sensitive to demand changes in Synchro. This is because the increase in the g/C ratio for the movements counteracted the increase in v/c ratio. Both the WB through movement at the NW intersection and the EB through move at the SE intersection had unusual patterns. These were caused by the fact that the progression factor that is automatically computed in Synchro.
 4. In sensitivity tests focused on saturation flow rate, control delay did not appear to depend on saturation flow rate. This is because the higher the saturation flow rate is, the higher the progression factor that is estimated.
 5. Regarding the maximum green time sensitivity test, as the max green parameter input increased, the cycle length also increased. As a result, the highest maximum green yielded the lowest green split and resulted in higher control delay. Finally, the offset change solely affected the progression factor.
 6. For the RCI, most of delay is caused by the minor street traffic, primarily for the EB-R movement at the west intersection. Also, control delay for all the movements increased as demand increased. This was especially true when the v/c ratios exceeded 1.0. The saturation flow rate sensitivity tests yielded expected trends; that is, higher saturation flow rates resulted in lower control delays. However, some movements were not affected by the change in saturation flow rate. This was because of the negative correlation between v/c ratio and the value of the progression factor in Synchro; c) regarding the maximum green sensitivity test, control delay was not significantly affected from the overall intersection perspective. This is due to the fact that as the EB-R movement at the west intersection (which mostly contributed to the overall delay) went down, other movement delays went up and finally, d) The change of the offset value did not yield significant differences in delays between scenarios and a small change in the progression factor.

11.2 General Guidance

- 1- The study measured saturation flow rates that were in general lower than expected. In only one case did we measure a saturation flow rate more than 1,800 pc/hr/lane. The observed range varied from a low of 1,530 to a high of 1,780. This is based on measurements taken at sites in five different NC counties. The team recommends the use of an ideal saturation flow rate of 1,750 pc/hr/lane for capacity analysis purposes.
- 2- Under congested conditions, it is important to account for the effect on delays of the presence of initial and final queues. Thus, when traffic counts are being conducted the team recommends that the size of the initial queue at the start of the count, and the final queue at the conclusion of the count, be recorded. The initial and final queue lengths, in particular have a significant effect on the resulting delays and LOS.

- 3- An additional precaution is required when queues are present at the start of the data collection. Delays to vehicles in the initial queue should not be included; only the vehicles joining that initial queue should be tracked for their delays.
- 4- To overcome some of the issues related to initial and final queues, the team has relied instead on travel times between key points to validate the models. Both SIDRA and TransModeler can generate this performance measure, while SYNCHRO cannot. It would be useful to recommend that such a measure be supplemented in its output.
- 5- Under congested conditions, the team found it difficult to track the back of the queue because of sight (and video) distance limitations. Both the analytical and simulation models calculate delays on the basis of a difference from an ideal travel time at the free flow or posted speed limit. In the event the back of queue cannot be tracked, the team recommends the use of a reduced free flow speed, consistent with field observations.
- 6- There are many definitions of what constitutes model calibration and validation. Throughout this study, we limited the calibration parameters to those describing user behavior and characteristics (saturation flow, crossing speed, critical headway, fraction of heavy vehicles, etc.) and control schemes (signal plans, LT phasing, etc.). The team's guidance is NOT to calibrate a model by attempting to match measures of performance such as delays, stops or travel time. This is likely to lead to model overfitting, and make it less transferable to other conditions.

11.3 Model Use Guidance

- 1- Alternative intersections capacity analysis should be based on Origin-Destination (OD) delays and travel times, per the HCM. Neither SIDRA nor SYNCHRO in their current versions can report OD-based delays. These movement-based delays are highly sensitive to the green time at the origin and offset to the next intersection. In analytical models (including HCM) delays are computed for the combined merging movements at each intersection, and therefore are not OD-based. NCDOT should be aware of this limitation, which is not present in microsimulation models such as TransModeler.
- 2- Another limitation emerged when testing the delay for the major street LT movement at the main intersection of the CFI site. Analytical models assume *traffic arrives at the main intersection throughout the cycle*, in its delay computations. This leads to an overestimation of that delay. In reality, LT traffic arrives only during the upstream crossover signal release period therefore that movement delay will also depend on the length of the upstream green and the offset between the crossover and main intersection green times. NCDOT should cautiously interpret SYNCHRO results for that movement.
- 3- The research team could not identify any documentation on a procedure to calibrate the critical headway for roundabout operations in TransModeler in NC. We understand that there is a default headway buffer of 0.5 sec being employed. We have provided guidance on how to calibrate that value in Chapter 4 of this report and recommend that NCDOT review and adopt this guidance.
- 4- In TransModeler, saturation flow rates at signals are coded via a "headway buffer" parameter. A relationship between the saturation flow rate and this headway buffer value is shown in Figure 3-5 of this report. The team recommends the use of this graphic should site-specific values of saturation flow need to be entered in TransModeler.

- 5- Moreover, this headway buffer value pertains model-wide, which means every movement is affected. Sometimes, this is not appropriate, because the geometry of approaches can vary. We found, especially for the RCI analysis, to obtain consistency between the SYNCHRO and TransModeler saturation flow rates, we had to use the “parameter marker” feature that allows approach specific parameter values, like the headway buffer, to be employed. We encourage NCDOT to follow this practice.
- 6- In addition, NCDOT should be aware that the parameter marker feature pertains to approaches, not individual movements. So, if there are field-observed differences in saturation flow rates for through, left and right-turning movements on a given approach, these differences cannot be replicated in TransModeler. (They can in SYNCHRO and SIDRA.) NCDOT might encourage Caliper to make this adjustment be movement specific.
- 7- The CAP-X model v/c estimates were consistent with other analytical and simulation models when operating in the LOS A-C range. However, when those models reported LOS of E-F, CAP-X tended to produce a better indication of LOS. The research team recommends that when CAP-X generates an intersection v/c ~ 0.85 to view this condition as approaching capacity for some critical movements. Intersections with sufficient demand to trigger this v/c in CAP-X are very sensitive to signal timing, turn bay length and other geometric and control features requiring additional modeling detail.
- 8- In Synchro, there are no U-turn specific adjustment factors to saturation flow rates; the team recommends overriding the left turn saturation flow rate adjustment factor default values and use a lower factor for U-turns consistent with the HCM6 recommendations. This adjustment is applicable in the analysis of both RCI and MUT junctions.
- 9- In summary, the following guidance is presented on the use of analytical and microsimulation models.
 - a. In cases where the current or projected operations are anticipated to be at LOS A-C both analytical and simulation models will yield consistent results. This is based on our validation findings at the single lane roundabout, for the through movement at the offset intersection, at the traditional diamond interchange, and for the through movement on the major road CFI.
 - b. In cases where the current or projected operations are consistent with LOS D-F we find that the analytical models *tend to overestimate delays* and travel times. This is based on our validation findings at the isolated and coordinated signalized intersections, for the LT movement at the offset intersection, and for the LT movement at the main intersection of the CFI.
 - c. For all alternative intersections including CFI, RCI, DDI, MUT the current analytical models including SYNCHRO and SIDRA are not able to properly estimate delays and LOS by OD movement correctly, and therefore the team recommends that microsimulation be used for operational assessment of those intersections.

References

1. Alexiadis, V., Jeannotte, K., Chandra, A. *Traffic Analysis Toolbox Volume I, Traffic Analysis Tools Primer*. No. FHWA-HRT-04-038. Office of Operations, Federal Highway Administration, Washington, D.C., United States. 2004.
2. Park, B., and Schneeberger, J.D. Microscopic simulation model calibration and validation: case study of VISSIM simulation model for a coordinated actuated signal system. *Transportation Research Record*, No.1856., 2003, pp.185-192.
3. Dowling, Richard Gerhard, Joseph R. Holland, and Allen Huang. *California Department of Transportation: Guidelines for Applying Traffic Microsimulation Modeling Software*. Dowling Associates, 2002.
4. Jeannotte, K., Chandra, A., Alexiadis, V., Skabardonis, A. *Traffic analysis toolbox Volume II: Decision support methodology for selecting traffic analysis tools*. No. FHWA-HRT-04-039. 2004.
5. FDOT. *Traffic Analysis Handbook*. Florida Department of Transportation, Tallahassee, FL, 2021.
6. VDOT. *Traffic Operations and Safety Analysis Manual – Version 1.0*. Virginia Department of Transportation, Richmond, VA, 2015.
7. PennDOT. *Traffic Engineering Manual*. Pennsylvania Department of Transportation, Harrisburg, PA, 2014
8. ODOT. *Protocol for VISSIM Simulation*. Oregon Department of Transportation, Salem, OR, 2011
9. Click, S.M., and Roupail, N.M. *Field Assessment of the Performance of Computer-based Signal Timing Models at Individual Intersection in North Carolina*. North Carolina Department of Transportation, Raleigh, 2000.
10. Fang, F.C., and Elefteriadou, L. Some Guidelines for Selecting Microsimulation Models for Interchange Traffic Operational Analysis. *Journal of Transportation Engineering*, Vol.131(7), 2005, pp.535-543.
11. Dowling, R. *Traffic Analysis Toolbox Volume VI: Definition, Interpretation, and Calculation of Traffic Analysis Tools Measures of Effectiveness*. Report No. FHWA-HOP-08-054, Federal Highway Administration, Washington, D.C., 2007.
12. Brilon, W. *Traffic Flow Analysis Beyond Traditional Methods*. Proceedings of the 4th International Symposium on Highway Capacity. Washington, DC, USA: Transportation Research Board, 2000.
13. Dowling, R., Skabardonis, A., and Alexiadis, V. *Traffic Analysis Toolbox, Volume III: Guidelines for Applying Traffic Microsimulation Modeling Software*. Report No. FHWA-HRT-04-040, Federal Highway Administration, Washington, D.C., 2004.
14. Rakha, H., Hellenga, B., Van Aerde, M., Perez, W. *Systematic Verification, Validation and Calibration of Traffic Simulation Models*. Presented at the 75th Annual Meeting of the Transportation Research Board, Washington, DC. 1996.
15. Park, B., Won, J., and Perfater, M.A. *Microscopic Simulation Model Calibration and Validation Handbook*. Report No. FHWA/VTRC 07-CR6, Virginia Transportation Research Council, 2006.

16. Gagnon, C., Sadek, A.W., Touchette, A., and Smith, M. Calibration Potential of Common Analytical and Microsimulation Roundabout Models: New England Case Study. *Transportation Research Record: Journal of the Transportation Research Board*, 2008, Vol. 2071: 77–86.
17. Li, Z., DeAmico, M., Chitturi, M.V., Bill, A.R., and Noyce, D.A. *Calibration of VISSIM Roundabout Model: A Critical Gap and Follow-up Headway Approach*. Presented at 92nd Annual Meeting of the Transportation Research Board, Washington, D.C., 2013.
18. Chun, G., Roupail, N., Samandar, S., List, G., Yang, G. *Analytical and Microsimulation Model Calibration and Validation: Application to Roundabouts under Sight-Restricted Conditions*. Presented at 101st Annual Meeting of the Transportation Research Board, Washington, D.C., 2022.
19. Giuffrè, O., Granà, A., Tumminello, M.L., and Sferlazza, A. Calibrating a Microscopic Traffic Simulation Model for Roundabouts Using Genetic Algorithms. *Journal of Intelligent and Fuzzy Systems*, 2018, Vol. 35(2): 1791-1806.
20. Mathew, T.V., Radhakrishnan, P. Calibration of Microsimulation Models for Nonlane-Based Heterogeneous Traffic at Signalized Intersections. *Journal of Urban Planning and Development*, Vol.136, No.1, 2010, pp.59-66.
21. Bhattacharyya, K., Maitra, B., Boltze, M. Calibration of Micro-Simulation Model Parameters for Heterogeneous Traffic using Mode-Specific Performance Measure. *Transportation Research Record*, Vol. 2674(1), 2020, pp.135–147.
22. Schroeder, B.J., Salamati, K., Hummer, J. Calibration and Field Validation of Four Double-Crossover Diamond Interchanges in VISSIM Microsimulation. *Transportation Research Record*, No. 2404, 2014, pp.49-58.
23. Guo, Y., Sayed, T., Zheng, L., Essa, M. An extreme value theory based approach for calibration of microsimulation models for safety analysis. *Simulation Modelling Practice and Theory*, Vol.106, 2021, <https://doi.org/10.1016/j.simpat.2020.102172>
24. TRB. *Highway Capacity Manual, Sixth Edition: A Guide for Multimodal Mobility Analysis*. Transportation Research Board, National Research Council, Washington, DC. 2016.
25. Lochrane, T., J. Bared, and W. Zhang. *Capacity Analysis for Planning of Junctions (Cap-X) Tool*. FHWA, US Department of Transportation, 2018, Available: <https://www.fhwa.dot.gov/software/research/operations/cap-x/>
26. Akçelik, R., and M. Besley. *SIDRA 10 User Guide*. Akcelik & Association Pty Ltd, Victoria, Australia, 2018.
27. Cubic ITS, Inc. *Synchro Studio 11 User Guide*. Cubic ITS Inc., Sugar Land, TX, 2019.
28. Benekohal, R.F., . El-Zohairy, Y.M., and Saak, J.E. *Comparison of Delays from HCM, Synchro, PASSER II, PASSER IV and CORSIM for an Urban Arterial*. Report No. FHWA-IL/UI-TOL-1, Illinois Department of Transportation, 2001.
29. Caliper Corporation. *Transmodeler User Guide*. Caliper Corporation, Newton, MA, 2021. <https://www.caliper.com>
30. Troutbeck, R. J. Estimating the critical acceptance gap from traffic movements. Queensland University of Technology, 1992.
31. Siegloch, W. Die Leistungsermittlung an Knotenpunkten Ohne Lichtsignalanlagen. *STRASSENBAU U STRASSENVERKEHRSTECH*, 1973
32. Raff, M. S. A Volume Warrant for Urban Stop Signs. Eno Foundation for Highway Traffic Control, Saugatuck, Connecticut, 1950, pp. 1–121.